WEAK INTERACTIONS OF QUARKS AND LEPTONS: EXPERIMENTAL STATUS*

STANLEY WOJCICKI
Physics Department and
Stanford Linear Accelerator Center
Stanford University, Stanford, CA. 94305

Lectures presented at the
12th SLAC Summer Institute on Particle Physics
The Sixth Quark

Stanford, California
July 23 - August 3, 1984

* Work supported by the Department of Energy, contract numbers DE-AC03-76SF00515 and DE-AC03-ER40050, and The National Science Foundation.

TABLE OF CONTENTS

1. Introduction

The work on the subject of weak interactions spans the last half a century. In assessing where we are today and where we might be going in the near future it is useful to look at the historical development of this field. Furthermore, we can say that the task of the high energy physicist is to understand the basic constituents of matter and of the forces that govern their behavior. Thus, in the spirit of the title of this talk, I start out by outlining the development[1] of our present picture of the constituents and the present picture of the weak force which determines at least a part of their mutual interactions.

Figure 1 attempts schematically to outline the major milestones in the development of the picture we shall be discussing. There is undoubtedly certain arbitrariness in the choice of these milestones but hopefully they do represent reasonably fairly the logical development of the subject. In the "constituent sector" I take the discovery of the muon as the logical starting point since that was the first indication that the spectrum one is dealing with is richer than initial observations might have indicated. The unexpected discovery of strange particles followed by observation of the electron neutrino and the famous 2 neutrino experiment were other key steps in the initial elucidation of the quark-lepton picture.

The decade of the 1960s saw the birth of the quark concept and its subsequent growth to maturity. The initial spectroscopic measurements led to the quark postulate and culminated in the discovery of the predicted Ω^- particle. The dynamical reality of the quarks was demonstrated beautifully in a series of deep inelastic scattering experiments, first with electrons using the SLAC accelerator and subsequently with the neutrinos and muons, mainly at Fermilab and CERN. The decade of the 1970s brought us an enlargement of both the quark and lepton sectors with the observation of the postulated charm quark and the totally unexpected τ lepton. The subsequent measurements of the properties of these two new constituents confirmed the initial belief that they represent an

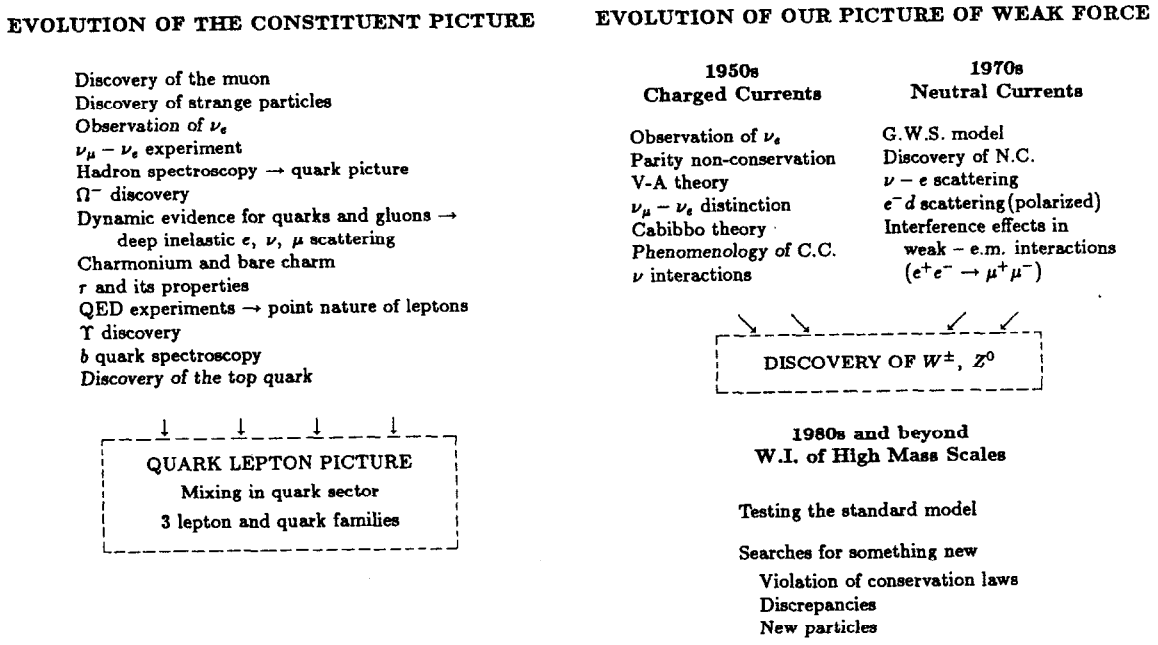

Figure 1 A rough outline of the historical development of our present picture of quarks and leptons and their weak interactions.

addition to the family of the fundamental building blocks.

Finally the late 1970s and early 1980s provided us with evidence for, and properties of, the fifth quark. Just now we may be in the process of completing the quark sextet with the recent observations at CERN.

One should not neglect the important contributions to this picture from the many beautiful QED experiments demonstrating the point nature of the leptons, ranging from the ultra-high precision static experiments to the highest energy e^+e^- QED processes.

Thus we have arrived at our present picture of the three doublet families of quarks and three doublet families of leptons. In addition we have learned that the mass eigenstates and weak interaction eigenstates are different in the quark sector. The reasons for the similarities and differences in this quark-lepton picture are one of the key puzzles in high energy physics today.

We turn now to the evolution of our present understanding of the weak interactions. I find it natural to distinguish between two different topics associated with two different eras in the study of this field - the charged current sector with its golden age in the 1950s and the neutral current sector with the height of its development in the 1970s. The key nuclear physics experiments in the 1950s on the nature of the weak interaction, parity nonconservation, and neutrino helicity, coupled with the seminal theoretical ideas about parity violation and the conserved vector current hypothesis led to the establishment of the presently accepted V-A picture of charged current interactions. The experiments on decays of elementary particles and the program on neutrino interactions reinforced this picture and developed further the phenomenology of weak interactions.

Our understanding of neutral currents also progressed very rapidly with the height of activity in the late 1970s. A few years after the formulation of the Glashow-Weinberg-Salam model (GWS), neutral currents were discovered at CERN and their existence confirmed soon afterwards at Fermilab. There followed several important experiments culminating in the key polarized electron-deuteron

scattering asymmetry measurement at SLAC. The subsequent experimental work provided even more stringent tests, all of them reinforcing our belief in the validity of the GWS picture.

Both of those rather separate lines of investigation have culminated in the recent discoveries at CERN of the W and Z gauge bosons. This key experiment can be viewed as bringing to a successful end the previous 50 years of work on weak interactions. We can justifiably ask where do we go from here.

It is my opinion that the next decade will emphasize the weak interactions of higher mass scales. Thus we shall try to answer the questions that will address the existence and the properties of the postulated (as well as the unexpected) higher mass particles and their roles as mediators of the weak interactions. This physics will span a range of investigations including detailed tests of the standard model with the hope of discovery of small discrepancies as well as searches for totally new phenomena, whether these be violations of existing laws, new particles, or something totally unexpected. The techniques employed will undoubtedly be numerous, ranging from atomic and nuclear experiments, through proton decay, ν decay and oscillation searches and cosmic ray studies, to the experiments at the highest energies which will hopefully be opened up by the next generation of accelerators. Finally, it may also be hoped that these "high mass scale investigations" will at the same time shed light on the puzzles that are present today in the constituent sector.

The choice of topics adopted for these lectures can be understood in the context of the above discussion. My emphasis will be less on how we got here rather than on where we are and where we are going from here. Hence, I will discuss the present experimental status of weak interactions, with the emphasis on the problems and questions and on the possible lines of future investigations.

2. The Quark Mixing Matrix

In our present picture of the quark sector, we have three left-handed doublets:

$$\begin{pmatrix} u \\ d' \end{pmatrix}_L , \begin{pmatrix} c \\ s' \end{pmatrix}_L , \text{ and } \begin{pmatrix} t \\ b' \end{pmatrix}_L$$

It is furthermore known experimentally that the quark mass eigenstates (denoted by the unprimed symbols) are not the same as the quark gauge group eigenstates (denoted by primed symbols). There is a certain arbitrariness in parametrizing this fact. The convention is to define the phases in such a way that the two sets of eigenstates are identical for the q = 2/3 quark states i.e., $u = u', c = c'$, and $t = t'$. We can then define a unitary matrix, U, which is totally specified by four real parameters conventionally taken to be three angles and one phase. This matrix can then be thought of as giving us the relationship between the (d', s', b') states and the (d, s, b) states i.e., schematically

$$q' = Uq \tag{2.1}$$

Alternatively, the matrix U can be said to specify the quark couplings in the charge-changing weak interaction current, i.e.

$$J^\mu = \bar{q}^+ \gamma^\mu (1 - \gamma_5) U q^- \tag{2.2}$$

with the $q^+(q^-)$ symbols standing for the positive (negative) charge quark states.

The matrix U is similar to the Euler matrix representing a rotation in the three-dimensional space. There are several parametrizations of this matrix. The original one, due to Kobayashi and Maskawa,[2] is

$$\begin{pmatrix} C_1 & -S_1C_3 & -S_1S_3 \\ S_1C_2 & C_1C_2C_3 - S_2S_3e^{i\delta} & C_1C_2S_3 + S_2C_3e^{i\delta} \\ S_1S_2 & C_1S_2C_3 + C_2S_3e^{i\delta} & C_1S_2S_3 - C_2C_3e^{i\delta} \end{pmatrix}$$

where $C_i \equiv \cos\theta_i, S_i \equiv \sin\theta_i$; $i = 1, 2, 3$ and $\theta_1, \theta_2, \theta_3$ are three angles equivalent to Euler angles and δ is the phase mentioned above. It was the contribution of

Kobayashi and Maskawa to point out that the CP violation can be introduced naturally if one has 6 quarks (rather than 4 known at that time) and provided that the phase $\delta \neq 0$ or π .

The other representation that finds frequent use is due to Maiani[3] and is given by

$$\begin{pmatrix} C_\beta C_\theta & C_\beta S_\theta & S_\beta \\ -S_\gamma C_\theta S_\theta e^{i\delta} - S_\theta C_\gamma & C_\gamma C_\theta - S_\gamma S_\beta S_\theta e^{i\delta} & S_\gamma C_\beta e^{i\delta} \\ -S_\beta C_\gamma C_\theta + S_\gamma S_\theta e^{i\delta} & -C_\gamma S_\beta S_\theta - S_\gamma C_\theta e^{-i\delta} & C_\gamma C_\beta \end{pmatrix}$$

where $C_\theta \equiv \cos\theta, S_\theta \equiv \sin\theta$, etc.

Even within the framework of each representation there are several different phase conventions that are used in the literature. These do not present a problem for us since the experiments that we shall discuss determine only the absolute magnitude of each particular matrix element. Finally, we should remark that one can define each angle to be in the first quadrant. The phase δ can then range from 0 to 2π and must be determined by experiment.

There are certain advantages to each representation. In the original K-M representation all the angles, $\theta_1, \theta_2, \theta_3$ are relatively small and thus the form of the matrix explicitly shows that the U_{13} element, for example, is second order in these small quantities. In the Maiani representation, θ, β, and γ are also small, and in that approximation the matrix becomes simply

$$\begin{pmatrix} 1 & \theta & \beta \\ -\theta & 1 & \gamma \\ -\beta & -\gamma & 1 \end{pmatrix} \quad .$$

Thus the angles θ, β, γ are approximately related to the size of the amplitude describing the couplings $u \to s, u \to b$, and $c \to b$ respectively.

A third parametrization of the mixing matrix has been recently introduced by Wolfenstein.[4] That particular parametrization is convenient for the analysis of the CP problem insofar that it explicitly shows that the CP violation enters only multiplied by a third power of a small parameter λ.

Our procedure in this discussion will be to describe the experimental input that allows us to measure the general matrix elements, i.e.,

$$\begin{pmatrix} U_{ud} & U_{us} & U_{ub} \\ U_{cd} & U_{cs} & U_{cb} \\ U_{td} & U_{ts} & U_{tb} \end{pmatrix} \quad .$$

At the end we shall try to relate that experimental input to the values of the K-M representation parameters θ_1 , θ_2 , θ_3 and δ .

Before embarking on this task, it might be worthwhile to summarize the phenomenological need for the top quark that would complete the third doublet. In other words, the question that one asks is whether the experimental data is compatible with the b quark being a singlet. This question might be moot in light of the recent evidence[5] for a possible new quark state from CERN, but until these data are shown to be completely conclusive, it is worthwhile to keep an open mind on this point.

A rather general argument on this point has been recently presented by Kane and Peskin[6] and we reproduce here its general qualitative features. The authors show that in any model in which the b quark is an SU(2) singlet with conventional $W^\pm$ and Z° couplings the following inequality involving semileptonic decays has to be satisfied:

$$\frac{\Gamma(B \to X\ell^+\ell^-)}{\Gamma(B \to X\ell^+\nu)} \geq 0.12 \qquad (2.3)$$

where $\ell^\pm$ is the generic symbol for charged leptons. Furthermore, the alternative models, which do not make this standard coupling assumption, are either already ruled out by the data or extremely unattractive.

The essence of the argument is as follows. The b quark is known to decay and thus must decay by virtue of mixing. The two weak eigenstates representing

$q = -1/3$ quark states can then be written as:

$$d' = \sum_{i=1}^{3} \alpha_i q_i \qquad \text{and}$$
$$s' = \sum_{i=1}^{3} \beta_i q_i \tag{2.4}$$

where α_i , β_i are mixing coefficients and $q_i = d$, s , or b . In Fig. 2 we show the diagrams that must be responsible for leptonic decays of the b quark. As can be seen from these diagrams the decay rates are given solely by the couplings of the gauge bosons to the leptons and to the quarks. The former are determined entirely in the framework of the Glashow-Weinberg-Salam model[7]; the latter are given by the model if the mixing coefficients (α's and β's) are known. Accordingly, the problem reduces to finding these coefficients which minimize the ratio given in 2.3 and at the same time are compatible with the other experimental data. To put it in other words the Glashow-Weinberg[8] theorem which shows that the GIM mechanism for suppression of neutral currents is applicable for any number of weak doublets, is no longer relevant if b quark is a weak singlet. Hence, the mixing coefficients have to be adjusted "by hand" so as to minimize the flavor changing neutral current amplitude in b decay and to make those amplitudes in other decays compatible with the very stringent experimental limits.

One makes now the observation that the mixing angles are rather well constrained already by the existing data. Specifically if the first equation in 2.4 is rewritten as

$$d' = C_1(C_c d + S_c s) + S_1 b \ ,$$

C_1 is constrained to be very close to 1 by Cabibbo universality and S_c is the sine of the Cabibbo angle that is well measured in K and hyperon decays. Additional constraints are imposed by the requirements of orthogonality of s' and d' and the requirement that the strangeness changing $d \longleftrightarrow s$ neutral current amplitude be small enough to be compatible with the $K_L - K_S$ mass difference. The net effect

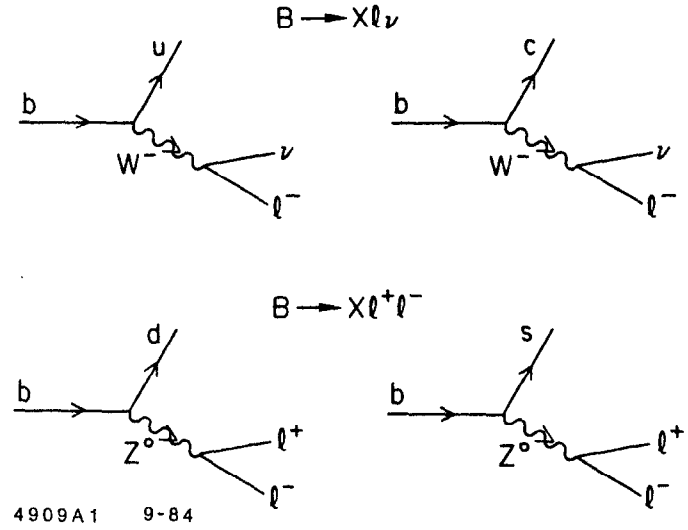

Figure 2 Diagrams contributing to semileptonic b decay.

of these constraints is that the mixing parameters are strongly constrained and the lower bound stated in 2.3 is obtained.

The best experimental limit comes from the data taken by the CLEO collaboration which obtains[9)]

$$\frac{B \to X\ell^+\ell^-}{B \to All} < 0.3\% \ (90\% \ C.L) \quad . \tag{2.5}$$

Coupled with the world average [9)] for each (i.e. electron and muon) semileptonic branching ratio of the B meson of $11.6 \pm 0.5\%$, this yields

$$\frac{\Gamma(B \to X\ell^+\ell^-)}{\Gamma(B \to X\ell^+\nu)} < 1.3\% \quad . \tag{2.6}$$

Thus the experimental value is clearly in contradiction with the Kane-Peskin bounds and excludes the b singlet possibilities. We next proceed to the discussion of the experimental determination of six out of the nine total elements U_{ij} .[10)]

a) U_{ud} responsible for $u \to d$ and $d \to u$ transitions.

We determine this matrix element by comparing the strength of nuclear vector beta decays to muon decay rate. To assure pure vector, i.e., Fermi transitions we have to limit ourselves to $0^+ \to 0^+$ decays. In addition, it is important that the nuclear matrix element be perfectly understood, which in turn implies use of superallowed transitions.

Several transitions satisfying these requirements exist in nature and have been studied experimentally. They generally are decays within the same $T = 1$ multiplet and the two that provide the most accurate information are ^{14}O and $^{26}Al^m$ decays. The data on those and other decays, satisfying the criteria outlined above, are presented in Table I below (reproduced from Paschos and Turke[11)]).

Table I

ft-values, corrections and corresponding results for more accurate decays.

Nucleus	ft(s)	$\delta_R(\%)$	$\delta_C(\%)$	$\delta_W(\%)$	$\lvert U_{ud}\rvert$
^{14}O	3047.6 ± 3.6	1.57	0.18	2.10	0.97223
$^{26}Al^m$	3037.9 ± 2.9	1.61	0.24	2.10	0.97377
^{34}Cl	3052 ± 12	1.68	0.51	2.10	0.97255
$^{38}K^m$	3063 ± 10	1.74	0.44	2.10	0.97015
^{42}Sc	3052 ± 13	1.81	0.44	2.10	0.97154
^{46}V	3039 ± 16	1.87	0.40	2.10	0.97311
^{50}Mn	3038.1 ± 7.1	1.95	0.47	2.10	0.97322
^{54}Co	3041.4 ± 5.0	2.01	0.56	2.10	0.97289

The relevant corrections are: δ_R , the "outer" electromagnetic correction, δ_C - the nuclear isospin correction to correct for isospin impurity in the transitions in question, and δ_W - the difference in "inner" electroweak correction between the nuclear ft values and the muon decay rate.

Paschos and Turke obtain from their analysis

$$U_{ud} = 0.9730 \pm 0.0004 \pm 0.0020$$

where the first error is statistical and the second represents theoretical uncertainties. An independent analysis by Shrock and Wang[12)] using compilations by Towner and Hardy and by Wilkinson[13)] as the basic input yields

$$U_{ud} = 0.9737 \pm 0.0025$$

Clearly these numbers are compatible with each other. As the best value I shall

take the average of the two, obtaining

$$U_{ud} = 0.9733 \pm 0.0024. \qquad (2.7)$$

b) U_{us} responsible for $u \to s$ and $s \to u$ transitions.

There are two alternative approaches to measuring this matrix element and we shall discuss each one in turn.

1 - Analysis of the Ke_3 decays, i.e., of the processes

$$K^+ \to \pi^\circ e^+ \nu \qquad \text{and}$$
$$K_L^\circ \to \pi^\pm e^\mp \nu \qquad .$$

There are several theoretical difficulties that have to be kept in mind when discussing these decay modes. First, we might expect some SU_3 breaking effects, even though they should be small here by virtue of the Ademallo-Gatto theorem[14] Second, the momentum transfer involved is no longer negligible as in the case of the nuclear beta decay; hence the form factor behavior must be understood insofar as it is the rate at $q^2 = 0$ that is directly related to U_{us}^2.

Experimentally, the input consists of the lifetimes of the two K mesons, the branching ratio into the $\pi e \nu$ mode and the form factor dependance allowing the extrapolation to obtain $f_+(0)$.

Shrock and Wang[12] apply radiative and SU_3 breaking corrections to the data to obtain

$$U_{us} = 0.221 \pm 0.003 \qquad \text{from } K^+ \text{ decays} \qquad \text{and}$$
$$U_{us} = 0.212 \pm 0.005 \qquad \text{from } K_L^\circ \text{ decays.}$$

Combining these we obtain

$$U_{us} = 0.219 \pm 0.003. \qquad (2.8)$$

2 - The other method consists of analysis of the combined hyperon and neutron decay rates. We first briefly describe qualitatively the formalism that is used in this analysis. The general matrix element for hyperon (or neutron) decay can be expressed in terms of 6 form factors, three of which: f_1 , f_2 , f_3 are vector form factors and the other three, g_1 , g_2 , g_3 axial form factors. Only f_1 and g_1 , and to much lesser extent f_2 , give significant contribution to the experimentally observable quantities.

The amplitude of the strangeness conserving decays is proportional to U_{ud} ($\cos\theta$ in the old 4 quark formalism); of the strangeness changing decays to U_{us} ($\sin\theta$ in the 4 quark formalism). Furthermore, both f_1 and f_2 are determined entirely by the CVC hypothesis. The g_1 form factor for each decay is expressible as a linear combination of 2 parameters, F and D, which represent the strength of the symmetric and anti-symmetric 8 $\otimes$ 8 couplings. The exact parametrization of these 3 form factors is specified in Table II.

Table II

Parameters of the baryon weak matrix

Decay	Amplitude	$f_1(0)$	$f_2(0)$[a]	$g_1(0)$
$n \to pe\nu_e$	$\cos\theta$	1	$\mu_p - \mu_n$	F + D
$\Sigma^\pm \to \Lambda e\nu_e$	$\cos\theta$	0	$-\sqrt{3/2}\mu_n$	$\sqrt{2/3}D$
$\Sigma^- \to \Sigma^\circ e\nu_e$	$\cos\theta$	$\sqrt{2}$	$\sqrt{2}[\mu_p + (\mu_n/2)]$	$\sqrt{2}F$
$\Lambda \to p\ell\nu_e$	$\sin\theta$	$-\sqrt{3/2}$	$-\sqrt{3/2}\mu_p$	$-\sqrt{3/2}$(F+D/3)
$\Sigma^- \to n\ell\nu_\ell$	$\sin\theta$	-1	$-(\mu_p + 2\mu_n)$	$-(F - D)$
$\Xi^- \to \Lambda\ell\nu_\ell$	$\sin\theta$	$\sqrt{3/2}$	$\sqrt{3/2}(\mu_p + \mu_n)$	$\sqrt{3/2}(F - D/3)$
$\Xi^- \to \Sigma^\circ\ell\nu_\ell$	$\sin\theta$	$1/\sqrt{2}$	$1/\sqrt{2}(\mu_p - \mu_n)$	(F+D)$/\sqrt{2}$
$\Xi^\circ \to \Sigma^+\ell\nu_\ell$	$\sin\theta$	1	$\mu_p - \mu_n$	F+D
$\Xi^- \to \Xi^\circ\ell\nu_\ell$	$\cos\theta$	1	$\mu_p + 2\mu_n$	$F - D$

[a] The values of the anomalous magnetic moments are: $\mu_p = 1.793, \mu_n = -1.913$.

Every measurable in these decay processes (decay rates, asymmetry parameters, angular correlation coefficients) can be expressed in terms of the form factors discussed above. Thus once $\sin\theta$ (and hence $\cos\theta$) is known, each independent piece of data determines a straight line in the D , F space. Hence the analysis can be thought of as consisting of finding that value of $\sin\theta$ which results in all of those straight lines intersecting in a common point, or more specifically, minimizing the "circle of least confusion."

The latest experimental results from the hyperon decay experiment at CERN[15] are displayed in Fig. 3. In addition, data on neutron lifetime and neutron decay angular correlations are also shown on the same figure. There is some controversy and inconsistency in the neutron lifetime data. For the purpose of this plot a value of $\tau_n = 925.3 \pm 11.1$ sec has been used by the authors of Ref. 15. The lines labeled (g_1/f_1) represent the angular correlation measurements; the other lines come from the partial rate measurements. The shaded area represents the extent of the experimental errors. Clearly the data are quite consistent and a least squares fit yields for the best values of the parameters:

$$F = 0.477 \pm 0.012 ,$$
$$D = 0.756 \pm 0.011 , \quad \text{and}$$
$$\sin\theta \equiv U_{us} = 0.231 \pm 0.003.$$

This value of U_{us} is somewhat different from the K decay value ($\sim 3\sigma$). This probably reflects the theoretical uncertainties in both analyses. Accordingly, it is probably best to take the average value and increase the error somewhat to take into account these uncertainties. Thus we quote

$$U_{us} = 0.225 \pm 0.005 . \tag{2.9}$$

Before leaving this topic, one should mention that there exists one set of data that is inconsistent with the above picture, namely the measurements of the α_-,

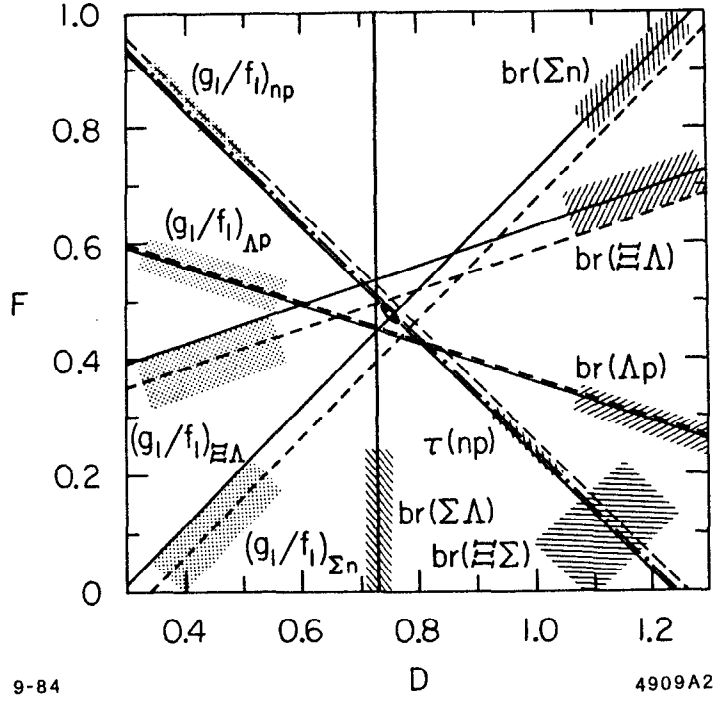

Figure 3 Summary of the hyperon decay data (from CERN experiment) and the neutron decay rate.

the decay asymmetry parameter for Σ^-. These data are illustrated in Fig. 4, together with the prediction from the overall fit to the CERN data. The present consensus is to discount this disagreement somewhat, since all these data points come from low statistics experiments, done in less than optimum conditions. There is an experiment[16] at Fermilab, which just completed its data-taking phase, which uses a polarized Σ^- beam and attempts to reconstruct the full Σ^- decay by measuring both the decay neutron and the decay electron. The results from that experiment should definitely settle this particular question.

c) U_{cd} responsible for $c \to d$ and $d \to c$ transitions.

In principle, there are two ways of extracting this parameter out of the data and we shall discuss each one in turn.

1 - We can study the $c \to d$ transitions in the charm decays. The ideal processes would be the decays

$$D \to \pi \ell \nu \qquad \text{and}$$
$$D \to \rho \ell \nu$$

since these are unencumbered by the effects of strong interactions in the final state.

In practice neither of these decay modes has been observed as yet. Even when some data on these channels will be accumulated, there will still be certain conceptual difficulties with the proper analysis e.g., SU_4 breaking effects, mass of the charm quark to be used and form factor dependance. The pure hadronic decays $D \to 2\pi$ and $D \to K^+K^-$ have been observed but the extraction of U_{cd} out of these data does not appear to be possible at the present time. The fundamental difficulty lies in the fact that the hadronic effects simply are not understood well enough theoretically to be able to extract quantitative results. To illustrate this fact we remind the reader that experimentally[17]

$$\frac{\Gamma(D^\circ \to K^+K^-)}{\Gamma(D^\circ \to \pi^+\pi^-)} \approx 3.5$$

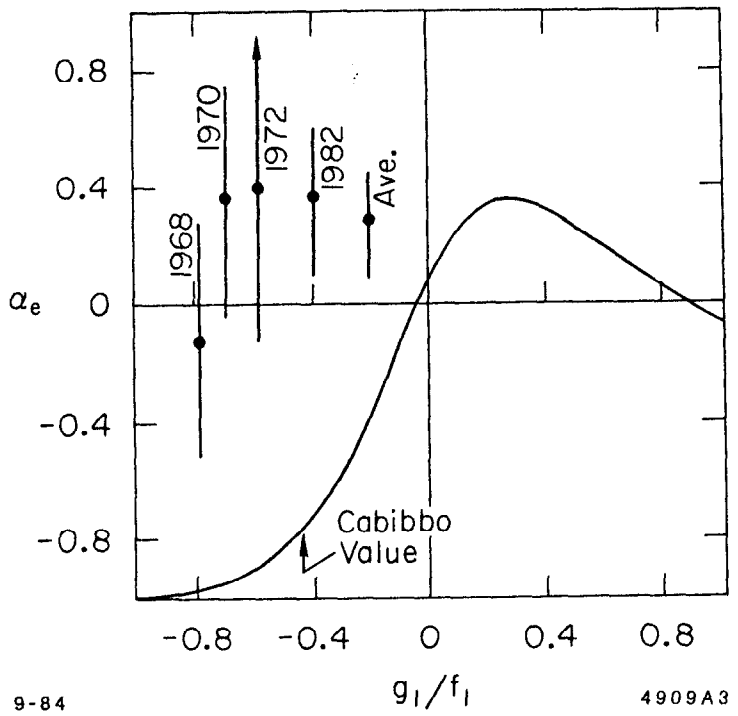

Figure 4 The four measurements of the Σ^- asymmetry parameter (α_e) compared with the prediction of the overall fit. The curve shows the dependance of the α_e on the ratio of form factors (g_1/f_1).

whereas the phase space effects would tend to favor the $\pi^+\pi^-$ mode. To my knowledge, no satisfactory explanation of this discrepancy has been given.

In addition there is the experimental fact that the lifetimes of D° and D^+ do not appear to be equal. Specifically using Hitlin's compilation[18] we have

$$\tau^+/\tau^\circ = 2.78^{+0.86+0.31}_{-0.60-0.42} \quad .$$

This can be understood at least qualitatively on the basis of the fact that the exchange diagrams that contribute to the D° decay are absent in the case of the D^+ decay (see Fig. 5). However, I am not aware of any reliable theoretical calculations that are able to reproduce accurately this number.

Thus at best we can conclude from the non-leptonic decay modes that the $c \to d$ transition is suppressed with respect to the $c \to s$ rate. Extraction of any quantitative information out of the charm Cabibbo forbidden decays, however, will have to await better experimental data or better theoretical understanding or both.

2 - Quantitative information on the U_{cd} matrix element can be obtained from the charm production by neutrinos. More specifically, one studies a $\mu^+\mu^-$ final state that is dominated by the sequence

$$\nu + p \text{ (or n)} \to \text{charm} + \mu^-$$
$$\quad \lfloor\!\!\to \mu^+ + X$$

which on the quark level can be written as

$$\nu + d \to \mu^- + c$$
$$\quad \lfloor\!\!\to s + \mu^+ + \nu$$

or

$$\nu + s \to \mu^- + c$$
$$\quad \lfloor\!\!\to s + \mu^+ + \nu$$

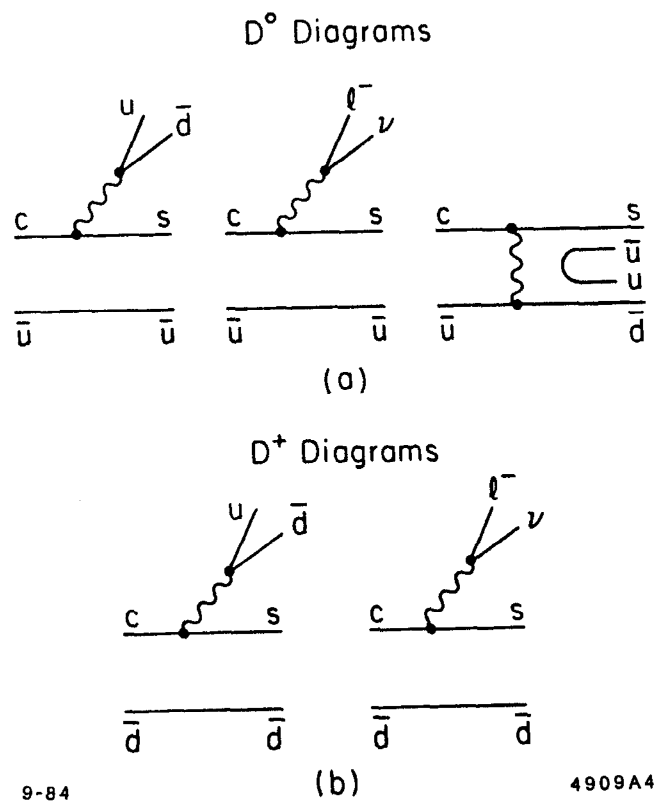

Figure 5 The standard diagrams that contribute to D° (a) and $D^\pm$ (b) decay (Cabibbo allowed).

and comparable reaction for the incident $\bar{\nu}$'s.

To obtain the value of U_{cd} we must separate the two quark contributions. The expressions for differential charm production cross sections by neutrinos and anti-neutrinos on an isoscalar target (a good approximation for heavy target experiments) are given by:

$$\frac{d^2\sigma^\nu}{dxdy} = \frac{G^2 M E_\nu x}{\pi} \left\{ |U_{cd}|^2 [u(x) + d(x)] + |U_{cs}|^2 \cdot 2s(x) \right\} , \qquad (2.10)$$

$$\frac{d^2\sigma^{\bar{\nu}}}{dxdy} = \frac{G^2 M E_{\bar{\nu}} x}{\pi} \left\{ |U_{cd}|^2 [\bar{u}(x) + \bar{d}(x)] + |U_{cs}|^2 \cdot 2\bar{s}(x) \right\} \qquad (2.11)$$

where $u(x)$ and $d(x)$ are the u and d quark distributions in the proton and we have utilized the fact that $u(x)$ in proton is the same as $d(x)$ in neutron.

Experimentally, the best measurement is of the $2\mu/1\mu$ ratios i.e. of $\sigma^\nu_{+-}/\sigma^\nu_-$ and of the $\sigma^{\bar{\nu}}_{+-}/\sigma^{\bar{\nu}}_+$. We note that for single muon production we have

$$\frac{d^2\sigma^\nu}{dxdy} \propto q(x) + (1-y)^2 \bar{q}(x) , \qquad (2.12)$$

$$\frac{d^2\sigma^{\bar{\nu}}}{dxdy} \propto \bar{q}(x) + (1-y)^2 q(x) \qquad (2.13)$$

where $q(x)$ stands for $u(x)$, $d(x)$, and $s(x)$ and similarly for $\bar{q}(x)$. We can now define

$$R = \sigma^{\bar{\nu}}_+ / \sigma^\nu_- \qquad (2.14)$$

and integrate the expressions 2.10 - 2.13. Using the fact that $s(x) = \bar{s}(x)$, after some algebra we obtain

$$B|U_{cd}|^2 = \frac{(\sigma^\nu_{+-}/\sigma^\nu_-) - (R\sigma^{\bar{\nu}}_{+-}/\sigma^{\bar{\nu}}_+)}{1-R} \frac{2}{3} \quad , \qquad (2.15)$$

with B being the weighted average semileptonic branching ratio of the charmed particles, the weighting being determined by the relative production cross section of various charm particles in $\nu(\bar{\nu})$ interactions and the relative muon detection efficiency for those decay modes.

The detailed analysis of this reaction has been performed[19] by the CDHS group who used $R = 0.48 \pm 0.02$ and $B = 7.1 \pm 1.3\%$, the latter value obtained by studying relative charmed particle production in emulsions. The dimuon to single-muon cross section ratios used came from the CDHS experiment. For the value of $|U_{cd}|$ the authors obtain

$$|U_{cd}| = 0.24 \pm 0.03 \quad . \qquad (2.16)$$

The CCFRR collaboration at Fermilab obtains a similar value[20] (0.25 ± 0.07) from the analysis of their $\mu^+\mu^-$ data.

d) U_{cs} responsible for the $c \to s$ and $s \to c$ transitions.

Again, information here can be obtained both from the charm decays and from the charm production by neutrinos.

1 - The optimum charm decay channel to use is the process

$$D \to \bar{K} \ell^+ \nu$$

since this decay combines the best experimental input and fewest theoretical uncertainties. Nevertheless some problems remain and they tend to limit the accuracy with which we can measure this matrix element.

On the theoretical side we need to cope now with the potential SU_4 breaking effects which could be larger here than in the case of K decays. The form factor dependance could also be more important here since q^2 involved can be quite large. At present, there is no information on the Dalitz plot density for this decay. Finally the relationship of the decay rate to the value of $|U_{cs}|^2$ depends on the masses of the c and s quarks used.

Experimentally, for a specific decay, for example:

$$D^+ \to \bar{K}^\circ e^+ \nu_e$$

we need to know the D^+ lifetime, exclusive branching ratio $D^+ \to e^+ X$, and the fraction of that exclusive mode that goes to $\bar{K}^\circ e^+ \nu_e$. The difficulty in extracting

the rate of interest lies in the fact that τ_D^+ and τ_D° appear to be different and thus their leptonic branching ratios will not be equal. Most of the exclusive $D \to eX$ branching ratio measurements came from high energy e^+e^- annihilations, where the precise $D^\circ/D^\pm$ production rate is not known very well experimentally.

The numbers we shall use are:

$$\begin{aligned}
\tau_+/\tau_- &= 2.78 && \text{(Ref.18)}, \\
\tau_D^+ &= (8.3 \pm 1.0) \times 10^{-13}\text{sec} && \text{(Ref.21)}, \\
B(D \to eX) &= (8.4 \pm 0.6)\% && \text{(Ref.21)}, \\
\sigma(D^\circ)/\sigma(D^+) &= 2.3 \pm 1.2 && \text{(Ref.22)} \quad \text{and} \\
\Gamma(D \to Ke\nu)/\Gamma(D \to eX) &= 0.55 \pm 0.14 && \text{(Ref.23)}.
\end{aligned}$$

These values give

$$\begin{aligned}
B(D^+ \to e^+X) &= (15 \pm 3)\% , \\
B(D^+ \to \bar{K}^\circ e^+\nu_e) &= (8 \pm 3)\% , \\
\text{and} \quad \Gamma(D^+ \to \bar{K}^\circ e^+\nu_e) &= (1.0 \pm 0.3) \times 10^{11}\text{sec}^{-1} .
\end{aligned}$$

Finally, to relate the last value to $|U_{cs}|$ we use[24]

$$\Gamma(D^+ \to \bar{K}^\circ e^+\nu_e) = 1.5 \times 10^{11}\text{sec}^{-1} \times |f_+^{D\to K}(0)|^2 \times |U_{cs}|^2 \quad ,$$

where the numerical coefficient was derived by using the F^* dominance of the form factor. Assuming perfect SU_4 symmetry, i.e., $f_+^{D\to K}(0) = 1$, we obtain

$$|U_{cs}| = .82 \pm .13 ,$$

where the uncertainty quoted represents merely a propagation of the errors in the input quantities and does not reflect any additional theoretical uncertainties.

2 - Independent information on this matrix element can be obtained from the charm production by neutrinos, i.e. from the analysis of $\mu^+\mu^-$ events in the final state. The differential cross section has been given in Equation 2.10 and thus one must separate the two contributions. This can be done because the valence and sea quark distributions have quite different x dependance.

In more detail the procedure is as follows. The $s(x)$ distribution is assumed to be the same as $\bar{s}(x)$ and can be obtained directly from the $\mu^+\mu^-$ events produced by the ν interactions. Because U_{cd} is small, $\bar{u}(x)$ and $\bar{d}(x)$ contribute very little to this process, and in addition they are very similar to $s(x)$ as can be ascertained from single μ production by ν's at high y. This fact is illustrated in Fig. 6a where the actual $\mu^+\mu^-$ x distribution is compared with the prediction from the single μ data analysis. Finally, the u and d quark distributions can be obtained from the structure functions using the relation

$$x[u(x) + d(x)] = \frac{1}{2}[F_2(x) + xF_3(x) - 2xs(x)] , \qquad (2.17)$$

where F_2 and F_3 are derived from the analysis of single muon data.[25] As can be seen from Fig. 6b the data can be fit quite well[19] by a linear combination of these two distributions with the result

$$\frac{|U_{cs}|^2 \cdot 2S}{|U_{cd}|^2 \cdot (U + D)} = 1.19 \pm 0.09 \qquad (2.18)$$

where $S = \int_o^{\prime} xs(x)dx$ and similarly for U and D. Again, using the results of the single μ experiment, this result can be converted to

$$\frac{|U_{cs}|^2 \cdot 2S}{|U_{cd}|^2 \cdot (\bar{U} + \bar{D})} = 9.3 \pm 1.6 .$$

To go any further we have to make some assumptions. We expect that $2S < (\bar{U} + \bar{D})$ because of the heavier s quark mass. If we take the extreme case of SU_3

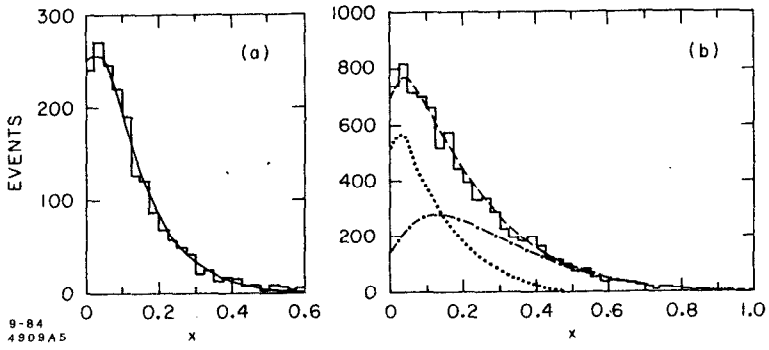

Figure 6 The x distribution for $\mu^+\mu^-$ events from Ref. 19.
(a) Histogram represents the $\bar{\nu}$ data, the curve is the prediction from single μ analysis.
(b) Histogram represents the ν data; dotted curve is the contribution due to $s(x)$, dash-dot curve due to $u(x) + d(x)$, and the dashed curve the sum of both.

symmetry i.e., $2S = \bar{U} + \bar{D}$ then we obtain

$$|U_{cs}|^2 = (9.3 \pm 1.6)|U_{cd}|^2 .$$

Clearly, this assumption gives a lower limit for U_{cs}. We can plug in the previously derived value of U_{cd} to obtain the inequality

$$|U_{cs}| > 0.59 \text{ at } 90\% \text{ C.L.} .$$

This value is obviously consistent with the result obtained from the charmed meson decay analysis.

c) U_{ub} responsible for the $u \to b$ or $b \to u$ transitions.

By far the best limit on this parameter comes from the new information on the b quark lifetimes and the upper limit on $b \to u$ branching ratio. Before discussing these data, for historical reasons we mention briefly the information that can be extracted from the like sign dimuon data resulting from $\bar{\nu}$ interactions. These events could originate (in the quark picture) from:

$$\begin{aligned} \bar{\nu} + u &\to \mu^+ + b \\ &\quad\; |\to c + X \\ &\quad\; |\to s + \mu^+ + \nu_\mu . \end{aligned}$$

In the actual calculation,[26] it is convenient to compare the rates for $\mu^+\mu^-$ and $\mu^\pm\mu^\pm$ since some of the uncertainties cancel out in that procedure. Threshold factors due to finite c and b quark masses have to be included. The most stringent limit can be obtained by assuming that at least a part of the $\mu^+\mu^+$ rate is due to some background process that also contributes with the same strength to ν interactions, and is responsible there for all of the $\mu^-\mu^-$ events (the cross section

for $\nu\bar{u} \to \bar{b}\mu^-$ would be much smaller). Under those assumptions one obtains the limit

$$|U_{ub}| < 0.18 \quad . \tag{2.19}$$

A much better value is obtained by studying the b decays directly. The important input here is the ratio $\Gamma(b \to u\ell\nu)/\Gamma(b \to c\ell\nu)$ which can be obtained from the study of the lepton momentum spectra resulting from the semileptonic b decays. The 4S Υ region is the ideal point to study this question since the B mesons produced are almost at rest and Doppler broadening is relatively small.

This problem was studied by the two collaborations working at CESR and they have obtained the following limits at the 90% C.L.

$$\Gamma(b \to u\ell\nu)/\Gamma(b \to c\ell\nu) < 5.5\% \qquad \text{CUSB collaboration}^{27)} \qquad \text{and}$$

$$\Gamma(b \to u\ell\nu)/\Gamma(b \to c\ell\nu) < 4\% \qquad \text{CLEO collaboration.}^{28)}$$

There is some model dependance in the extraction of these limits from the data since one has to make some assumptions that affect the exact functional dependance of the curve that is fitted: i.e., spectator quark model or well defined final state mass, Fermi momentum of the b quark, mass of the spectator quark. The end result, however, is only mildly sensitive to these assumptions provided that reasonable values of relevant parameters are taken. The relevant lepton spectra and the fits to different hypotheses are shown in Fig. 7 for the CUSB data and Fig. 8 for the CLEO data.

Taking the more stringent CLEO limit and correcting for phase space effects due to different masses of the u and c quarks we obtain an upper bound

$$|U_{ub}|/|U_{cb}| < 0.14 \qquad \text{with 90\% C.L.} \quad . \tag{2.20}$$

f) <u>U_{uc} responsible for $c \to b$ and $b \to c$ transitions.</u>

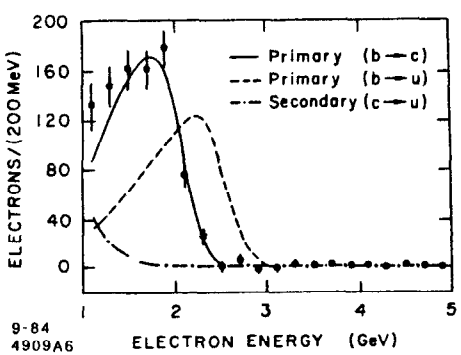

Figure 7 The electron energy spectrum from b decay as obtained by the CUSB collaboration.

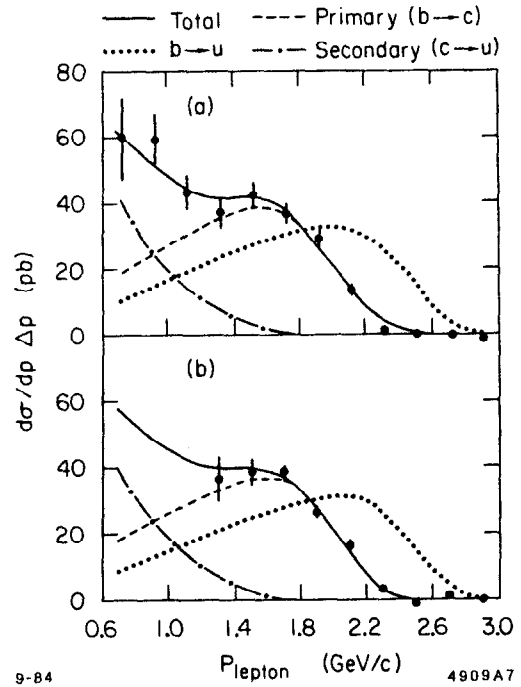

Figure 8 Electron (a) and muon (b) energy spectra from b decay as obtained by the CLEO collaboration. The solid curve represents the calculated spectrum on the assumption of no direct $b \to u\ell\nu$ decay.

The lifetime of the b quark can be related to the linear combination of $|U_{cb}|^2$ and $|U_{uc}|^2$. The exact values of the coefficients depend on the quark masses used and on the magnitude of the dynamical enhancement for the non-leptonic modes. We follow the treatment of Gaillard and Maiani[29] who derived the relationship:

$$\tau_B = 0.93 \times 10^{-14}/(2.75|U_{cb}|^2 + 7.7|U_{ub}|^2) \text{ sec} \quad . \qquad (2.21)$$

Note that the ratio of the 2 coefficients, i.e., 0.36 is somewhat different than the ratio of 0.45 used by the CLEO collaboration[28] in relating their 4% experimental limit to 0.14 limit on matrix elements previously quoted (using 0.36 would reduce the limit to 0.125).

The b quark lifetime has been shown about a year ago to be surprisingly long[30] and the present situation has been summarized by Jaros[31] at this Institute. The results are tabulated in Table III below.

Table III

Summary of b lifetime results

Collaboration	Value (ps)	Reference
Mark II	$0.85 \pm 0.17 \pm 0.21$	31
MAC	$1.6 \pm 0.4 \pm 0.4$	31
DELCO	$1.16^{+.37}_{-.34} + .23$	32
JADE	$1.8^{+.5}_{-.3} \pm .35$	33
TASSO	$1.9 \pm .4 \pm .6$	33

All of these experiments use the impact parameter method[30,31] to extract the lifetime value. Thus the systematic errors could be similar and it is probably incorrect to take a weighted average of all the values. For the purpose of the

following discussions we shall take

$$\tau_b = (1.0 \pm 0.3) \times 10^{-12} \text{ sec} .$$

This value yields

$$|U_{cb}| = 0.058 \pm 0.009 \qquad (2.22)$$

since the U_{ub} contribution can be neglected here in light of Equation 2.20.

Furthermore, combining this with the Equation 2.20 we also obtain

$$|U_{ub}| < 0.01 \qquad 90\% \text{ C.L.} . \qquad (2.23)$$

Clearly this limit is much more stringent than the one obtained in 2.19.

g) Other 3 matrix elements.

Clearly no direct experimental information exists at the present time on the other 3 matrix elements that link the t quark to d , s , and b quarks. For completeness, it might be worthwhile to end this discussion by discussing the eventual prospects for measuring these elements.

As will be apparent from the discussion below, we expect the inequality $|U_{tb}| >> |U_{ts}| >> |U_{td}|$ based on the extracted values of θ_1, θ_2 , and θ_3. If the mass of the t quark is in the vicinity of 40 GeV, we would expect an appreciable decay rate[34] of the toponium state into $t\bar{b}\ell^-\nu$ and $\bar{t}b\ell^+\nu$. Since $\Gamma(t\bar{t} \to e^+e^-)$ can be measured from the height of the toponium peak, the relative branching ratio of $(t\bar{t}) \to e^+e^-$ vs $t\bar{b}\ell\nu$ can give us the value of $|U_{tb}|^2$. We expect here the usual difficulties associated with measuring an angle by measuring its cosine when $\cos\theta \approx 1$.

In principle the values, or more likely, the limits on the other t quark matrix elements can be obtained by looking at the lepton energy spectra in toponium decays, or bare top decays, in a manner similar to the CESR work on b quarks discussed above. However, because of the high t quark mass, this technique will be rather difficult.

Again, in principle, the top production by neutrinos can yield information on U_{ts} and U_{td}. This method, however, will have to await ν beams of much higher energy than are currently available.

Calculations of the 4 basic parameters: $\theta_1, \theta_2, \theta_3, \delta$.

We can proceed now to the extraction of the 4 basic parameters from the experimental input. We shall use the original Kobayashi-Maskawa parametrization for this purpose. We proceed in several steps:

1 - Since $U_{ud} = C_1$ in K-M parametrization, we obtain directly from Equation 2.5 that

$$S_1 = 0.230 \pm 0.011 . \qquad (2.24)$$

2 - We can perform a consistency check using the elements of the first row, which also gives us a value of S_3. Since

$$U_{us}^2 + U_{ud}^2 = 1 - S_1^2 S_3^2$$

by substituting the experimental values for the expressions on the left hand side of the equation, we obtain

$$S_1 S_3 = .045 \, ^{+.05}_{-.045} .$$

Clearly, the unitarity condition is satisfied but the information on S_3 is limited. Dividing by S_1 we obtain

$$S_3 = 0.20 \, ^{+.21}_{-.20} . \qquad (2.25)$$

This method of obtaining S_3 is much less sensitive than the more direct evaluation discussed below.

3 - Using Eq. 2.23 and definition of U_{ub} we obtain

$$S_1 S_3 < 0.01 \qquad 90\% \text{ C.L.}$$

and dividing by S_1 we have

$$S_3 \leq 0.043 \qquad 90\% \text{ C.L.} . \tag{2.26}$$

4 - From the expression for U_{cb} and Eq. 2.22 we obtain

$$|U_{cb}| = |C_1 C_2 S_3 + S_2 C_3 e^{i\delta}| = 0.058 \pm 0.009$$

which gives us the inequality

$$|S_3 + S_2 e^{i\delta}| \geq 0.058 \pm 0.009 . \tag{2.27}$$

The above expression gives us correlated limits on S_2 and S_3 which will occur when $\delta = 0$ and $\delta = \pi$. More precisely, the allowed space for S_2 and S_3 will be a triangular region bounded by the three lines i.e.,

$$\left.\begin{array}{ll} S_2 = 0.058 + S_3 & \delta = \pi \text{ case} \\ S_2 = 0.058 - S_3 & \delta = 0 \text{ case} \\ S_3 = 0.043 & S_3 \text{ limit} \end{array}\right\} . \tag{2.28}$$

The intermediate values of δ give well defined contours inside this triangle. These limits as well as contours for other values of δ are displayed in Fig. 9 (adapted from L.-L. Chau and W.-Y. Keung[35]).

5 - As is apparent from the discussion in the preceding section δ can be determined if both S_2 and S_3 are known. The functional form of the 6 matrix elements discussed above demonstrates that even if the experimental errors were considerably reduced, a unique determination of these two angles is impossible without

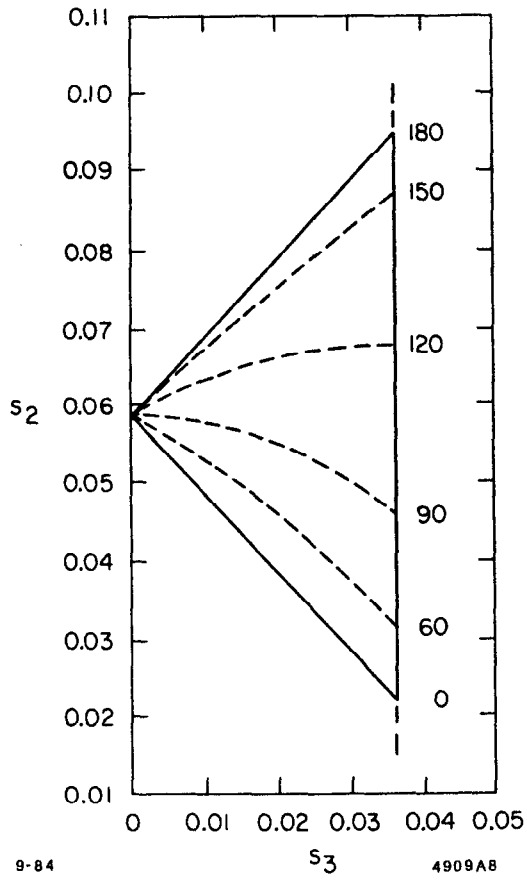

Figure 9 The relationship between S_2 and S_3 values and the value of δ. The allowed S_2 and S_3 values must lie within the triangle bounded by the three solid lines.

additional input. Hence we might discuss briefly which other experiments can provide auxiliary information on these parameters. A full discussion of these questions would take us too far into the theoretical domain; in addition it would unnecessarily duplicate a much more erudite treatment given in the parallel lectures by H. Harari. For completeness, however, we should mention briefly some of the relevant points.

The basic idea is that the off diagonal $K^\circ - \bar{K}^\circ$ mass matrix element is related to several experimentally measurable quantities and that a major (?) contribution to this element is expressible in terms of the K-M matrix elements and hence $\theta_1, \theta_2, \theta_3$, and δ. Some of the quantities related to this matrix element are $\Delta m, K_1 - K_2$ mass difference, CP violation parameter in $K^\circ - \bar{K}^\circ$ system and part of the amplitude for $K^\circ \to \mu^+\mu^-$. We shall have occasion to return to this point in several instances later on in these lectures. Below we elaborate briefly on the second point.

The off-diagonal $K^\circ - \bar{K}^\circ$ matrix element can be expressed as[36]:

$$M_{12} = < K^\circ|H_2|\bar{K}^\circ > + \sum_n \frac{< K^\circ|H_1|n >< n|H_1|\bar{K}^\circ >}{M_K - E_n} \qquad (2.29)$$

where the first part, involving a local $\Delta S = 2$ Hamiltonian can be related to the box diagram shown in Fig. 10, and the second, dispersive part represents a time ordered product of two local $\Delta S = 1$ Hamiltonians. It has been customary to neglect the second part on the grounds that the different contributions enter with both positive and negative signs and hence will cancel out. The contribution of the box diagram,[37] $M_{12}^{\rm box}$, which in this approximation equals M_{12}, can be written as

$$M_{12}^{\rm box} \propto \sum_{ij}^{u,c,t} \lambda_i \lambda_j A_{ij} K_{12} \qquad (2.30)$$

where $\lambda_i = U_{is}U_{id}$ and $i = u, c, t$, and A_{ij} are well defined functions of the quark masses, generally calculated under the assumption that $m_q < m_W$. The matrix

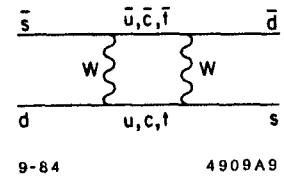

Figure 10 The box diagram used to calculate the short range approximation of $K^\circ - \bar{K}^\circ$ transition amplitude.

element of the $\Delta S = 2$ Hamiltonian is K_{12}. Thus it follows from the above that if

a) masses of all the quarks are known

b) one knows how to calculate K_{12} and

c) the neglect of the long distance contributions is valid,

then the measurement of the quantities expressible in terms of M_{12} will give us information about elements of matrix U. It is important to emphasize these limitations and approximations inherent in these analyses. In practice the approximation (c) is considered to be better for calculations of some parameters than for the others[38] (e.g. better for ϵ than for Δm). The uncertainty in K_{12} has been traditionally parametrized by[39]

$$K_{12} = B(K_{12})_{\text{vac}}$$

where $(K_{12})_{\text{vac}}$ is the vacuum saturation approximation of the matrix element, first used successfully by Gaillard and Lee[40] in predicting the value of the charmed quark mass and B is usually called the "bag factor" that can be calculated theoretically with a certain degree of reliability.[41] The mass of the top quark has been either used as a parameter in calculating other quantities or has been predicted from other measurements.[42]

It should be clear from the above that when the top quark mass is known and the value of B is well understood, quite accurate determination of the basic parameters should be possible. Furthermore, different pieces of the experimental input can then be required to be self-consistent. Any discrepancy would be an indication of the new physics that is not contained in the K-M matrix parameters.

Summary.

It is useful to put together all the results on the matrix elements of U. We first compile together the raw experimental data (we quote here magnitudes of the matrix elements):

$$U = \begin{pmatrix} .9733 \pm .0024 & .225 \pm .005 & < 0.01 \\ .24 \pm .03 & .82 \pm .13 & .058 \pm .009 \\ — & — & — \end{pmatrix} .$$

We can obtain more precise values by assuming the unitarity of the U matrix and utilizing the values of θ_1, θ_2, and θ_3 derived above to calculate the elements of U. This procedure then yields (again magnitudes only):

$$U = \begin{pmatrix} .9733 \pm .0024 & .225 \pm .005 & 0 - 0.01 \\ .225 \pm .006 & .971 \pm .002 & .058 \pm .009 \\ .013 \pm .009 & .058 \pm .009 & .998 \pm .001 \end{pmatrix} .$$

3. CP Violation

It has been 20 years almost to the day since the initial observation[43] of the CP violation through the decay $K_L^\circ \to \pi^+\pi^-$. The subsequent decade has witnessed a great flurry of activity which established the validity of CP violation interpretation as the explanation of the $K_L^\circ \to 2\pi$ decay, uncovered no evidence of CP violation in any other process, and led to quite accurate measurement of the fundamental CP violation parameters in the $K^\circ - \bar{K}^\circ$ system.[44]

The last few years have seen a revival of the interest in the CP violation question. Part of the stimulation came from the discovery of the heavy quark systems, which could provide a new laboratory for studying these phenomena. More important, however, has been the realization that more precise measurements of the CP violation parameters could shed light on any potential new physics since the prediction of these parameters from the K-M matrix phase δ appears possible.[45]

In this chapter we shall discuss the most recent work on the $K \to 2\pi$ decays, the prospects for improvement during the next few years, other CP violation experiments planned, and possibilities for observation of CP violation in the heavy quark systems. We shall begin by a brief summary of the formalism needed to describe the $K^\circ - \bar{K}^\circ$ system phenomena.

We define $|K_1^\circ>$ and $|K_2^\circ>$ as CP eigenstates, i.e.

$$|K_1^\circ>=\frac{1}{\sqrt{2}}\{|K^\circ>+|\bar{K}^\circ>\} \text{ and } |K_2^\circ>=\frac{1}{\sqrt{2}}\{|K^\circ>-|\bar{K}^\circ>\} \qquad (3.1)$$

and the actual states observed, $|K_S^\circ>$ and $|K_L^\circ>$ as

$$|K_S^\circ>=\frac{1}{\sqrt{1+|\epsilon|^2}}\{|K_1^\circ>+\epsilon|K_2^\circ>\} \text{ and } |K_L^\circ>=\frac{1}{\sqrt{1+|\epsilon|^2}}\{|K_2^\circ>+\epsilon|K_1^\circ>\}\ . \qquad (3.2)$$

From the above it is clear that ϵ represents the amount of the "wrong" CP state admixture and thus is a measure of the amount of CP violation in the $K^\circ - \bar{K}^\circ$ system.

One can also have CP violation directly in the $K \to 2\pi$ decay. This would be the result of a non-zero phase difference between A_0 and A_2, amplitudes leading to T=0 and T=2 2π states respectively. The standard convention is to define phases in such a way that A_0 is real. Then the direct CP violation parameter ϵ' can be expressed as

$$\epsilon' = \frac{1}{\sqrt{2}}\ \mathrm{Im}\left(\frac{A_2}{A_0}\right) e^{i(\delta_2-\delta_0+\pi/2)} \qquad (3.3)$$

where δ_2 and δ_0 are T=2 and T=0 $\pi\pi$ scattering phase shifts that can be measured in independent experiments.

It is also customary to define 2 other amplitudes that are linear combinations of ϵ and ϵ'. These are

$$\eta_{+-} \equiv \frac{A(K_L^\circ \to \pi^+\pi^-)}{A(K_S^\circ \to \pi^+\pi^-)} = \epsilon + \epsilon' \qquad \text{and} \qquad (3.4)$$

$$\eta_{oo} = \frac{A(K_L^\circ \to \pi^\circ\pi^\circ)}{A(K_S^\circ \to \pi^\circ\pi^\circ)} = \epsilon - 2\epsilon' \qquad . \qquad (3.5)$$

Finally, one should mention the types of experiments that can provide information on these parameters:

a) The rate of $K_L^\circ \to \pi^+\pi^-$ gives us $|\eta_{+-}|^2$.

b) The rate of $K_L^\circ \to \pi^\circ\pi^\circ$ gives us $|\eta_{oo}|^2$.

c) The charge asymmetry in semileptonic modes is proportional to Re ϵ .

d) Interference between coherent K_L° and K_S° beams decaying into $\pi^+\pi^-$ yields phase of η_{+-} .

e) Interference between coherent K_L° and K_S° beams decaying into $\pi^\circ\pi^\circ$ yields phase of η_{oo} .

The first 4 experiments provide by far the most precise information on the CP violation parameters. One should also mention an important relation that provides a constraint on arg ϵ, which follows from unitary arguments

$$\tan \arg \epsilon = \frac{2(m_L - m_S)}{\Gamma_S}\ . \qquad (3.6)$$

The experiments mentioned above are all consistent[44] with the superweak model of CP violation[46] which demands that ϵ' be zero to a very high level of precision. For ϵ they yield the value

$$\epsilon = (2.27 \pm 0.08) \times 10^{-3} e^{i(43.7\pm0.2)^\circ}\ .$$

In the last few years there has been a renewed interest in precision measurements of ϵ'/ϵ. Experimentally, this measurement is attractive since due to the relation

$$|\eta_{oo}|^2/|\eta_{+-}|^2 = 1 - 6\epsilon'/\epsilon \qquad (3.7)$$

which follows immediately from 3.4 and 3.5, a measurement of $|\eta_{oo}|^2/|\eta_{+-}|^2$ gives an amplified precision for ϵ'/ϵ by a factor of 6. Furthermore, this measurement

represents a ratio of two ratios, namely

$$\frac{|\eta_{oo}|^2}{|\eta_{+-}|^2} = \frac{\Gamma(K_L^\circ \to 2\pi^\circ)/\Gamma(K_S^\circ \to 2\pi^\circ)}{\Gamma(K_L^\circ \to \pi^+\pi^-)/\Gamma(K_S^\circ \to \pi^+\pi^-)} \tag{3.8}$$

and one can propose experimental arrangements where at least a part of the systematic errors will cancel out by virtue of this fact.

On the theoretical front, theoretical advances and improved experimental input on the K-M parameters allow one to predict the value of ϵ'/ϵ within the standard model.[47] The spirit of these calculations involve basically the assumptions that the ϵ parameter is dominated by the box diagram in Fig. 10, the ϵ' by the quark diagram illustrated in Fig. 11. Experimental results at variance with this theoretical prediction would have to imply additional sources of CP violation (for example more complicated Higgs structure or right-handed currents).

There have been recently two new experiments that try to extend our knowledge of ϵ'/ϵ ratio. The first one of these, Fermilab E617, is a Chicago-Saclay collaboration and its final results have been presented by Winstein at the 1984 neutrino conference in Dortmund[48] and by Cronin at this Institute.[49] The second one, BNL experiment 749, by a BNL-Yale collaboration, is still in the analysis stage and only preliminary results are available at this time.[50]

Because the new results are discussed in much more detail by Cronin[49] we limit ourselves here only to several brief comments. One could first make some general statements that apply to both of these experiments:

a) The goal is to measure ϵ'/ϵ to better than 1 % . Since ϵ itself is small, good control of backgrounds is mandatory.

b) By measuring either $2\pi^\circ$ and $\pi^+\pi^-$ modes simultaneously, or K_L° and K_S° decays simultaneously, some of the uncertainties drop out (e.g. dependance on flux measurement).

c) Since in either procedure one tries to utilize as much of the same apparatus as possible, lot of experimental uncertainties do cancel out and reliance on

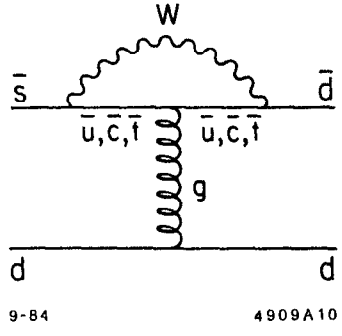

Figure 11 The diagram which gives a major contribution to the ϵ' parameter in the standard picture.

Monte Carlo is lessened.

The basic idea of the Chicago-Saclay experiment is indicated schematically[48] in Fig. 12. The modes $2\pi^\circ$ and $\pi^+\pi^-$ are observed at different times, but one does look simultaneously at 2 separate beams, a direct K_L° beam and a regenerated K_S° beam. The regenerator is moved from one beam to another on a pulse to pulse basis to average out any possible variations in the flux or differences in efficiencies in different areas of the apparatus. An identical regenerator is used for both $\pi^+\pi^-$ and $\pi^\circ\pi^\circ$ running. In the $2\pi^\circ$ mode, one of the γ rays is required to convert in a thin converter which also defines the end of the decay volume. Finally, the rate of decays in both beams is maintained roughly constant by another absorber in the regenerated beam that is located far upstream and moved from one beam to another in phase with the regenerator.

One has to be careful about several potential sources of trouble:

a) The 2 beams (K_L° and K_S°) have to be well separated so that after reconstruction one can identify unambiguously the source of each 2π event.

b) The resolutions for the $\pi^\circ\pi^\circ$ and $\pi^+\pi^-$ modes are inherently different, both in mass and also in direction. This has the effect that the background that has to be subtracted, both under the K° mass peak and under the 0° regenerated beam (due to incoherent regeneration) is larger for the $2\pi^\circ$ mode.

c) Because of lifetime differences, the longitudinal decay distribution of K_L° and K_S° will be different. This does introduce some dependance on Monte Carlo calculation of efficiency.

The extent of these potential difficulties and/or the level at which they have been taken care of by the experimenters is illustrated in Figs. 13 - 16. Figure 13 shows that the decays from the two beams are well separated in both the $2\pi^\circ$ and $\pi^+\pi^-$ modes. Figures 14 and 15 illustrate for 2 typical energies the effects of different resolution for the 2 decay modes. The background is essentially negligible for the $\pi^+\pi^-$ mode; for $2\pi^\circ$'s it is at the level of few percent both

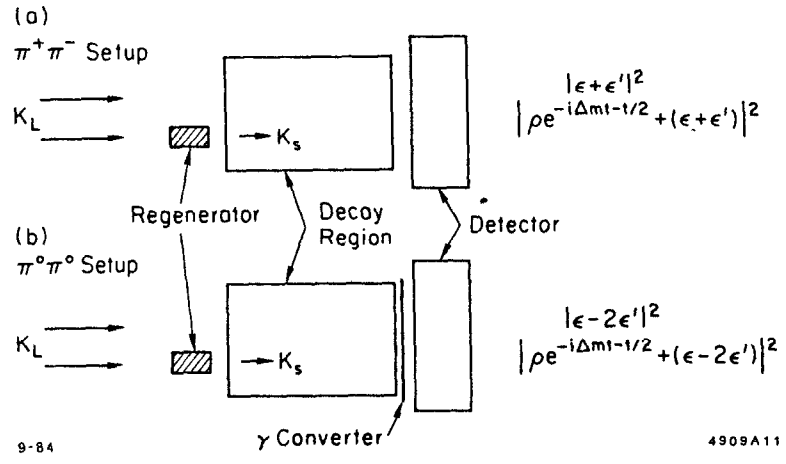

Figure 12 Schematic drawing of the basic idea of the Chicago-Saclay experiment. The amplitudes being measured in each beam are indicated at right.

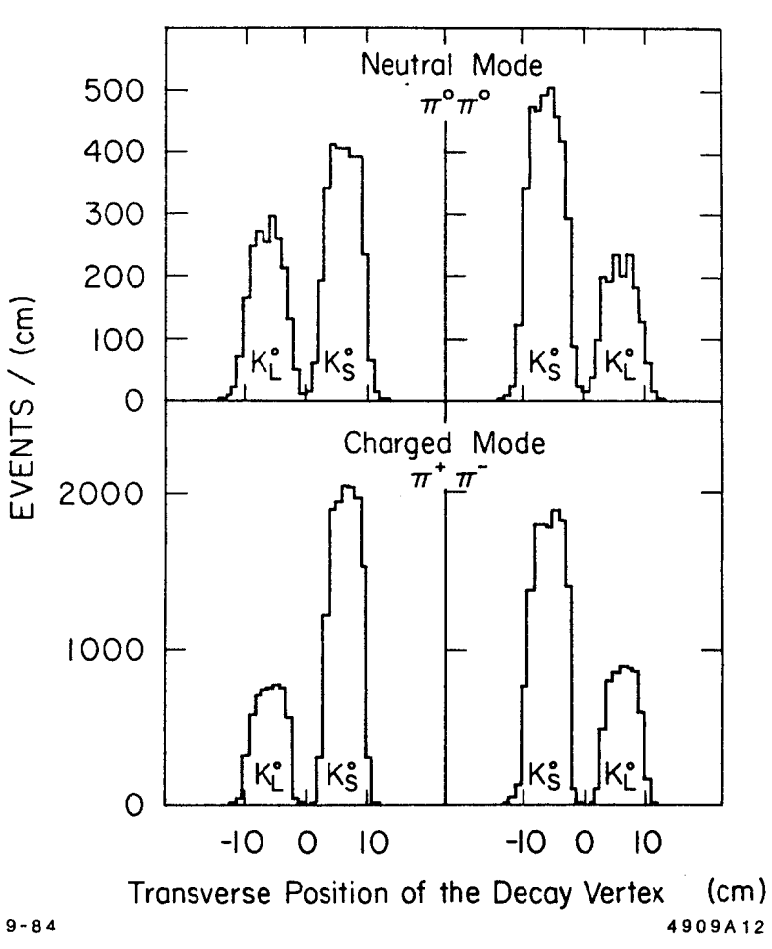

Figure 13 The transverse decay point distribution of the detected events in the Chicago-Saclay experiment.

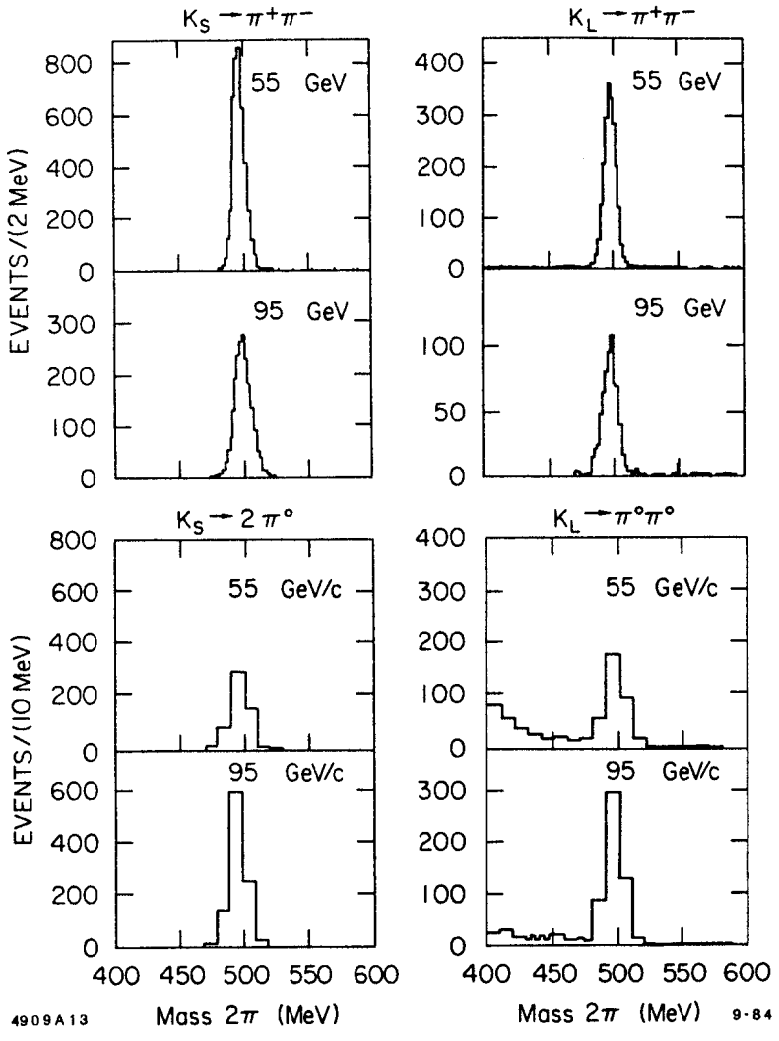

Figure 14 Distribution of the effective mass of the dipion system in the Chicago-Saclay experiment for 2 representative energies.

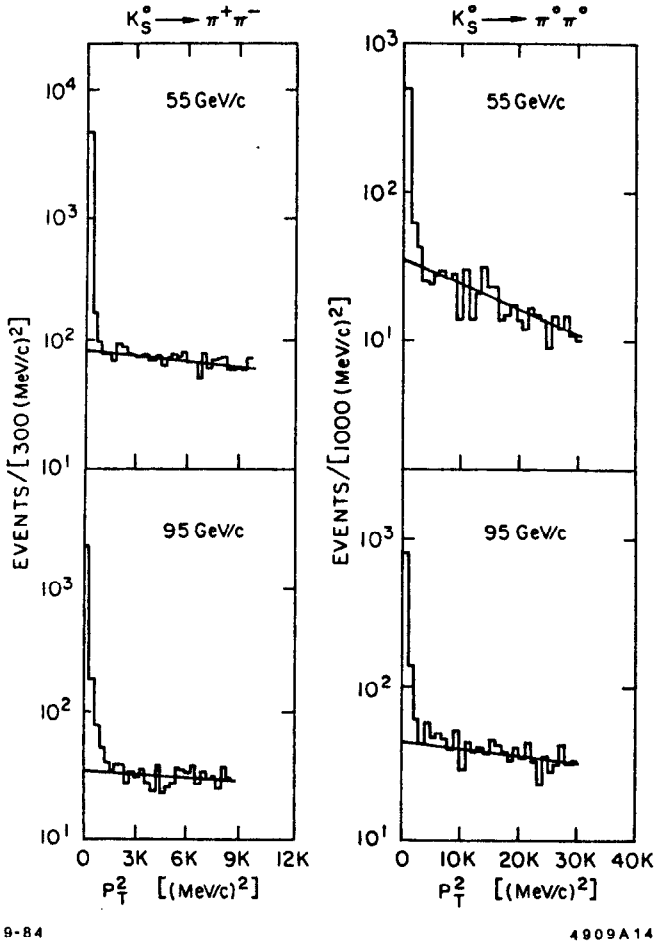

Figure 15. The P_T^2 distribution of the reconstructed 2π decay events in the regenerator beam for 2 representative energies (from the Chicago-Saclay experiment).

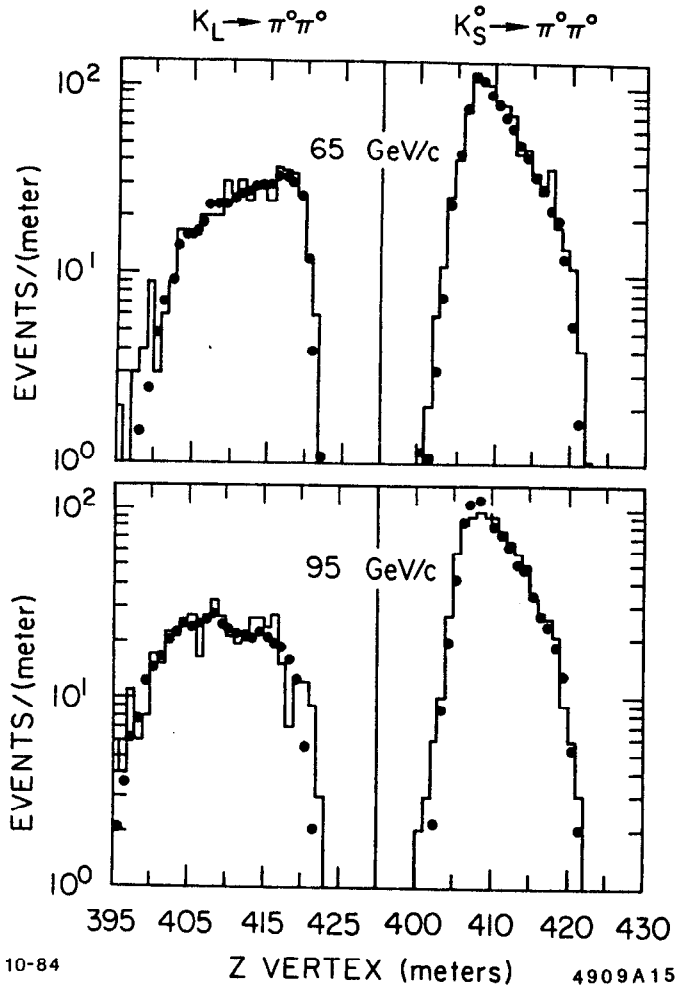

Figure 16 The z distribution of the reconstructed $\pi\pi$ decays of K_L° and K_S° for 2 representative energies (from the Chicago-Saclay experiment). The solid lines represent the data; the dots the Monte Carlo prediction.

under the mass peak and under the forward coherent regeneration peak. Finally the z dependance of the reconstructed decays and the Monte Carlo prediction is shown in Fig. 16.

In addition, various checks on the systematics have been performed by the group which give one an ability to estimate quantitatively the magnitude of the systematic errors. The final result is

$$\epsilon'/\epsilon = -0.0046 \pm 0.0053(\text{stat}) \pm 0.0024\ (\text{syst})\ . \qquad (3.9)$$

The BNL experiment takes a different approach and collects $\pi^+\pi^-$ and $\pi^\circ\pi^\circ$ events simultaneously. The datataking alternates between K_L° and K_S°, the latter being generated by moving an 80 cm carbon regenerator into the beam. The highly preliminary result quoted by Winstein[48] at the Dortmund Conference is

$$\epsilon'/\epsilon = -0.0027 \pm 0.0061\ (\text{stat})\ . \qquad (3.10)$$

The systematic errors are still in the process of being calculated.

These experimental numbers should be compared with the most recent theoretical calculations[47] of lower bounds on ϵ'/ϵ displayed in Fig. 17. The important point to be made here is that the sign of ϵ'/ϵ is predicted by these calculations and thus there appears to be $\sim 3\sigma$ discrepancy with the experiment.

In light of these results there is a considerable interest in improving the ϵ'/ϵ measurement. There are at present plans for two major new experiments with that goal in mind. The first one, a Chicago-Fermilab-Princeton-Saclay[51] experiment at Fermilab (E731) uses similar techniques as its predecessor, E617. It does, however, take advantage of several improvements, namely better duty cycle at the Tevatron, new and improved beam line, better acceptance, and an improved detector. A datataking rate some 30 times higher than what was achieved previously is anticipated.

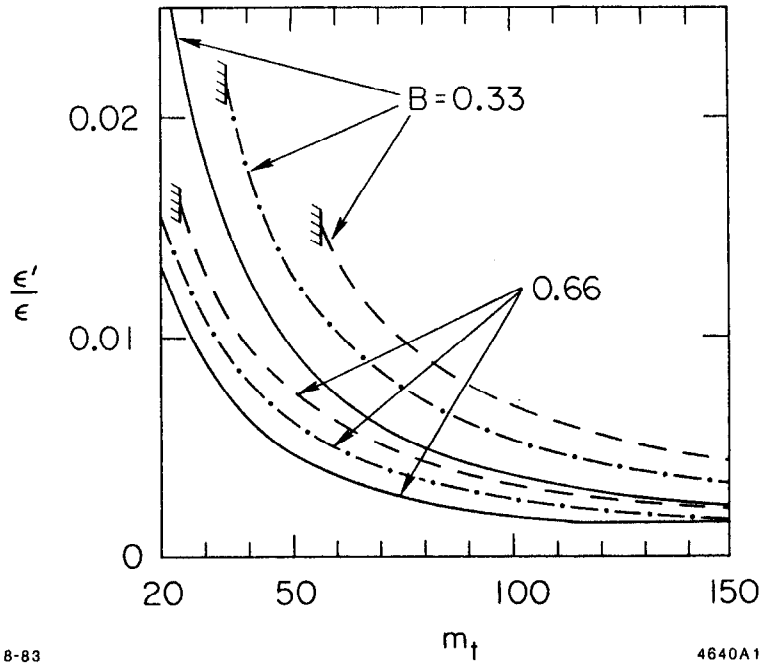

Figure 17 Lower bounds on ϵ'/ϵ as calculated by Gilman and Hagelin. Two different values (0.33 and 0.66) of the bag factor B are used, and three different b quark lifetimes: 0.6 psec (solid line), 0.9 psec (dash-dot) and 1.2 psec (dashed line).

A quite different approach has been proposed at CERN[52] by the CERN-Pisa-Dortmund-Orsay-Siegen-Edinburgh collaboration. The plan is to take $\pi^+\pi^-$ and $\pi^\circ\pi^\circ$ data simultaneously like in the BNL experiment. There are several important and ambitious innovations. The K_S° beam is obtained not by regeneration but by targeting the primary proton beam near the detector. This K_S° target is movable, the idea being to vary the targeting point along the z direction through the decay volume during the experiment. Thus the K_S° and K_L° z decay distributions should be very similar. The experiment uses no converter and no magnet and thus achieves very high acceptance. The background to $\pi^+\pi^-$ mode is suppressed by good particle identification, good angular measurements, and use of a hadron calorimeter to measure pion energies. A liquid argon detector is used to measure γ-ray energies and impact points.

These experiments strive for accuracy in the ϵ'/ϵ ratio in the neighborhood of 10^{-3}. The first results should be available in three years.

I would like to summarize next some of the other experiments on CP violation, either performed in the recent past or planned for the near future, that attempt to extend our knowledge of that phenomenon.

a) The CP-nonconserving polarization of μ^+ from the decay $K^+ \to \pi^\circ\mu^+\nu$, normal to the decay plane, has been measured recently by the Yale-BNL group.[53] For events satisfying $\vec{P}_\mu \cdot \vec{P}_\nu \approx 0$ they obtain a value

$$P = (-3.0 \pm 4.7) \times 10^{-3} .$$

This result, especially when coupled with the earlier companion work on μ polarization from K_L° decay,[54] precludes unusually large contributions to CP violation from the Higgs sector.

b) There are tentative plans at CERN to look for a difference in the branching ratios for $K^\circ \to 2\pi^\circ$ and $\bar{K}^\circ \to 2\pi^\circ$, which is allowed if CP invariance is violated. The proposed letter of intent[55] plans to exploit the fact that at LEAR one has a very good source of tagged K° and $\bar{K}^\circ$ decays resulting from the channels

$$\bar{p}p \to K^+\pi^-\bar{K}^\circ \text{ or } K^-\pi^+K^\circ .$$

The authors propose to look at about 2×10^8 $2\pi^\circ$ decays which would yield sensitivity on the ϵ'/ϵ ratio of about 3×10^{-3}.

c) A search for CP violation in a new channel is at present under way in a new experiment at Fermilab[56] by a Rutgers-Wisconsin-Michigan-Minnesota collaboration. The experiment will measure the rate for the decay $K^\circ \to \pi^+\pi^-\pi^\circ$ as a function of the proper time in the K° rest frame. The major contribution to this decay will come from the decay of K_L°, but this rate will be modulated at a level of about 10^{-3} by simultaneous presence of a CP violating amplitude due to $K_S^\circ \to \pi^+\pi^-\pi^\circ$ decay. The interference of this small amplitude will give some time dependance to this rate. If one defines

$$\eta_{+-\circ} \equiv \frac{A(K_S^\circ \to \pi^+\pi^-\pi^\circ)}{A(K_L^\circ \to \pi^+\pi^-\pi\circ)}$$

one expects a precision on $\eta_{+-\circ}/\epsilon$ of about 0.25. This can be compared with the present limit of

$$|\frac{\eta_{+-\circ}}{\epsilon}| < 150 \quad .$$

d) A recently approved experiment at BNL, E791, proposes[57] to look for CP violating mode

$$K_L^\circ \to \pi^\circ e^+e^- \quad .$$

The single γ or Z° diagram which contributes to this decay is CP violating and its contribution to the branching ratio can be estimated from the rate of $K^+ \to \pi^+e^+e^-$ decay if the decay occurs solely through the K_1° admixture in the K_L° state. This rate would involve CP violation in the mass matrix and thus be proportional to $|\epsilon|^2$. The estimated branching ratio from this contribution is 6×10^{-12}.

On the other hand there can also be "direct" CP violation in this decay mode which has been estimated[58] to generate a branching ratio at the level of 3×10^{-11}. Thus the situation could be quite different here than in the case of $K \to 2\pi$ decay where the "direct" CP violation amplitude ϵ' is $\lesssim 10^{-2}\epsilon$. The proposed experiment hopes to achieve sensitivity to be able to see the "direct" CP violation.

e) The same experiment[57] plans also to look for the longitudinal polarization of the μ^+ in the decay

$$K_L^\circ \to \mu^+\mu^- \quad .$$

Two amplitudes can contribute to this process[59]:

$a \equiv {}^1S_\circ$ which is P and CP conserving, and

$b \equiv {}^3P_\circ$ which is P and CP violating.

Since a longitudinal polarization of μ^+ violates parity, both of the above amplitudes must be present if that polarization is non-zero, and hence CP must also be violated. In the standard picture, the polarization is expected to vanish at the level of 10^{-3}, so a significant non-zero polarization observed must be evidence of new physics contributing to the process.

The decay rate can be expressed as

$$\Gamma \; \alpha \; (|a|^2 + \nu^2|b|^2) \tag{3.11}$$

and the polarization P as

$$P = \frac{2\nu(ba^*)}{|a|^2 + \nu^2|b|^2}$$

where ν is a phase space factor that is numerically ≈ 0.91.

The important point here is that considerable theoretical uncertainties exist in calculating the rate for $K_L^\circ \to \mu^+\mu^-$. The pure weak interaction quark diagrams are not able to account for a significant fraction of the remaining $K_L^\circ \to \mu^+\mu^-$ amplitude after the contribution of the 2γ intermediate state is subtracted out.[60] Thus from the rate measurement alone, one cannot exclude a significant CP violating amplitude b and a polarization close to 100% cannot be ruled out. Furthermore, there is no experimental information at the present time on the polarization in this process.

f) Finally, one should mention the electric dipole moment of the neutron as a potential testing ground of the different models of T violation (and hence also CP violation within the framework of CPT invariance). The present upper limit,[61] quoted as

$$d_n = (0.4 \pm 1.5) \times 10^{-24} e \; cm$$

is already restricting some of the more exotic models of CP violation, but still about 6 orders of magnitude away from the prediction of the standard model.[62] Thus even with the experimental improvements anticipated in the near future, the experimental accuracy will not be sufficient to expect a non-zero answer if the K-M phase is the sole source of CP violation.

Heavy quark systems.

We conclude this chapter with a brief discussion of potential CP violation effects in the heavy quark neutral states. The uniqueness of the $K^\circ - \bar{K}^\circ$ system lies in the fact that the only quantum number distinguishing K° from its antiparticle is strangeness, i.e., a quantity that is not absolutely conserved. The heavy quark neutral states, $D^\circ - \bar{D}^\circ$, $B^\circ - \bar{B}^\circ$, and $T^\circ - \bar{T}^\circ$ duplicate these conditions insofar as they also differ by a flavor quantum number that is violated by weak interactions. Hence we should ask to what extent the mixing phenomena and mass matrix CP violation, seen in the $K^\circ - \bar{K}^\circ$ system, can be expected to be reproduced also in these heavier neutral systems.

We should first point out that the $B^\circ - \bar{B}^\circ$ system is the most favorable one of the three for the observation of the mixing phenomena.[63] The two heavier

quark doublets can be generically represented as

$$\begin{pmatrix} H \\ L \end{pmatrix} \equiv \begin{pmatrix} c \\ s \end{pmatrix} \text{ or } \begin{pmatrix} t \\ b \end{pmatrix} \quad .$$

In general $\Gamma(L) < \Gamma(H)$ because of enhanced phase space for heavy quark (H) decays and even more importantly because the light quark (L) has to decay out of its doublet and hence is Cabibbo suppressed. In addition, if the mass difference is dominated by the box diagrams we would expect

$$(\Delta m)_L \; \alpha \; M_H^2 \; ,$$
$$(\Delta m)_H \; \alpha \; M_L^2$$

and hence

$$(\Delta m)_L > (\Delta m)_H \; .$$

We shall have large mixing if the mass difference is large enough so that the phase between Q_S and Q_L (Q is used as a generic name for a neutral system, e.g. K_S , D_S , etc.) can change appreciably during an average lifetime of that system. Thus $(\Delta m/\Gamma)$ is a measure of the size of that mixing and from the arguments given above we expect that

$$(\frac{\Delta m}{\Gamma})_L > (\frac{\Delta m}{\Gamma})_H \; .$$

Hence the K and the B systems should exhibit the greatest mixing effects. Parenthetically, we should mention that experimentally[64] the $D^\circ - \bar{D}^\circ$ mixing is limited to less than 4%.

In the remainder of this chapter we shall comment very briefly on some of the theoretical calculations regarding the possible mixing and CP violation effects in the $B^\circ - \bar{B}^\circ$ system. One measure of mixing is the parameter r defined as

$$r \equiv \frac{\Gamma(B^\circ \to \ell^+)}{\Gamma(B^\circ \to \ell^-)} \quad .$$

The physical meaning of r is the relative probability that a particle which starts out as a B° changes into a $\bar{B}^\circ$, as evidenced by its decay into the "wrong" sign lepton. It goes without saying, that the leptons discussed above refer to primary leptons only, i.e. do not include secondary leptons from intermediate charm particles. One can show[65] that r is given by

$$r = \left|\frac{1-\epsilon_B}{1+\epsilon_B}\right|^2 \frac{(\Delta m)^2 + \frac{1}{4}(\Delta\Gamma)^2}{2\Gamma^2 + (\Delta m)^2 - 1/4(\Delta\Gamma)^2}$$

where ϵ_B is the ϵ in the B system (parameter characterizing CP violation in the mass matrix) and $\Delta\Gamma \equiv \Gamma_S - \Gamma_L$. Thus we see that r can be non-zero either by virtue of $\Delta m \neq 0$, i.e. mixing due to phase difference or $\Delta\Gamma \neq 0$, which gives rise to mixing by virtue of one linear combination of B's decaying away faster than the other. Both of those terms are appreciable in the $K^\circ - \bar{K}^\circ$ system. For the B's we expect $\Delta m >> \Delta\Gamma$ since the states that couple to both B° and $\bar{B}^\circ$ and hence give rise to $\Delta\Gamma$, couple to them relatively weakly[66] in contrast to the situation with the 2π state in $K^\circ\bar{K}^\circ$ system.

The CP violation arises if r and $\bar{r}$ are different. In that case the lepton charge asymmetry, which is a true measure of observability of CP violation in the $B^\circ - \bar{B}^\circ$ system is non-zero and is given by

$$A_\ell \equiv \frac{N(\ell^+) - N(\ell^-)}{N(\ell^+) + N(\ell^-)} = \frac{r - \bar{r}}{2 + r + \bar{r}} \quad .$$

Clearly mixing is essential if CP violation effects are to be observed.

The $B^\circ - \bar{B}^\circ$ mixing will also lead to like-sign primary dileptons in e^+e^- annihilations. Again we define a mixing parameter R

$$R = \frac{N^{++} + N^{--}}{N^{++} + N^{--} + N^{+-}} = \frac{r + \bar{r}}{r + \bar{r} + r\bar{r} + 1}$$

and a CP violation parameter

$$a \equiv \frac{N^{++} - N^{--}}{N^{++} + N^{--}} = \frac{r - \bar{r}}{r + \bar{r}} \; .$$

Because the $B^\circ\bar{B}^\circ$ pair is produced in a coherent state, the effects of Bose statistics have to be included and the magnitude of R will depend on whether the $B\bar{B}$ is in a relative even or odd angular momentum state.

The magnitude of these parameters have been estimated recently by a number of authors.[35,47,63,65,66] The calculations can be made for both the $B_d(b\bar{d})$ and $B_s(b\bar{s})$ states and they all depend on the values of the K-M mixing angles and the K-M phase. Using the experimental input on these parameters, one reaches the general conclusion that the mixing parameter can be quite large for B_s but the CP violation parameter a is very small. For B_d, the CP violation parameter is somewhat larger but the mixing effects are correspondingly smaller. The net result is that the CP violation effects due to mass matrix-term will probably be unobservable in the $B-\bar{B}$ system. This situation is summarized in Fig. 18 taken from Ref. 35.

Another possible source of CP violation in the $B^\circ - \bar{B}^\circ$ system would be CP violation in the decay process itself. This could occur in those final states which can be fed by either B° or $\bar{B}^\circ$, e.g. $\psi + K_S^\circ + \pi$'s . CP violation effects would exhibit itself in a lepton asymmetry in association with such exclusive states. The calculations performed indicate that such asymmetries could be appreciable[63] but the statistics will be much more limited because of the requirement to observe an exclusive state.

4. RARE DECAYS

The last several years have seen a renewal of interest in rare decays, more specifically in experimental searches for decays of μ's, K^+'s and K_L°'s which are forbidden in the standard model because they violate one or more conservation laws. These searches are driven in part by the theoretical arguments that new physics might indeed require processes that do not observe these symmetry laws. But they are also fueled by improvement in experimental techniques which make feasible exploration of new domains. In general, most of the ideas for new physics require existence of some new processes and very frequently different schemes make quite different quantitative predictions. Thus experiments on rare decays

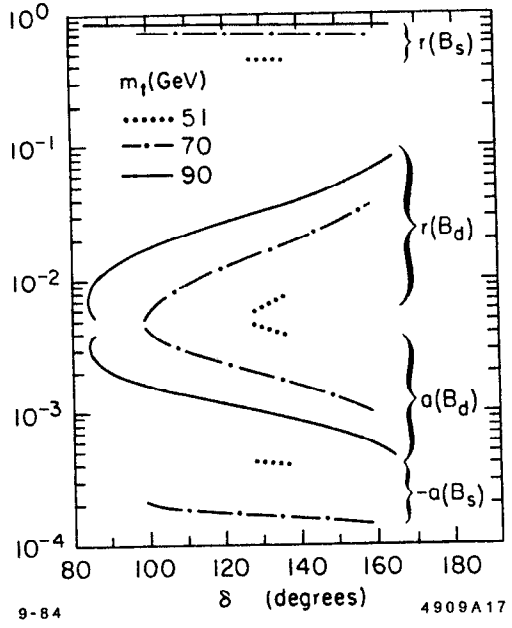

Figure 18 The $B^\circ - \bar{B}^\circ$ mixing parameter r and the CP violation parameter a calculated for B_s and B_d as a function of the top quark mass and the K-M phase δ. The input data uses 1 psec as the b quark lifetime. The allowable range of δ (indicated) is obtained by fitting the ϵ parameter to the box diagram calculation with B = 0.33 (from Ref. 35).

are, at least in principle, capable of narrowing down the spectrum of viable new models.

A useful phenomenological classification of different processes has been provided by Cahn and Harari[67] who utilize the fact that quarks and leptons appear to come in three generations: (u, d, ν_e, e) , (c, s, ν_μ, μ) , and (t, b, ν_τ, τ) each one classified by a generation number G: G1 for the first one, G2 for the 2nd one, etc. with G1 - G2 $\equiv 1$. In this scheme different diagrams can be classified by their ΔG value. In addition, the reactions can be diagonal or non-diagonal, depending whether the reaction is purely leptonic or hadronic or whether it is mixed. This scheme is illustrated in Fig. 19 which shows the diagrams and Cahn-Harari classification for several processes of interest.

The symmetry violating processes could depend on ΔG and thus different reactions could proceed at quite different rates. But there are other possible relevant factors. Thus if the mediating interaction is of the vector nature, the process $K_L^\circ \to e^\pm \mu^\mp$ will not occur. The same is true for $K^+ \to \pi^+ e^- \mu^+$ if the relevant interaction is axial. Finally the reaction $K^+ \to \pi^+ \nu\nu$ is allowed in the standard model with a reasonably well defined rate. But new interactions or phenomena could enhance it or other effects (like large ν_τ mass) could suppress it. The main point of this discussion is that there exists a great wealth of different possibilities in different models and only experiments can resolve these issues.

In contrast to the new K decay experiments that are not scheduled to start taking data for another year or so, the muon rare decay program has been pursued vigorously during the last decade. The main lepton number violating channels that have been studied are:

$$\mu^+ \to e^+ \gamma \,,$$
$$\mu^+ \to e^+ e^+ e^- \,,$$
$$\mu^- N \to e^- N \,,$$
$$\text{and} \quad \mu^+ \to e^+ \gamma\gamma \,.$$

No positive evidence for any of these processes has been found but the great deal

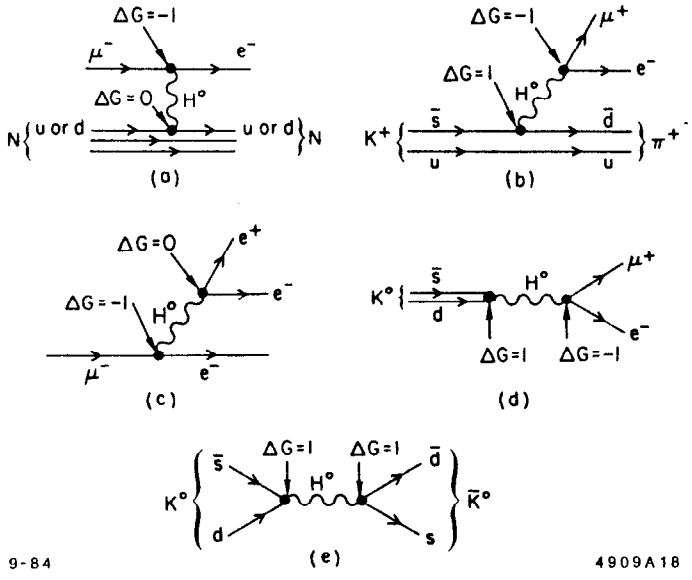

Figure 19 (a) The μ conversion to e by nuclear capture, $\Delta G = -1$;

(b) The $K^+ \to \pi^+ \mu^+ e^-$ decay, $\Delta G = 0$;

(c) The diagonal process $\mu \to 3e$, $\Delta G = -1$;

(d) The non-diagonal, $\Delta G = 0$, $K_L^\circ \to \mu e$ decay; and

(e) The $\Delta G = 2$ diagonal interaction which can contribute to $K_L^\circ - K_S^\circ$ mass difference.

of progress that has been accomplished during the last 40 years in this field is illustrated in Fig. 20. The branching ratio for the μ^- capture process is defined as its relative rate with respect to the standard μ^- capture reaction, i.e.,

$$\mu^- N \rightarrow \nu_\mu N'.$$

At present there are extensive experimental programs at the three pion and muon factories: LAMPF, SIN, and TRIUMF on the above 3 decay modes and the forbidden conversion process. The present and anticipated branching ratio sensitivity for both μ and K channels is indicated in Fig. 21 where the different processes are explicitly tagged by their ΔG value.

I would like next to discuss several of the planned experimental programs on the rare K decays. They are all scheduled to run at the BNL AGS and can be expected to start yielding results in a period of 1 to 3 years. The first process is the channel

$$K^+ \rightarrow \pi^+ \nu \bar{\nu}$$

or, more correctly, since ν's are not observed

$$K^+ \rightarrow \pi^+ + \text{ nothing visible}.$$

In the standard model, this process is allowed in second order and proceeds via a modified box diagram illustrated in Fig. 22, which effectively turns the $\bar{s}$ quark into the $\bar{d}$ quark. The u quark acts as a spectator. In addition there is an induced Z° contribution, also illustrated in Fig. 22. The strength of these contributions can be calculated and the results of the most recent calculations[47] are shown in Fig. 23 as a function of the top quark mass.

Assuming high experimental sensitivity and a narrowing of the theoretical uncertainties the measurement of this rate could shed light on the number of lepton generations within the framework of the standard picture. The rate for

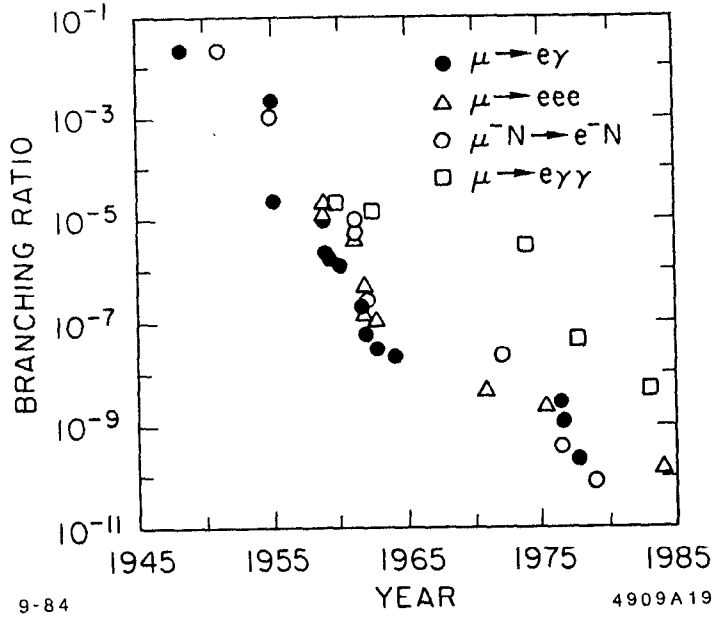

Figure 20 Upper limits for separate lepton number violating processes as a function of time.

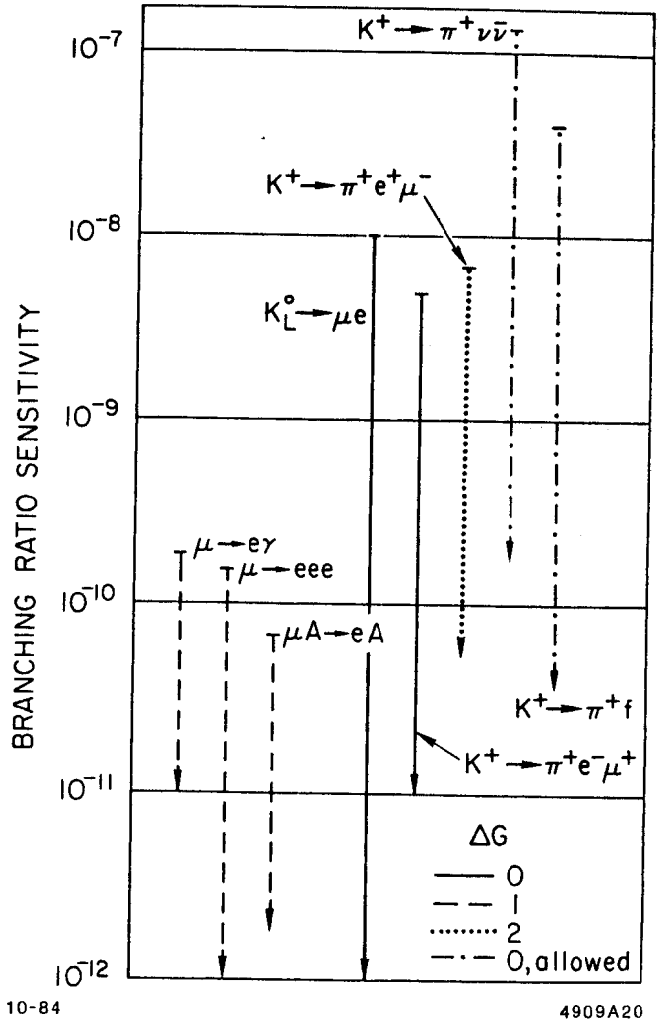

Figure 21 Present and anticipated branching ratio sensitivities for various rare decays.

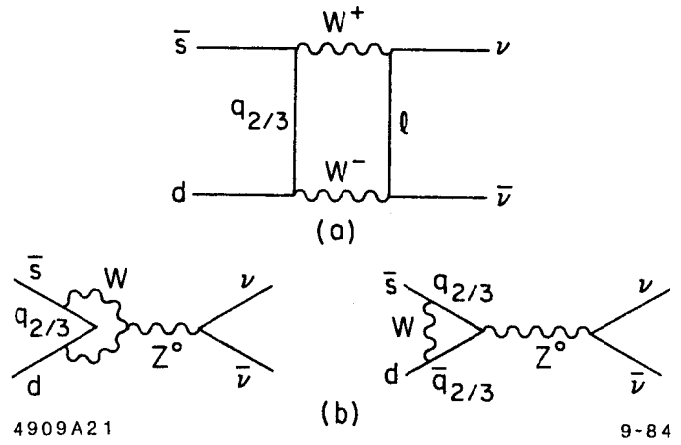

Figure 22 The box diagram contribution to the process $K^+ \to \pi^+ \nu\bar{\nu}$ (a) as well as some of the diagrams contributing to the induced Z° process (b).

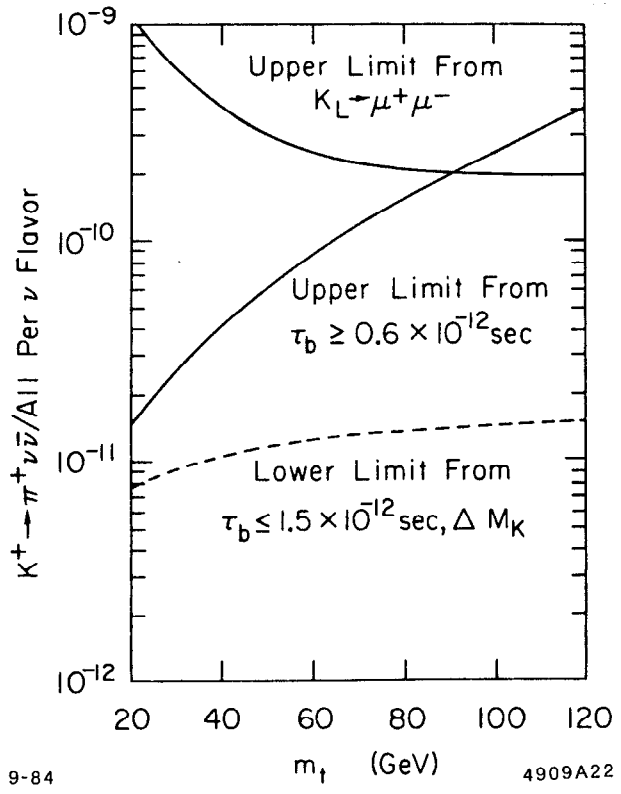

Figure 23 Theoretical limits on the branching ratio $K^+ \to \pi^+ \nu_i \bar{\nu}_i$ (for each neutrino flavor) as a function of the top quark mass.

each generation has some dependance on the lepton mass(es) in the next generation(s) due to the explicit form of the box diagram,[68] but this dependance is weak if $m_\ell << m_W$. In addition if the ν_τ has an appreciable mass (several MeV or more) the total rate and the π^+ spectrum would be affected.

Probably more interesting is the possibility that there is new physics which contributes to this process. One is the existence of new massless and non-interacting particles, like some of the "*nuinos*" postulated within the framework of the supersymmetry models. Another new physics possibility is the existence of a new massless Goldstone boson postulated by Wilczek[69] to explain the lepton and quark masses. This new postulated particle, commonly called familon and denoted by f would exhibit itself in the process under discussion as a decay mode

$$K^+ \to \pi^+ + f$$

and would result in a peak in π^+ energy spectrum.

Recently an experiment[70] has been proposed at Brookhaven to investigate this process down to the level of 2×10^{-10}, about three orders of magnitude better than the present upper limit.[71] The main experimental problems center around a clean identification of π^+ and total hermiticity, i.e. ability to detect all the known particles except neutrinos over the full 4π solid angle. The proposed experiment achieves the former, i.e. a good $\pi - \mu$ separation by combining range and curvature information for the momentum measurement and insisting on observation of the full $\pi^+ \to \mu^+ \to e^+$ decay chain. The apparatus looks very much like a modest colliding beam detector except that it is totally enclosed by live detectors. The entrance end is capped by a BaFl scintillator which serves simultaneously to degrade the K^+ beam to a low energy and to detect any decay particles heading in that direction. A fully live and finely segmented target is used to suppress various second order processes that could simulate the decay in question.

Figure 24 shows the range distribution of π^+ and μ^+ from the more frequent K^+ decays at rest. A ± 1 cm range resolution is folded in. As can be seen from the figure, approximately 20% of the π^+ from $K^+ \to \pi^+\nu\bar{\nu}$ lie beyond the $\pi^+\pi^\circ$ peak. Thus unambiguous identification of π^+ with a range above that value would by itself constitute a signature of $K^+ \to \pi^+\nu\bar{\nu}$. Clearly the acceptance for $K^+ \to \pi^+ + f$ is complete in π^+ momentum space.

The experiment is also sensitive to other rare decay modes like $K^+ \to \pi^+e^+\mu^-$ (a $\Delta G = 2$ transition) and $K^+ \to \pi^+\gamma\gamma$. In addition, the decay $K^+ \to \pi^\circ\pi^+$ can be used as a source of tagged π°'s and provide a mechanism to search for $\pi^\circ \to$ nothing observed.

An ongoing parallel effort is an experiment[72] to measure the decay mode

$$K^+ \to \pi^+e^-\mu^+$$

down to a level of 10^{-11}, roughly a factor of 500 better than the existing present limit.[73] Experimentally, the advantage here lies in the fact that the initial and all final state particles are charged, facilitating the overall kinematic constraint of energy and momentum conservation. The main experimental challenge lies in the particle identification since the main background appears to be due to the reaction

$$K^+ \to \pi^+\pi^+\pi^-$$

followed by the $\pi^+ \to \mu^+\nu$ decay and misidentification of the π^- as an electron. Specifically a π^-/e^- rejection of 10^{-7} is required which is obtained by a pair of gas Čerenkov counters and a lead-scintillator shower detector. The plan view of the apparatus is shown in Fig. 25. The Čerenkov counter in the muon arm is used to suppress the background from the decay $K^+ \to \pi^+\pi^\circ$ with a subsequent decay $\pi^\circ \to e^+e^-\gamma$.

This experiment will also obtain several thousand of the examples of the decay $K^+ \to \pi^+e^+e^-$. This final state will allow one to search for states with mass

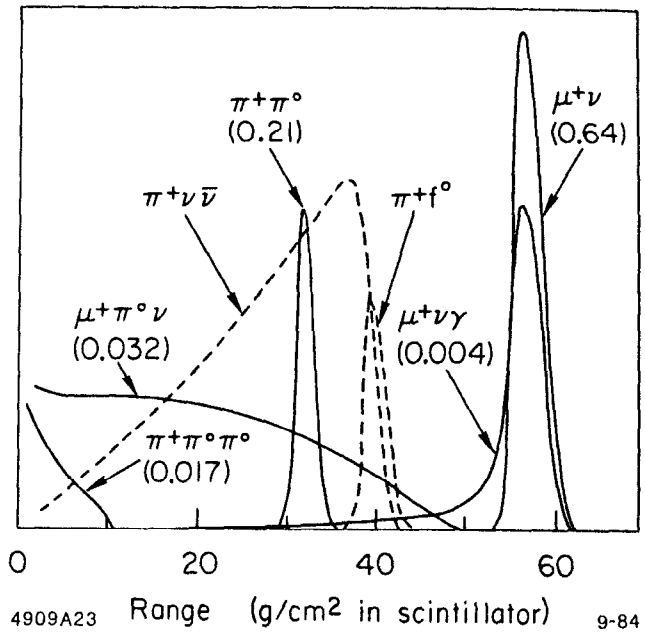

Figure 24 Range distribution in scintillator for π^+ and μ^+ from the known K^+ decays and from the rare decays searched for. The branching ratios of the known decays are indicated in parentheses.

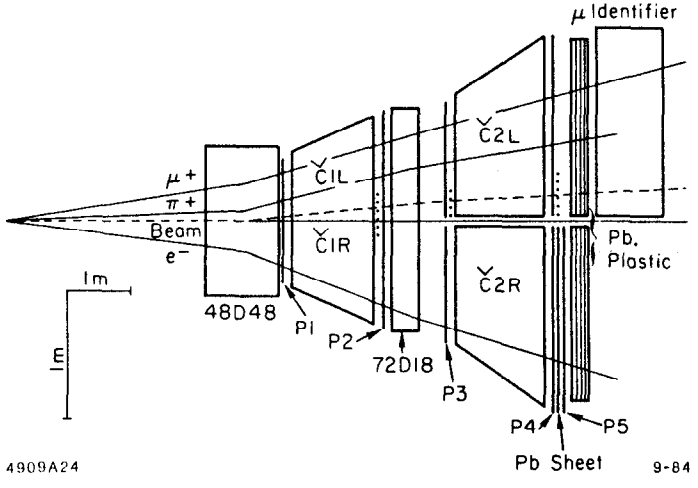

Figure 25 Plan view of the detection apparatus for the experiment searching for the decay mode $K^+ \to \pi^+\mu^+e^-$.

between 140 and 340 MeV decaying into e^+e^- and will provide an improvement of our knowledge of the branching ratio $\pi^\circ \to e^+e^-$.

The decay $K_L^\circ \to \mu^\pm e^\mp$ is being looked for by 2 experiments at BNL.[74,57] The decay $K_L^\circ \to \mu e$ is also a lepton number violating process but the same branching ratio sensitivity as in the $K^+ \to \pi\mu e$ decay translates into a limit on the strength of the interaction almost 2 orders of magnitude better. This is because of the longer K_L° lifetime and larger phase space for the 2 body final state. The main background comes from the relatively copious $K_L^\circ \to \pi e\nu$ decay followed by the $\pi \to \mu\nu$ decay. If the 2 ν's carry off minimum amounts of energy in the lab, this process can closely simulate the decay mode of interest. This background is especially pernicious if the $\pi \to \mu\nu$ decay occurs in the analyzing magnet since the decay kink in the right direction can increase the muon apparent momentum and thus allow the event to come even closer to faking the $K_L^\circ \to \mu e$ decay.

The schematic views of the Yale-BNL experiment are shown in Fig. 26. The electrons are identified by the Čerenkov counter and a lead glass wall (the particle identification is not extremely crucial in this experiment). Muon range is measured in an iron range stack to provide additional redundancy in μ energy measurement. Mini-drift chambers are used to obtain good position measurement, which is especially crucial in this kind of an experiment.

The Monte Carlo calculations indicate that the background begins to come in at a level of about 10^{-11}. The experiment is designed to achieve at least a 10^{-10} branching ratio sensitivity which would represent almost a two order of magnitude improvement over the present limit. In addition, a comparable sensitivity exists for the decay mode $K_L^\circ \to e^+e^-$. Since the standard model prediction for this decay is only about 10^{-13} (branching ratio) because of helicity suppression, new physics could manifest itself in that decay mode.

An even more ambitious proposal[57] has been put forth recently. It attempts to push this limit down to a branching ratio level of 10^{-12}. To achieve this, very high intensities are required (10^{13} protons/pulse) and one has to be able

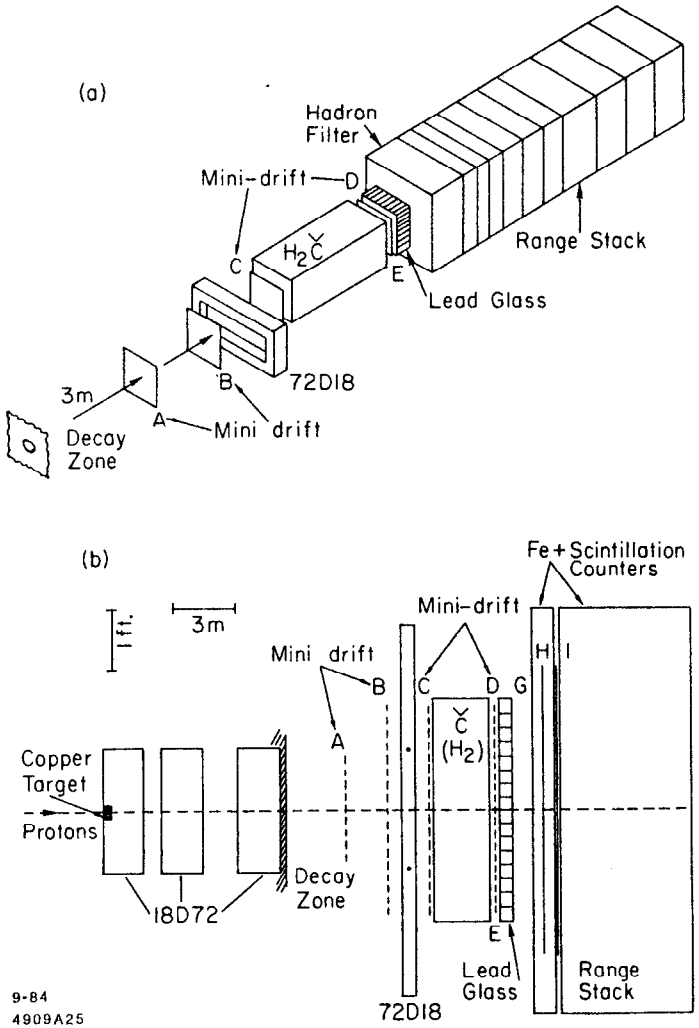

Figure 26 Schematic views, exploded (a) and plan (b) of the Yale-BNL detector used in E780.

to live in a flux of $6 \times 10^8 K_L^\circ$/pulse. The neutral beam has to be transported through the apparatus in a vacuum pipe, necessitating very good collimation upstream. To reduce the background below 10^{-12}, two independent spectrometers are used allowing one to perform two independent momentum measurements on both charged particles. In addition, the muon range stack is finely segmented to obtain an additional μ momentum measurement limited only by range straggling. The schematic of the proposed detector is shown in Fig. 27.

In addition to the comparable sensitivity for the decay mode $K_L^\circ \to e^+e^-$, the experiment also looks at the CP forbidden decay mode $K_L^\circ \to \pi^\circ e^+e^-$ and measures the polarization of μ^+ in the decay $K_L^\circ \to \mu^+\mu^-$. The physics interest in these processes has been discussed already in the chapter on CP violation. In addition, one should be also sensitive to $K_L^\circ \to \pi^\circ e\mu$, $e^+e^-\gamma$, $\mu^+\mu^-\gamma$, $4e$, $2\mu 2e$, etc.

I would like to end this chapter by emphasizing that if these proposed experiments can reach the advertised sensitivities, then they will be sensitive to propagators on the multi-TeV mass scale. In general, if these decays are mediated by some heavy object of mass m_H , then the rate for that decay is proportional to $f^2 f'^2 m_H^{-4}$ where the f's represent the coupling of the intermediate object at the 2 fermion vertices (see Fig. 28). Thus we have the simple relationship

$$\frac{\Gamma(K_L^\circ \to \mu e)}{\Gamma(K^+ \to \mu^+\nu)} \approx \left(\frac{ff'/m_H^2}{\sin\theta_c g^2/m_W^2}\right)^2$$

where g is the weak coupling constant and θ_c is the Cabibbo angle. Putting in known quantities we obtain:

$$m_H \approx 20\text{TeV}\left(\frac{10^{-8}}{BR(K_L^\circ \to \mu e)}\right)^{1/4}\left(\frac{ff'}{g^2}\right)^{1/2} .$$

Thus if $ff' \approx g^2$ and a $BR(K_L^\circ \to \mu e)$ of 10^{-12} can be reached, objects up to the masses of 200 TeV can be probed by those experiments.

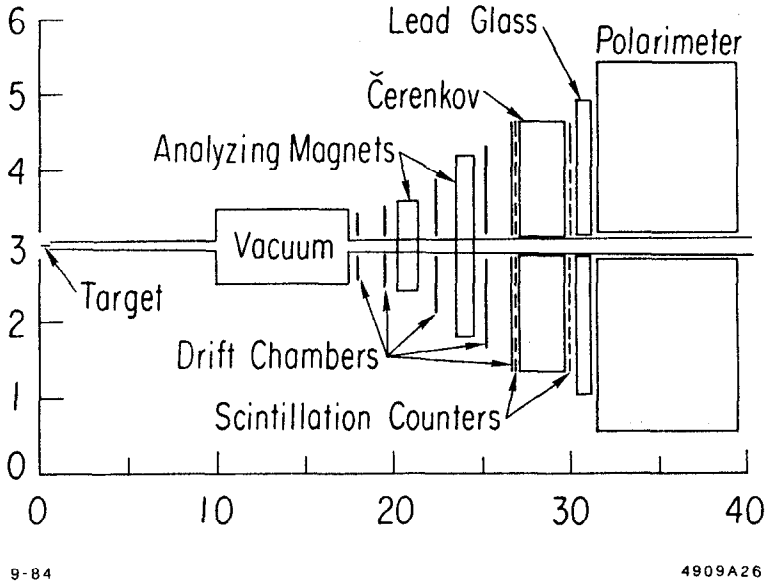

Figure 27 Schematic view of the E791 experiment. The dimensions are given in meters.

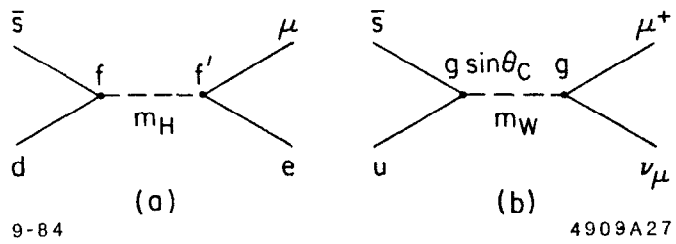

Figure 28 Comparison of the decays (a) $K_L^o \rightarrow \mu e$ mediated by a new heavy particle H and (b) $K^+ \rightarrow \mu^+ \nu$ mediated by the W boson.

5. LEPTON SECTOR

I would like to start this chapter by summarizing the status of our knowledge of the decays of the two heavy leptons, the μ and the τ. We have already mentioned in the previous section that the separate lepton number conservation, as tested in the muon decay, holds true to a very high level, approaching 10^{-10} in the branching ratios. A similar statement appears to hold true for the τ decays, although the experimental precision has not yet reached a comparable level. Specific neutrinoless τ decays have been looked for[75] with negative results, yielding following typical limits, e.g.

$$\begin{aligned} \tau &\rightarrow 3e \quad BR \quad < 4 \times 10^{-4}\,, \\ \tau &\rightarrow e\rho \quad BR \quad < 3.4 \times 10^{-4}\,, \text{ and} \\ \tau &\rightarrow \mu\gamma \quad BR \quad < 5.5 \times 10^{-4}. \end{aligned}$$

Other neutrinoless modes yield comparable upper limits.

Historically, muon decay has served as an ideal laboratory to study the weak interaction in some detail. Recent status has been summarized in a comprehensive review article by Scheck[76] and there have not been much new experimental input since that time. The Berkeley experiment[77] on the V-A nature of the μ decay will be discussed in the subsequent chapter on the searches for right-handed currents. One can summarize the μ decay situation with the statement that all of the data are consistent with the V-A interaction at a relatively high level of precision.

The τ decay provides another, considerably richer, area for the tests of our standard ideas of weak interactions. Within the standard model, the μ and τ decays should proceed by very similar diagrams illustrated in Fig. 29. The important difference stems from the fact that the τ is considerably heavier than the μ. This opens up the possibility of a number of different decay modes of the virtual W originating from the τ vertex. Thus a study of different τ decay modes is essentially a study of vertex B in Fig. 29 and represents a test as to whether

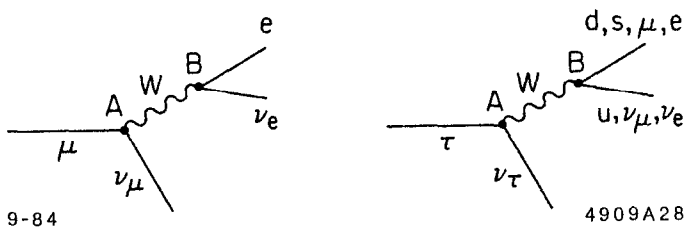

Figure 29 The μ and τ decay diagrams.

it is the standard W that is the sole mediator of the τ decay process. The net conclusion from all the data at hand is that no deviations from the standard picture have been observed here.

One can also look in detail at vertex A. A relatively old result[78] has shown that the τ decay is consistent with the V-A interaction. More specifically the Michel ρ parameter, predicted to be 0.75 for pure left-handed interaction has been measured to be 0.72 ± 0.10. The more recent experimental results have emphasized the measurement of the τ lifetime and hence the absolute strength of the $\tau - \nu - W$ vertex. The most recent comparison of the experimental value with the theoretical prediction yields[79]

$$\tau_\tau = (3.20 \pm 0.41 \pm 0.35) \times 10^{-13} \text{ sec} \qquad \text{experiment and}$$
$$\tau_\tau = (2.8 \pm 0.2) \times 10^{-13} \text{ sec} \qquad \text{theoretical prediction .}$$

Clearly, the experiment is in excellent agreement with the theoretical prediction. A better measurement of the τ leptonic branching ratios is needed if the comparison is to be pushed much further, since that is the limiting factor for the theoretical prediction.

We arrive thus at tentative conclusions based on the above experimental results that:

a) μ and τ are just "garden-variety" sequential leptons,

b) the separate lepton number is conserved to a high degree of accuracy.

Next we would like to consider to what extent other data might provide some additional information on the second statement. To elaborate on that we have to discuss briefly the formalism relevant to the lepton sector.

Given the fact that we have three lepton doublets, in analogy with the quark situation, namely,

$$\begin{pmatrix} e^- \\ \nu_e \end{pmatrix}, \begin{pmatrix} \mu^- \\ \nu_\mu \end{pmatrix}, \text{ and} \begin{pmatrix} \tau^- \\ \nu_\tau \end{pmatrix}.$$

We can ask whether the mass eigenstates in this sector are identical to the weak interaction eigenstates. As we discussed earlier, the answer to that question in the quark sector is an unequivocal NO. More formally, if we define

$|\nu_\alpha > \equiv$ neutrino "flavor" eigenstate (weak eigenstate) ,

$|\nu_i > \equiv$ neutrino mass eigenstate , and

$V \equiv$ lepton analogue of the K − M matrix

then we can write

$$|\nu_\alpha >= \sum_i V_{\alpha i} |\nu_i > \tag{5.1}$$

and the above question reduces to whether V is diagonal or not. Next, we shall explore the consequences that follow if V is <u>not</u> diagonal.

For simplicity we shall limit this discussion to the case of 2 flavors only. The 3 flavor situation has been discussed by several authors[80] in the literature. We have a mixing equation

$$\begin{pmatrix} \nu_e \\ \nu_\mu \end{pmatrix} = \begin{pmatrix} \cos\theta & \sin\theta \\ -\sin\theta & \cos\theta \end{pmatrix} \begin{pmatrix} \nu_1 \\ \nu_2 \end{pmatrix} \tag{5.2}$$

which relates the mass eigenstates to the flavor eigenstates by means of a lepton analogue of the K-M matrix. We consider a case when at $t = 0$ a pure flavor state is created, e.g. $|\nu_e >$. We can decompose it into mass eigenstates

$$|\nu_e >= \cos\theta \, |\nu_1 > + \sin\theta \, |\nu_2 > \qquad . \tag{5.3}$$

The mass eigenstates will have a time evolution that depends on their energy. Thus at some later time t we have a state

$$|\nu >_t = \cos\theta |\nu_1 > e^{-iE_1 t} + \sin\theta |\nu_2 > e^{-iE_2 t} \tag{5.4}$$

which can be transformed <u>back</u> to the $|\nu_e >, |\nu_\mu >$ basis to obtain:

$$|\nu >_t = (\cos^2\theta e^{-iE_1 t} + \sin^2\theta e^{-iE_2 t}) |\nu_e > + \cos\theta \sin\theta (e^{-iE_2 t} - e^{-iE_1 t}) |\nu_\mu > \ . \tag{5.5}$$

Thus we see that in general if a $|\nu_e >$ state is created at a time t=0 , at some

later time we shall have a finite probability of observing a $|\nu_\mu>$ state. We might thus be interested in two experimentally observable quantities:

a) probability of observing a $|\nu_e>$ state later on. This is defined as $P(\nu_e \rightarrow \nu_e) \equiv <\nu_e|\nu_e>_t$. Experiments looking for this phenomenon are called the "disappearance" experiments since in general the probability of observing ν_e will be less than 1.

b) probability of observing a $|\nu_\mu>$ state. Defined as $P(\nu_e \rightarrow \nu_\mu) \equiv <\nu_\mu|\nu_e>_t$, for only 2 neutrino states, this probability is given by $1 - P(\nu_e \rightarrow \nu_e)$. Experiments searching for ν_μ's in a beam originally composed of pure ν_e's are called "appearance" experiments.

Examining Equation 5.5 we see that the 2 necessary conditions for $P(\nu_e \rightarrow \nu_\mu) \neq 0$ are that $\theta \neq 0$ (i.e. matrix is non-diagonal) and that $E_1 \neq E_2$, implying that $m_1 \neq m_2$. It is convenient to express the latter requirement more explicitly. Taking advantage of the fact that $E >> m$, we can write

$$E_i \cong p + \frac{1}{2}\frac{m_i^2}{p} \approx E + \frac{1}{2}\frac{m_i^2}{E} \tag{5.6}$$

where E is the mean energy of the neutrino beam. Defining

$$\Delta = (E_i - E_j)t = \frac{\delta m^2}{2}\frac{L}{E}$$

with $\delta m^2 = m_i^2 - m_j^2$. With these approximations, we obtain

$$P(\nu_e \rightarrow \nu_e) = 1 - \sin^2 2\theta \frac{\sin^2 \Delta}{2} \text{ and} \tag{5.7a}$$

$$P(\nu_e \rightarrow \nu_\mu) = \sin^2 2\theta \sin^2 \frac{\Delta}{2} \ . \tag{5.7b}$$

Thus experiments on neutrino oscillations, if they yield negative results, can be interpreted as excluding a certain part of the $\sin^2 2\theta, \delta m^2$ space. We shall discuss them in more detail later, but first would like to review the independent evidence on the status of the masses of the three known (or expected) neutrinos.

Mass of the ν_e.

The classical reaction to investigate this question is the decay of tritium nucleus

$$H^3 \rightarrow He^3 + e^- + \bar{\nu}_e$$

with the electron kinetic energy endpoint (if $m_{\nu_e} = 0$) of 18.556 KeV. The technique relies on measuring the shape of the electron energy spectrum near the endpoint. The experiments of this kind present a number of challenges to the experimenters and are discussed in some detail in papers by Berquist.[81] Some of these problems are illustrated in Fig. 30. Since the nucleus changes its atomic number in the decay process, the final state He^3 ion can have its atomic electron not only in the ground state (n = 1), but also in (about 30% of time) one of the excited states (n = 2, 3, etc.) The difference in binding energy of these states reflects itself in the difference of masses of the whole system, and hence by energy conservation in the difference of endpoints of the decay electron energy spectrum. For example, the difference in binding energy between the lowest 2 states

$$M(^3He^+, n = 2) - M(^3He^+, n = 1) \approx 41eV$$

is of the same order as the typical energy resolution of the experiments. In reality, the actual situation is even more complicated, since the source used in neutrino mass experiments is not atomic tritium but part of some complicated molecule. Thus molecular physics must be well understood to interpret the results.

As seen in Fig. 30 a non-zero neutrino mass will result in curvature of the spectrum that is concave downward. But experimental resolution effects will smear this distribution and give it a curvature that is concave upward. Thus an overestimate of experimental errors can result in a false assignment of non-zero neutrino mass.

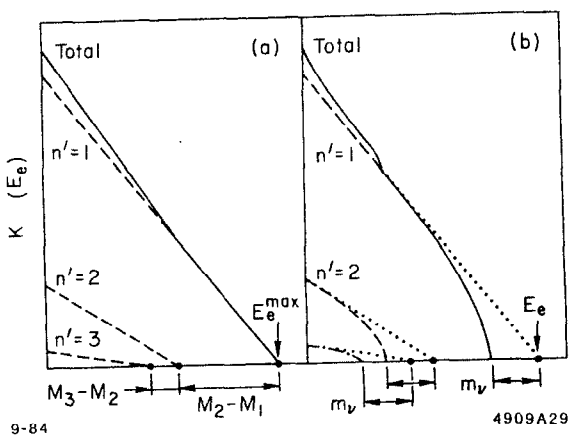

Figure 30 Detailed endpoint shape of the Kurie plot for atomic tritium β decay: (a) case of $m_\nu = 0$, and (b) case of $m_\nu \neq 0$. Effects of experimental resolution are not included (from Ref. 85).

The interest in the m_{ν_e} question has been revived recently by the experimental results from the ITEP group who in 1980 found[82]

$$14 < m_{\nu_e} < 46 \text{ ev} \qquad (99\% \text{ C.L.}) ,$$

i.e. evidence for a non-zero electron neutrino mass. The group has recently repeated their experiment with improved resolution, lower background, and higher counting rate.[83] The optimum m_ν value for the assumption of molecular valine (source of tritium in the ITEP experiment) final states is 33 ± 1 ev, but the hypotheses of molecular and atomic tritium states also give non-zero electron mass values. The edge of the experimental spectrum is shown in Fig. 31 with $m_\nu = 33$ ev and $m_\nu = 0$ hypotheses superimposed. The χ^2 for $m_\nu = 33$ ev is rather poor, 522 for 295 degrees of freedom, indicating that some systematic sources of error still need to be understood.

Recently J. J. Simpson raised the objection[84] that the calibration line used by the ITEP group to calculate their resolution has its own Lorentzian width of 9 ev; this fact was apparently overlooked by the experimenters. He claims that including this correction properly would decrease the resolution sufficiently to allow the zero mass hypothesis within the 90% C.L.

The ITEP results stimulated sufficient interest so that a large number of other groups around the world are attempting this experiment. The salient facts of the proposed experiments are reproduced below in Table IV, extracted from Shaevitz's review talk.[83]

A new approach to the problem of ν_e mass has been recently proposed by A. DeRujula[85] who suggested using a radiative electron capture process. In this process the final state consists of a nucleus, neutrino and the photon, and the measurement of the photon energy near its endpoint can give a value of the neutrino mass. The detection of photons in this energy range can be somewhat cleaner than detection of electrons, because there is no energy loss in the target in the photon case. On the other hand the counting rate at the endpoint is

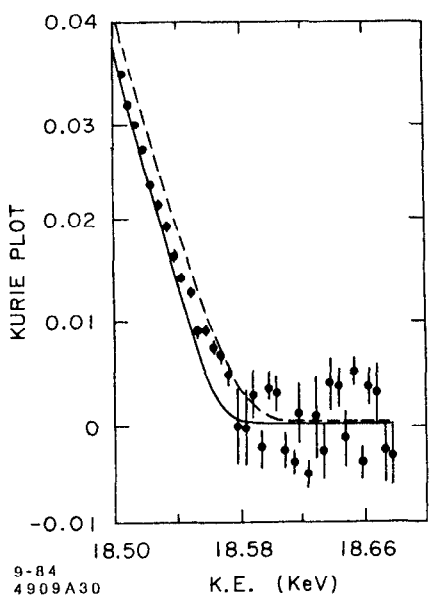

Figure 31 The edge of the Kurie plot from the 1983 ITEP experiment. The solid line is the best fit to the $m_\nu = 33$ ev hypothesis; the dashed line assumes $m_\nu = 0$.

strongly suppressed. DeRujula suggested overcoming this difficulty by using a substance that has an atomic resonance in the vicinity of the endpoint which could significantly enhance the rate in this region. The proposed best candidate isotope was ^{168}Ho and an experimental program has been initiated[86] to study this decay.

Table IV

Future β-Decay Experiments

Experiment	Source	Resolution (rms)	Sensitivity (m_{ν_e})
Fackler et al. Rock-FNAL-LLL	Solid Molecular ^3H	1-2 eV	> 4 eV
Boyd, Ohio State	Solid Molecular ^3H	10 eV	> 10 eV
Bowles et al., LAMPF	Atomic ^3H	40 eV	> 10 eV
Clark, IBM	Solid ^3H	5 eV	–
Heller et al. UC Berkeley	^3H in Semi-conductor	100 eV	> 30 eV
Graham et al. Chalk River	–	10 eV	>~ 20 eV
Bergkvist	^3H in valine	~ 25 eV	> 19 eV
Kundig, Zurich	–	5 eV	> 10 eV
INS, Japan	–	13 eV	> 25 eV

Finally one should mention that recently a K capture with a very low Q value, 156 ± 17 ev, has been discovered in ^{158}Tb isotope.[87] Raghaven has estimated that one could measure neutrino mass in this process down to 25 ev in the first generation mass experiments.

Mass of the ν_μ.

The measurement of ν_μ mass is intrinsically more difficult because no channels exist where the energy released is low. Traditionally, the two optimum processes to study this problem have been the decays

$$K_L^\circ \rightarrow \pi^\pm \mu^\mp \nu_\mu \qquad (5.8)$$

and $$\pi^+ \rightarrow \mu^+ \nu_\mu \, . \qquad (5.9)$$

The history of upper limits on ν_μ mass has been summarized by Shaevitz and is illustrated in Fig. 32. Channels 5.8 and 5.9 have alternated as sources of the best upper limit at any given time. The π decay has the advantage that the Q of the decay is about an order of magnitude lower. However, being a two body decay, the mass of the neutrino enters as the square into the energy balance equation. The K° decay channel suffers from a high Q value and the fact that the useful events, i.e. those with neutrino taking a negligible fraction of the total energy, are strongly suppressed by phase space factor.

The present best upper limit is

$$m_{\nu_\mu} \leq 0.49 \text{ MeV} \qquad (90\% \text{ C.L.})$$

and comes[88] from the study of the momentum of the decay muon from a π^+ at rest.

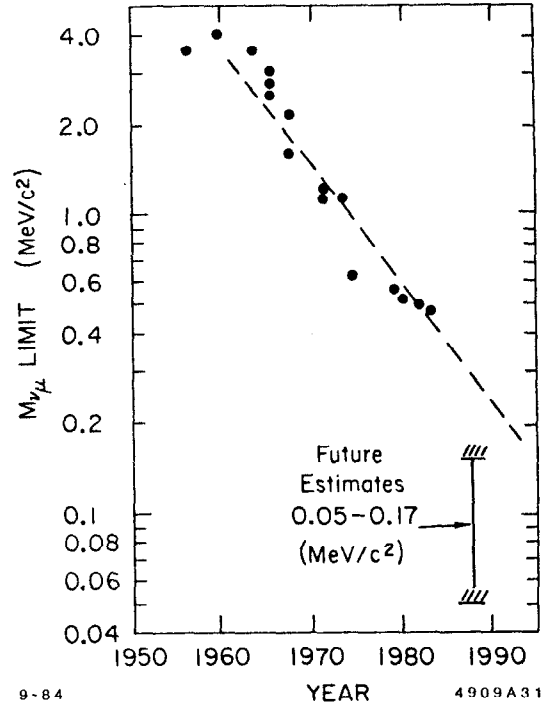

Figure 32 Muon neutrino mass limits as a function of time.

Mass of the ν_τ.

Similar difficulties, but considerably magnified, are also present in the ν_τ mass experiments. Here most useful are the τ decay channels where the observable final state products have as high a mass as possible. The present record holder is the reaction

$$\tau^{\pm} \rightarrow \pi^+\pi^{\pm}\pi^-\pi^0\nu_\tau \qquad (5.10)$$

since the 4π mass state can have high effective mass due to the ρ' intermediate state. The data on this question from the MarkII collaboration[89] is shown in Fig. 33. The quoted upper limit on the ν_τ mass is

$$m_{\nu_\tau} < 164 \text{ MeV} \qquad (95\% \text{ of C.L.}) \, .$$

Further progress on the ν_τ mass will have to await new techniques and new channels. Thus, for example, the decay modes

$$D(\text{or } F) \rightarrow \tau + \nu_\tau \qquad (5.11)$$

would be useful, if sufficient number of events could be obtained, because of the relatively low Q value. Similarly the rate for the decay

$$K^+ \rightarrow \pi^+\nu_\tau\bar{\nu}_\tau \qquad (5.12)$$

is obviously very sensitive to the ν_τ mass since the total energy released, and available for the two ν's is only 354 MeV.

Subdominantly coupled ν's.

We have already mentioned that non-zero ν masses and a non-diagonal V matrix can be detected through ν oscillations. Shrock[90] has pointed out that these phenomena can also be searched for by looking for multiple peaks in the

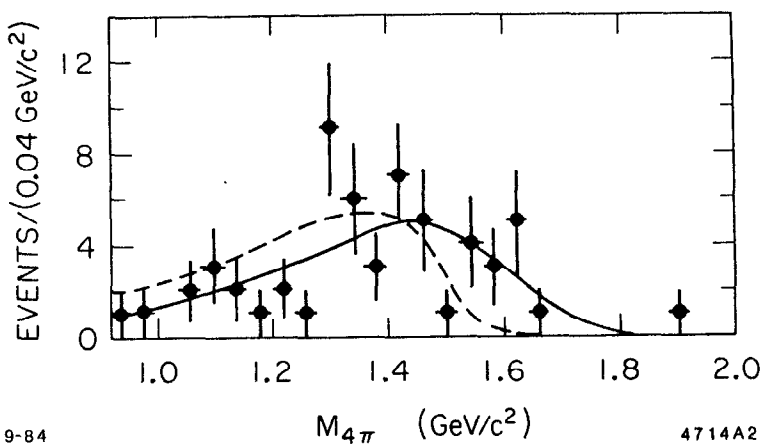

Figure 33 The 4π invariant mass distribution from the $\tau \rightarrow 4\pi + \nu$ decays. The solid line assumes $m_{\nu_\tau} = 0$, the dashed line $m_{\nu_\tau} = 250$ MeV. Both curves are drawn with the assumption of ρ' dominance with a mass of 1570 MeV and a width of 510 MeV.

lepton momentum spectrum in π and K decays. Thus if neutrino flavor states are written

$$\nu_\alpha = \sum_i V_{\alpha i} \nu_i \tag{5.13}$$

and if all the ν_i have different masses and if they are all kinematically accessible to a given decay, then this decay will exhibit as many peaks in the lepton momentum spectrum as there are neutrino mass states.

An analogous situation exists in the τ decay, where the 2 body decay can be written as

$$\tau^- \to \nu_\tau + (\bar{u}d') \tag{5.14}$$

and d', the weak interaction eigenstates is given by

$$d' = U_{ud}d + U_{us}s + U_{ub}b\ . \tag{5.15}$$

Because the decay into the b quark is energetically forbidden, we shall see <u>two</u> monoenergetic ν_τ peaks in τ decay corresponding to

$$\begin{aligned} &\tau^- \to \nu_\tau + (\bar{u}d) \ \text{ i.e. } \ \tau^- \to \pi^- + \nu_\tau \\ \text{and} \quad &\tau^- \to \nu_\tau + (\bar{u}s) \ \text{ i.e. } \ \tau \to K^- + \nu_\tau\ . \end{aligned} \tag{5.16}$$

An alternate technique to look for the same phenomena is to search for decays of heavy neutrinos in a neutrino beam. Thus if a K decay would result in a mixture of ν_μ's and some other heavy neutrino ν_H, we might expect to see subsequently

$$\nu_H \to \nu_\mu e^+ e^-\ .$$

Comprehensive discussions of these searches have been given by Shaevitz[83] and Winter[91] and will not be repeated here. No positive results have been found and the experiments can be interpreted as correlated upper limits on the mass of the heavy neutrino and the strength of mixing $|V_{\alpha i}|^2$. The limits on couplings to the electron and muon neutrino are reproduced in Fig. 34.

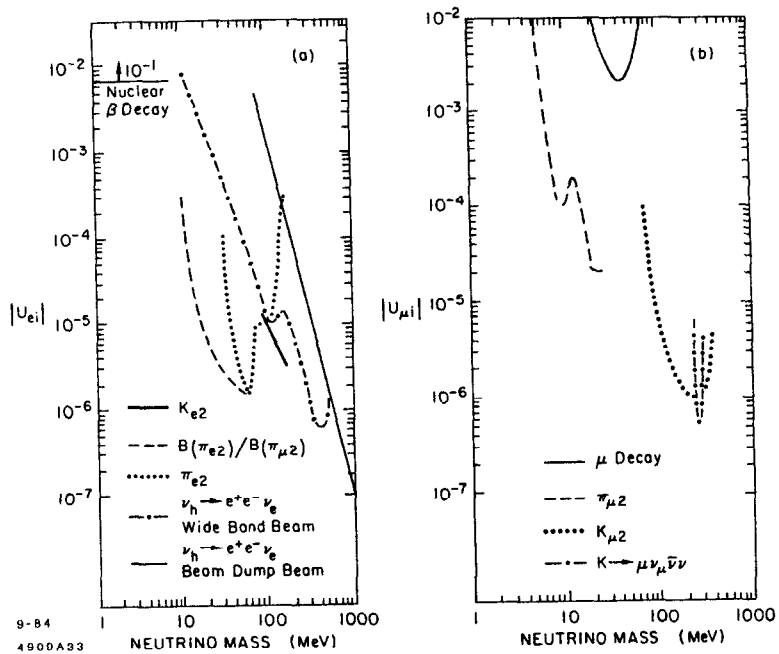

Figure 34 Limits on masses and couplings of heavy neutrinos to electron neutrinos (a) and muon neutrinos (b).

ν oscillations - general comments.

Before we discuss the ν oscillations experiments in detail, some general comments might be in order. First, we should again emphasize that all of the analyses to be discussed assume a two neutrino picture. Second, as we discussed previously, the figure of merit for the sensitivity of any experiment to the potential oscillations is the parameter Δ defined as

$$\Delta = \frac{\delta m^2}{2}\frac{L}{E} \quad . \tag{5.17}$$

It is convenient to identify three general ranges of Δ, i.e.

a) $\Delta << \pi$, corresponding to a situation where we are still close enough to the neutrino source so that the oscillations have not yet had sufficient time to develop. These experiments will be very insensitive to ν oscillations.

b) $\Delta \approx \pi$, corresponding to the optimum experimental situation for ν oscillation searches. Within the energy band of ν's accepted by the experiment, one can expect significant differences in behavior due to oscillations.

c) $\Delta >> \pi$, corresponding to the situation where the ν beam went already through several oscillation wavelengths. This will result in an inability to see the differences in behavior of ν's of different energies because in general we shall be integrating over too large a bandwidth. These experiments will still be sensitive to "disappearance" phenomena provided that $\sin^2\theta$ is large enough and our a priori knowledge of the flux good enough.

The neutrino oscillation experiments can be conveniently grouped into several categories, depending on the ν sources:

a) solar neutrino experiments. These have the advantage of large L/E but poor knowledge of the initial intensity. Thus they are sensitive to very small δm^2 , but only to large values of $\sin^2\theta$.

b) cosmic ray neutrino experiments. Similar comments apply here as to solar ν's, but L/E is typically lower; primary flux information could in principle be better. The neutrinos studied here are ν_μ's as opposed to solar neutrinos that are ν_e's.

c) reactor experiments. These give rise to $\bar{\nu}_e$'s with reasonably large L/E and high intensities. There is some flux uncertainty associated with many fission products that subsequently undergo β decay.

d) accelerator experiments. Those are characterized by the optimum control of the source, but rather small possible L/E values.

The various experiments (present and future) on ν oscillations have been summarized by Silverman and Soni.[92] The range that they cover in the L-E_ν space, together with their δm^2 sensitivity is shown in Fig. 35.

Solar neutrinos.

The detection of solar neutrinos on earth presents one possible method of searching for neutrino oscillations. The experiment relies on the fact that the sun is an intense source of electron neutrinos. These ν_e's have an energy low enough so that if they are transformed into ν_μ's or ν_τ's , the latter have too low an energy to participate in charged current reactions. Hence, ν oscillations will exhibit themselves as a deficiency of the detected neutrinos.

The experimental method relies on detecting the capture reaction

$$\nu_e + {}^{37}Cl \rightarrow {}^{37}Ar + e^- \tag{5.18}$$

in a large tank of liquid C_2Cl_4. The ^{37}Ar atoms are removed from the vessel by purging with helium gas and subsequently detected via their K capture reaction. The experimental details are described extensively in the available literature.[93]

The main advantage of this experiment is a very large L/E value giving rise to potential sensitivity down to a very small $\delta m^2 (\sim 10^{-11}\text{ev}^2)$. On the other hand, as mentioned previously, the sensitivity to $\sin^2 2\theta$ values is rather poor, due to theoretical uncertainties associated with the intensity of the source. The reason for the latter is illustrated in Table V which gives the reactions responsible for

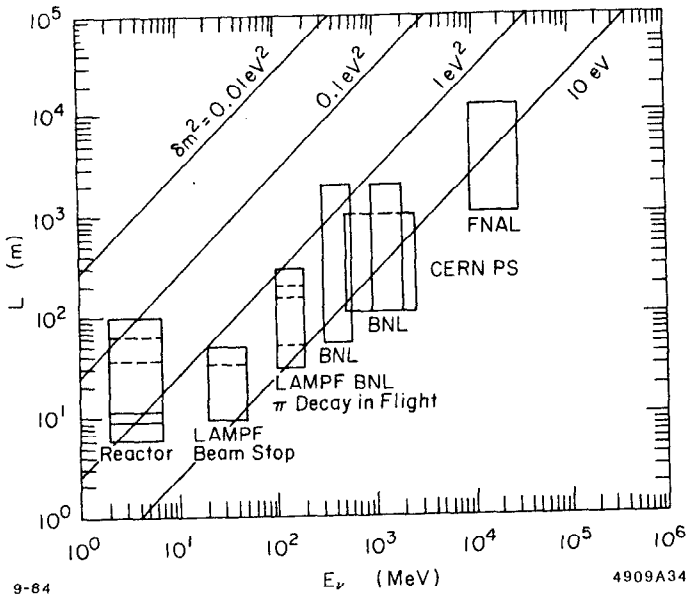

Figure 35 The neutrino source to detector distance (L) vs neutrino energy (E_ν) for various neutrino oscillation experiments together with their approximate sensitivity to the mass difference squared δm^2.

Table V

Neutrino Sources

Reaction	Energy (MeV)	Predicted Flux $10^{10}cm^{-2}sec^{-1}$	SNU (^{37}Cl)
$p + p \rightarrow D + e^+ + \nu_e$	0 - 0.4	6.1	0
$p + e^- + p \rightarrow D + \nu_e$	1.4	0.015	0.23
$^7Be + e^- \rightarrow {}^7Li + \nu_e$	0.86(90%) 0.34(10%)	0.34	1.03
$^8B \rightarrow {}^8Be^* + e^+ + \nu_e$	0 -14	0.00060	6.48
$^{13}N \rightarrow {}^{13}C + e^+ + \nu_e$	0 - 1.2	0.045	0.07
$^{15}O \rightarrow {}^{15}N + e^+ + \nu_e$	0 - 1.7	0.035	0.23
			8.04

the solar neutrinos, their energy and the expected contribution to the counting rate in a ^{37}Cl detector.[94] The unit that is convenient to use here is an SNU, a standard neutrino unit, defined as

$$1 \text{ SNU} \equiv 10^{-36}\nu_e \text{ captures/sec/target nucleus}(^{37}Cl) .$$

The difficulty lies in the fact that the threshold for the ^{37}Ar production is 0.814 MeV, and thus the majority of the ν_e flux from the sun is not able to contribute to the reaction in question. Hence the theoretical interpretation of the experimental results depends very strongly on our understanding of the production mechanisms of the high energy tail of the neutrino spectrum.

The experimental program of R. Davis et al.[95] has been going on now for over a decade. Their annual results until 1978 and the latest average are shown in Fig. 36. The average value of 2.2 ± 0.4 SNU is considerably lower than the theoretical prediction of 8.0 ± 3.3 SNU[94] obtained by summing over all the reactions listed in Table V. Whether this discrepancy is due to theoretical uncertainties in the solar neutrino flux calculations or new physics is unclear at the present time.

There has been a significant interest lately in exploring other avenues to probe this question, specifically by utilizing nuclear neutrino induced reactions with a significantly lower threshold.[94] One specific channel that has attracted a lot of attention is the $^{71}Ga\ (\nu, e)\ ^{71}Ge$ reaction that has a threshold of 0.236 MeV. Its relative advantage over ^{37}Cl reaction is well demonstrated when one compares the detection threshold energy with the energy spectra resulting from all of the solar reactions generating electron neutrinos (see Fig. 37). The total calculated rate for a ^{71}Ga target is 102 SNU's, considerably higher than for the ^{37}Cl reaction.

Cosmic ray neutrinos.

The cosmic ray hadronic showers are a source of muon neutrinos by virtue of the decay process $\pi \rightarrow \mu\nu$, where the pions come from the hadronic cascade initiated by the primary cosmic rays. Furthermore, the muon rate and spectrum observed on the earth's surface allow us to calculate the ν_μ flux and the energy distribution, since both μ's and ν_μ's come from the same source. The ν_μ flux can be measured in principle by observing ν_μ interactions in detectors located deep underground so that they will be shielded from other nuclear interactions. In practice, the fluxes are so low that one is forced to use the earth above the detector as the target, the detector serving only to observe the μ's resulting from the ν_μ interactions. Any deficiency of the μ's would constitute evidence of possible ν oscillations since ν_e interactions would give no μ's and ν_τ's only a much reduced number of μ's (from τ decay).

The experimental difficulty lies in the fact that the μ detectors discussed

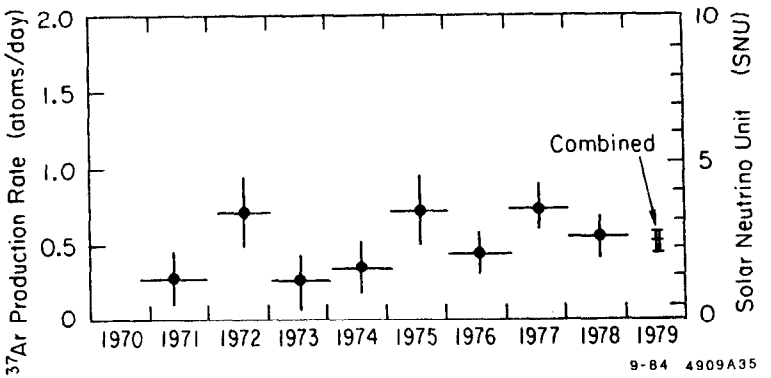

Figure 36 The annual average ^{37}Ar production rate from the experiment of R. Davis et al. The combined average is indicated on the right.

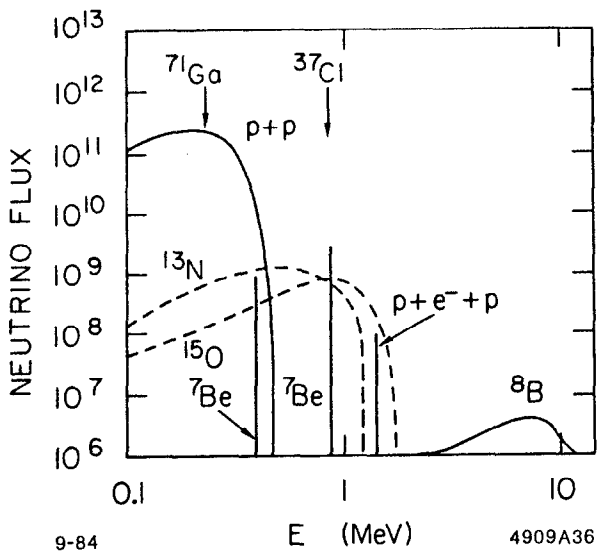

Figure 37 Energy spectrum of the solar neutrinos as indicated by the standard model. The thresholds for ^{37}Cl and ^{71}Ga reactions are indicated by the arrows. The fluxes are given in cm^{-2} sec^{-1} MeV^{-1} for continuum sources and in cm^{-2} sec^{-1} for line sources.

above will also be sensitive to the most energetic μ's that originate in the atmosphere from π decay and have enough energy to penetrate to the detector. That component can be separated out if one looks at the zenith angle distribution of the observed μ's. At large zenith angles the primary μ's will have to go through a large amount of earth; thus at those angles only μ's produced by ν_μ interactions should be present. Alternatively, if the detector can identify the direction of the muon by time of flight technique, it can isolate upward going μ's, i.e. those coming from interactions of ν_μ's originating from π decays on the other side of the earth. Those μ's should have no contamination from primary muons. All three of these sources are indicated very schematically in Fig. 38.

The results of the experimental observations and theoretical predictions are compatible with each other within experimental errors. Two of the underground setups[96] that do not measure time of flight give fluxes of neutrino induced muons that are mutually compatible and yield

$$I_\mu^{\text{theor}}/I_\mu^{\text{exp}} = 1.6 \pm 0.4 \ .$$

The Baksan-Valley experiment in the Soviet Union that does measure the time of flight obtains[97]

$$I_\mu^{\text{theor}}/I_\mu^{\text{exp}} = 1.0 \pm 0.26 \ .$$

Finally, a Soviet underwater muon detector,[97] operating at depths of 2000 m, 3000 m, and 3700 m finds

$$I_\mu^{\text{theor}}/I_\mu^{\text{exp}} = 1.19$$

based on 350 observed events.

The new generation proton decay detectors can in principle investigate this question in considerably more detail. The early results from the IMB experiment[98] are consistent with theoretical calculations: 69 events have been found, all of which are consistant with being due to ν interactions; 95 ± 30 are predicted.[99]

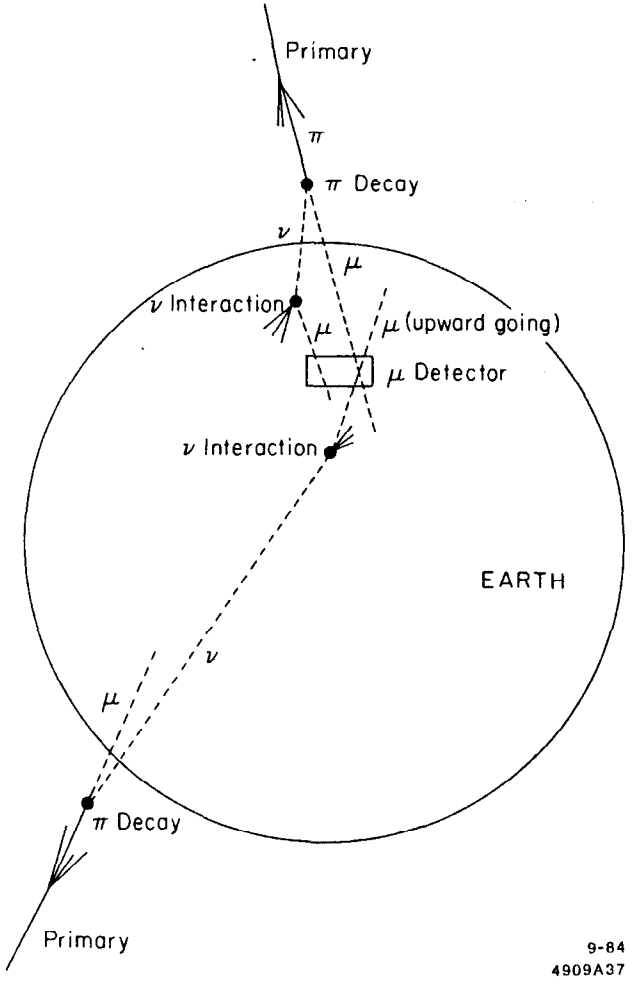

Figure 38 Schematic drawing of potential sources of μ's detected by an underground muon detector.

It should be pointed out, however, that this experiment is sensitive also to ν_e interactions as opposed to the μ detector experiments that can see only ν_μ's. Thus the results of these two kinds of experiments are not directly comparable.

Accelerator experiments.

The experimental input on the question of ν oscillations from the accelerator experiments can most naturally be classified into several different sources:

a) beam dump experiments,

b) disappearance experiments and

c) appearance experiments.

The beam dump experiments detect mainly "prompt" neutrinos, i.e. neutrinos originating from sources that have mean decay paths small compared to the typical interaction lengths. Various techniques are used to suppress and/or calculate the background from ν's resulting from π and K decays.

The dominant source of prompt neutrinos are expected to be charmed particle decays, predominantly decays of D° and $D^\pm$. Because of $\mu - e$ universality, the number of ν_μ and ν_e interactions should be the same, except for small phase space correction in the D decay process. Thus deviation from unity in the observed ν_e/ν_μ interaction ratio might be evidence for oscillation phenomena. The latest results have been recently reviewed by K. Winter[91] and are summarized in Table VI. Except for the anomaly observed by the CHARM experiment, the experiments are consistent with equal rates of ν_μ and ν_e interactions.

Table VI

Summary of the 1982 results on the ratio of electron- and muon-neutrino fluxes

Experiment	Electron ident. method*)	E_ν cut	$\phi(\bar{\nu}_e + \nu_e)/\phi(\bar{\nu}_\mu + \nu_\mu)$ (a)
CHARM	direct (extrap.)	2 GeV	$0.57 \pm {}^{0.11}_{0.10} \pm 0.07$
CHARM	subtraction (extrap.)	2 GeV	$0.59 \pm {}^{0.11}_{0.10} \pm 0.08$
CDHS	subtraction (extrap.)	20 GeV	$0.83 \pm 0.13 \pm 0.12$
BEBC	direct (subtraction and extrapol.)	20 GeV	$1.35 \pm {}^{0.65}_{0.34} \pm 12\%$
FMOW	direct	20 GeV	$1.09 \pm 0.10 \pm 0.10$
FMOW	subtraction (subtraction and extrap.)	20 GeV	$1.02 \pm 0.09 \pm 0.10$

(a) First error is statistical, second error is systematic.

*) In parenthesis is indicated the method used for determining the prompt fluxes.

There has been recently a renewed interest in dedicated accelerator experiments to search for ν disappearance phenomena.[100] These generally use two different (but as similar as possible) detectors located at two different distances from the neutrino source. Both of the detectors take data at the same time and are illuminated by the same neutrino beam. Thus sensitivity to detection efficiency and Monte Carlo calculations is considerably lessened. These experiments are generally sensitive to relatively large values of δm^2 (tens of eV^2) and moderate values of $\sin^2 2\theta (\gtrsim 0.1)$. The neutrino oscillations in these experiments would show up as a variation in the ratio of rates in the forward to backward detector as a function of ν energy that could not be explained by the relatively minor effects having to do with slightly different detection efficiencies in the two detectors. The results so far have been negative, yielding no evidence for neutrino oscillations. A typical result (from the CDHS experiment, Ref. 100) is shown in Fig. 39. The summary of all the experimental data will be presented at the end of this chapter after discussion of the reactor data.

The appearance experiments that have been performed so far can be classified into either $\nu_\mu \to \nu_e$ or $\nu_\mu \to \nu_\tau$ variety. They require clean beams without any original contamination of the potentially regenerated neutrino species. So far only ν_μ beams have satisfied this condition since the pure $\bar{\nu}_e$ beams from the reactors are too low in energy to be able to produce μ's or τ's if $\nu_e \to \nu_\mu$ or $\nu_e \to \nu_\tau$ transitions exist. The detectors for these experiments must have good spatial resolution because of the need to identify e's and τ's. Thus emulsions, bubble chambers and fine grain electronic detectors have made the principal contributions in the area. No evidence for neutrino oscillations have been seen in any of these experiments.

Reactor experiments.

Because of the very high fluxes and low energy, these experiments can probe rather low region of δm^2. The early experiments[101] concentrated on comparison of the experimental results on neutrino interaction rates and spectra with theoretical predictions; more recently, there has been a trend to dedicated oscillation experiments that operate the neutrino detector at two or more positions and thus can perform a relative rate measurement.

The Cal Tech - ISN Grenoble (later SIN) - TU Munich collaboration initiated their studies[102] at the ILL Grenoble reactor working at a distance of 8.75 m from the reactor core. They identify the reaction

$$\bar{\nu}_e p \to e^+ n$$

by detecting both the positron and the neutron in a coincidence. Aside from a small neutron recoil energy correction the neutrino energy is given by

$$E_{\bar{\nu}} = E_{e^+} + 1.8 MeV$$

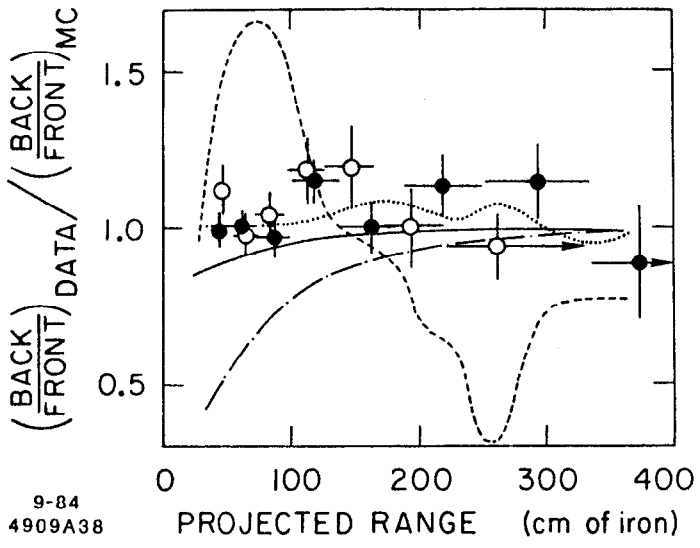

Figure 39 Ratio of Monte Carlo corrected event rates in the back and front CDHS detector as a function of projected range in iron. Also shown are curves indicating the expected behavior of these ratios in the case of oscillations for different choices of δm^2 and $\sin^2 2\theta$. Solid curve $\delta m^2 = 1$ eV^2 and $\sin^2 2\theta = 0.2$; dash-dotted curve $\delta m^2 = 1$ eV^2 and $\sin^2 2\theta = 1$; dotted curve $\delta m^2 = 32$ eV^2 and $\sin^2 2\theta = 0.2$; dashed curve $\delta m^2 = 16$ eV^2 and $\sin^2 2\theta = 1$. Solid circles refer to interactions in fine grained modules; open circles to the more coarse modules.

and thus a measurement of positron energy ($\delta E/E = 0.35\sqrt{E}$) yields the observed neutrino energy spectrum.

More recently this experiment has been continued[103] at the high power Gösgen reactor in Switzerland. Data were taken at 2 distances, 37.9 m and 45.9 m, allowing a test for the existence of neutrino oscillations independent of the knowledge of the neutrino flux. In addition, the data at the two positions can be combined and compared with the calculated ν_e spectrum that is based on the measured β decay spectrum from ^{235}U and ^{239}Pu. Neither one of the two analyses gives any evidence for the oscillations,[104] the combined data analysis yielding somewhat more restrictive limits on δm^2 and $\sin^2 2\theta$.

The LAPP, Annecy - ISN, Grenoble group recently presented results[105] from a high statistics experiment at the Bugey reactor in France. The neutrino flux at 13.6 m distance is $2 \times 10^{13}/\text{cm}^2/\text{sec}$, which is the highest intensity presently available for any experiment near a reactor. The experimental technique is very similar to that used by the other collaboration. The detector consists of liquid scintillator and ^3He proportional chamber sandwiches; the former is used to detect positrons and measure their energy, the latter to detect the neutron via the capture reaction

$$n + {}^3He \rightarrow t + p\,. \tag{5.19}$$

About 63000 $\bar{\nu}_e$ events have been observed at 2 different detector locations, 13.6 and 18.3 m away from the reactor core. The group have observed a difference in the counting rate and in the apparent energy spectrum at the two locations.

The measured ratio of fluxes at the two positions, as a function of positron energy is displayed in Fig. 40. The ratio appears not only to be different from unity, but also to have some energy dependance. The allowed region in the δm^2, $\sin^2 2\theta$ space, if this effect is interpreted as due to ν oscillations, is shown in Fig. 41. If we compare these results to the data from the Gösgen reactor, 2 location experiment, we find that values of the parameters $\delta m^2 \approx 0.2$ and $\sin^2 2\theta \approx 0.2$

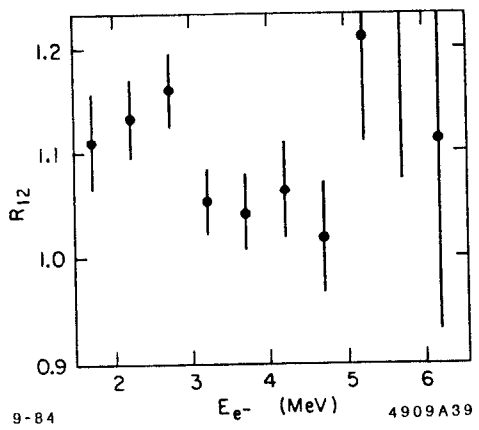

Figure 40 The ratio of $\bar{\nu}_e$ fluxes, as measured by $\bar{\nu}_e$ interactions, at the 2 locations in the Bugey experiment.

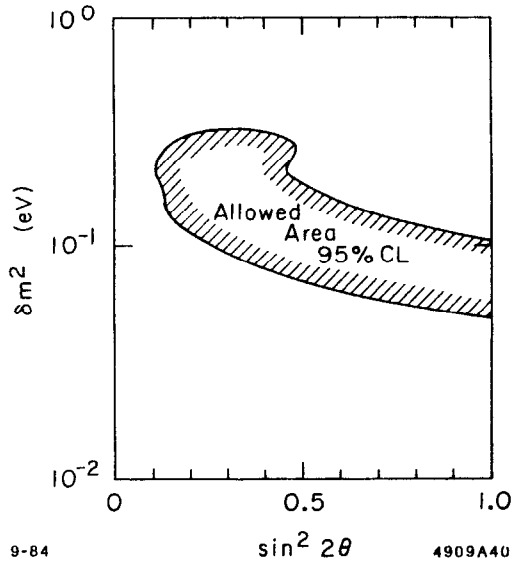

Figure 41 The parameter space allowed by the Bugey experiment, if the results are interpreted as due to ν oscillations.

are mutually compatible. On the other hand, the Bugey results contradict the Gösgen limits obtained by comparing the experimental results with the spectrum predicted from the experimental study of U and Pu fission and their byproducts.

ν oscillations - summary.

The best experimental upper limits for the correlated values of δm^2 and $\sin^2 2\theta$ are shown in Figs. 42 and 43. Figure 42 illustrates the upper limit envelopes extracted from all of the inclusive experiments (i.e. disappearance). Figure 43 shows the upper limit envelopes for the exclusive channels $\nu_\mu \to \nu_e$ and $\nu_\mu \to \nu_\tau$. If the inclusive limits are more stringent than the exclusive ones, the former are used in Fig. 43. One should emphasize once again, that these limits were obtained in the framework of the 2 neutrino flavor picture. The curves come mainly from Shaevitz's review talk[83] and have been updated by the most recent results.[100] The Bugey reactor experiment results are not included in these figures.

Double β decay.

The double β decay process

$$Z \to (Z-2) + 2e^- + 2\nu_e \tag{5.20}$$

occurs in nature by virtue of the fact that the expression for the mass of a nucleus has a term which depends on whether we are dealing with an odd-odd or even-even nucleus. Thus the mass of even A nuclei is described by two different curves, as exhibited in Fig. 44. The process (5.20) is not very interesting from the particle physics point of view since it merely represents a simultaneous beta decay of two d quarks. It does, however, present a rather formidable calculational problem to theoretical nuclear physicists.[106]

From the particle physics point of view, a very interesting question is whether the neutrinoless double β decays exist, namely the process:

$$Z \to (Z-2) + e^- + e^- \tag{5.21}$$

without the emission of any neutrinos. Very schematically, this decay would have

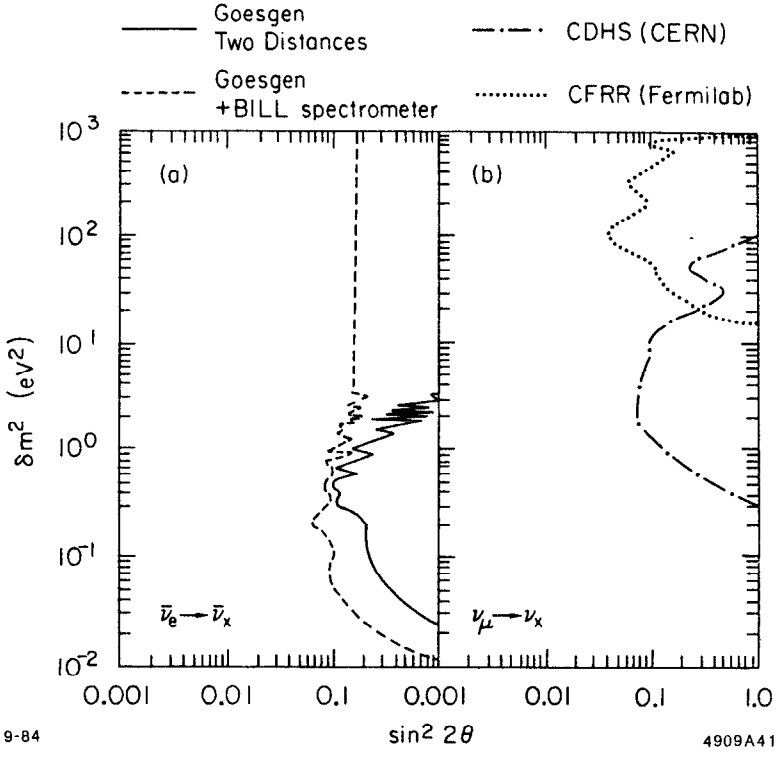

Figure 42 Upper limits on δm^2 and $\sin^2 2\theta$ obtained from the inclusive (disappearance) experiments.

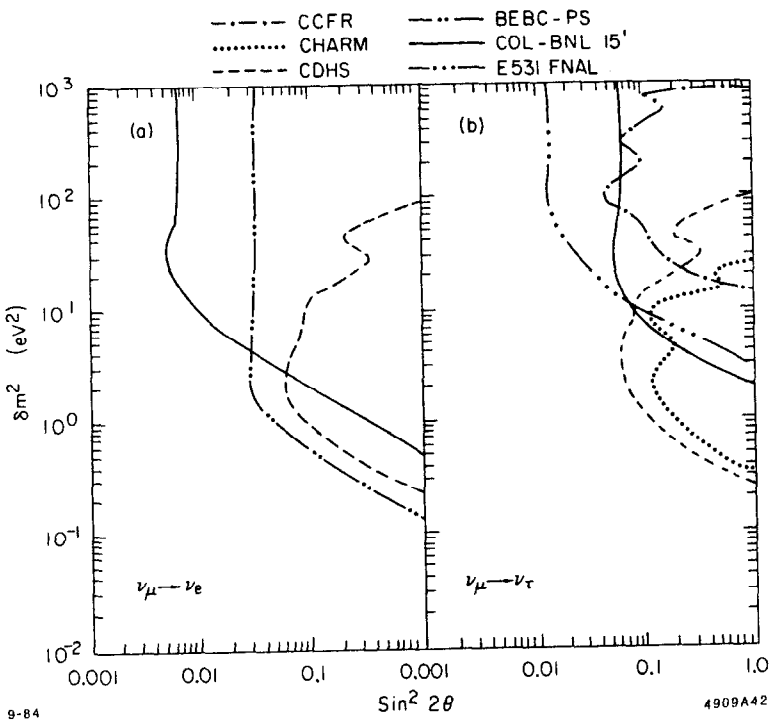

Figure 43 Upper limits on δm^2 and $\sin^2 2\theta$ obtained from the exclusive (appearance) experiments.

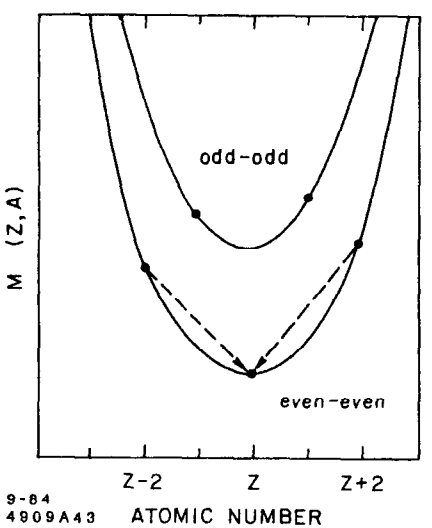

Figure 44 Energy systematics of even A nuclei. An allowed double β decay is indicated by an arrow.

to proceed as indicated in Fig. 45. In the conventional picture, since the same neutrino is both emitted and absorbed by the W^-, the process is forbidden both by lepton number conservation and helicity. Thus for the decay to proceed, the neutrino must be a Majorana particle, namely $\nu \equiv \bar{\nu}$ and the helicity requirement has to be somewhat relaxed. The latter can be accomplished in two ways: either by giving the neutrino some mass or by allowing some right-handed currents. The experimental implication of that fact is that negative results on neutrinoless double beta decay can be translated into correlated limits on neutrino mass and admixture of right-handed currents for a Majorana neutrino. The latter is usually parametrized by the ratio η of the masses squared of the two relevant vector bosons, namely

$$\eta \equiv |\frac{M_{W_L}}{M_{W_R}}|^2 . \tag{5.22}$$

Experimentally, there are several different experimental approaches to this question. The oldest technique relies on the geochemical means, namely detection by chemical analysis of the daughter nuclei trapped in the ores rich in the parent nuclei. Besides many serious difficulties connected with the proper interpretation of the source of the daughter nuclei, the method has two other very serious disadvantages. First, it cannot separate out the 2ν from 0ν decay modes but measures only the total rate, λ_T , i.e.

$$\lambda_T \equiv \lambda_{2\nu} + \lambda_{0\nu} . \tag{5.23}$$

This evidence for a non-zero $\lambda_{0\nu}$ comes from detection of excess of the daughter nuclei over and above what one would expect from the conventional 2ν double beta decay rate. This is where the second difficulty comes in, namely the necessity to rely on theoretical calculations to calculate $\lambda_{2\nu}$. As we mentioned previously, these calculations are difficult and those available in the literature show serious discrepancies.

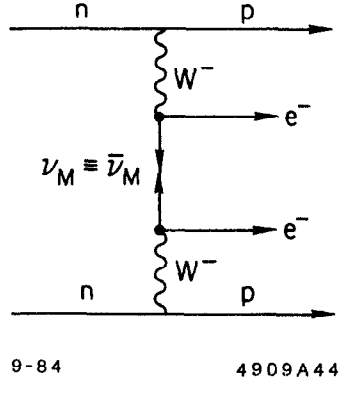

Figure 45 A diagram representing a neutrinoless double beta decay.

On the other hand the situation is somewhat helped by the phase space considerations. Since the energy released in a typical double beta decay is quite low, the phase space effects enhance the 2 body decay (no-ν decay) considerably - typically by a factor of $\sim 10^6$ relative to the conventional 4 body decay.

It has been pointed out by Pontecorvo[107] that these considerations lead one to conclude that considerable improvement in the accuracy of the final answer could be obtained if decay-rate ratios of pairs of similar nuclei are studied. The ratio of their respective nuclear matrix elements should be near unity, and generally, because of different phase space factor, the 0ν decay mode in one of the 2 channels would be significantly enhanced. Thus for example if one considers ^{128}Te and ^{130}Te, the Q values are 869 and 2533 keV respectively. Thus $\rho_{0\nu}$, defined as

$$\rho_{0\nu} \equiv {}^{128}\lambda_{0\nu} / {}^{130}\lambda_{0\nu}$$

will be much greater than $\rho_{2\nu}$, defined accordingly. Thus the overall ratio, $\rho_T >> \rho_{2\nu}$ if the neutrinoless decay mode occurs at all.

The early results on this Tellurium ratio, from the work of Hennecke et al. (Missouri group)[108] indicated some evidence for neutrinoless double beta decay. This result, however, has been contradicted by the recent publication of the Heidelberg group,[109] who find

$$\rho_T \equiv \frac{{}^{128}\lambda_T}{{}^{130}\lambda_T} = (1.03 \pm 1.13) \times 10^{-4} ,$$

i.e. no evidence for any enhancement due to neutrinoless decay mode. The implication of both of these results, in terms of limits (or values) of m_ν and η are shown in Fig. 46.

There is a program underway at UC Irvine to measure the double β decay process in ^{82}Se by measuring the energies of the 2 electrons resulting from the decay. The neutrinoless decay should exhibit itself as a spike in the total energy spectrum with a value corresponding to the total energy released. The early

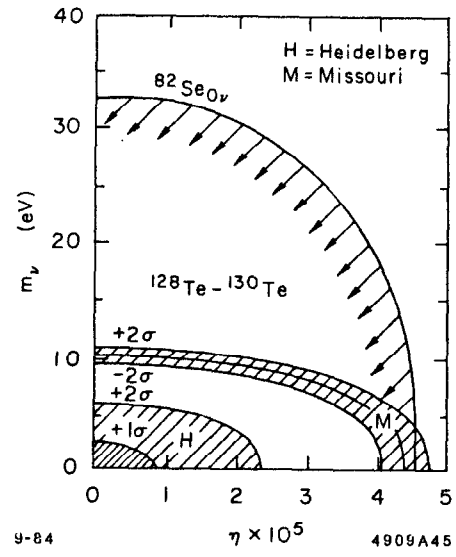

Figure 46 Allowed regions in the (m_ν, η) plane deduced from the measured ratios ρ_T of both the Heidelberg (H) and Missouri (M) analyses. The Se curve comes from the upper limit on $\lambda_{0\nu}$ from Cleveland et al., Phys. Rev. Lett. 35, 757 (1975).

experiment by Moe and Lowenthal[110] detected 20 clean $2e^-$ candidates using a cloud chamber, resulting in a half-life of $(1.0 \pm 0.4) \times 10^{19}$ years. This result was in significant disagreement with the previously accepted value, obtained by the geochemical means, of $(2.76 \pm 0.88) \times 10^{20}$ years, based on the analysis of the amount of selenium and krypton in tellurobismuthite.[111] The theoretical calculation for the 2ν rate[106] straddles these two experimental numbers with a value of 2.35×10^{19} years.

The UCI program is continuing, with a TPC detector scheduled to replace the previously used cloud chamber. If the cloud chamber result is correct, they should observe around 200 $2e^-$ events/month. A potential sensitivity to a no-ν partial lifetime of 2×10^{23} years is expected in two years of running.

A third general approach to the double β decay question involves attempts to observe $2e^-$ decays from ^{76}Ge using low background Ge detectors, generally located underground to reduce the cosmic ray background. There are at present 5 experiments in the preparation phase to perform this experiment. The *no* neutrino decay mode would exhibit itself as a line at 2.041 MeV and thus the goal of the experimenters is to reduce all the other backgrounds in this region as much as possible. The location and the preliminary background counting rates for those experiments as well as for the older Milano experiment are indicated below in Table VII.

Table VII

Preliminary Background Rates in Second Generation ^{76}Ge $\beta^-\beta^-$-Decay Experiments (given in counts/keV/hr/cm^3)

Experiment	Background at 2.041 MeV count/keV/hr/cm^3	Location
Milano (1983)	$\sim 1.6 \times 10^{-5}$	Mont Blanc Tunnel
Guelph-APTEC (1983)	$\sim 3.2 \times 10^{-5}$	Windsor Salt Mine
Battelle-Carolina (1983)	$\sim 2 \times 10^{-5}$	Battelle, above ground
Milano (1973)	$\sim 6.2 \times 10^{-5}$	Mont Blanc Tunnel
Battelle-Carolina (1982)	$\sim 6.2 \times 10^{-5}$	Battelle, above ground
Cal. Tech. (1983)	$\sim 2 \times 10^{-5}$	Pasadena, above ground

The ultimate sensitivity of the Ge experiments, assuming a running period of 4 years, is estimated to be about 10^{25} years. If this value is indeed achieved, it would correspond to[112]

$$m_\nu \leq 0.5 \text{ eV and } |\eta| < 10^{-6} .$$

This is probably the ultimate limit on the achievable neutrinoless double β decay sensitivity since the Ge detector combines very good energy resolution, good γ-ray background rejection, and favorable matrix element for this process. The present limits from all the studied doubled β decay sources are summarized[112] in Table VIII.

Table VIII

Present limits on $< m^{\mathrm{Maj}} >_\nu$ and $|\eta|$ from double beta decay experiments

Parent Isotope	$< m^{\mathrm{Maj}} >_\nu$	$\eta \times 10^5$	$< m^{\mathrm{Maj}} >_\nu^*$	$\eta \times 10^{5*}$
^{82}Se	$\leq$ 14 ev	$\leq$ 2	$\leq$ 33 eV	$\leq$ 4.6
^{130}Te	$\leq$ 8 eV	$\leq$ 2.3	$\leq$ 100 eV	$\leq$ 15
^{128}Te	$\leq$ 0.7 eV	$\leq$ 0.3	$\leq$ 8.7 eV	$\leq$ 3.5
^{48}Ca	$\leq$ 41 eV	$\leq$ 3.9	$\leq$ 44 eV	$\leq$ 4.2
^{76}Ge	$\leq$ 10 eV	$\leq$ 2.4	$\leq$ 24 eV	$\leq$ 4.5

*Values were analyzed with matrix elements renormalized to be in agreement with geochronological results in ^{130}Te and ^{82}Se. There is no compelling reason to do this.

6. RIGHT-HANDED CURRENTS

The original motivation for the right-handed currents rests in the explicit restoration of the right-left symmetry at the Lagrangian level. In this picture, we witness an asymmetry, i.e. predominantly a left-handed world, because we are in the low energy domain where this symmetry is broken. Explicitly, this is accomplished because $M_{W_R} >> M_{W_L}$ and as long as we are in the energy domain where $q^2 << M_{W_L}{}^2$, the observable weak interaction effects are due mainly to W_L. This framework might provide a natural mechanism of CP violation that is additional to that due to the presence of a phase in the Kobayashi-Maskawa matrix. That is accomplished by having a phase difference between W_L and W_R interactions. In this discussion, we shall limit ourselves strictly to the information that experiments provide about the question of the existence of the right-handed currents.

We shall compare the experimental situation with the classical model of right-left symmetry due to Bég, Budny, Mopatra, and Sirlin.[113] In that picture we have two states of well defined chirality W_R and W_L that mix to give mass eigenstates, W_1 and W_2 ,

$$W_1 = W_L \cos \varsigma - W_R \sin \varsigma, \text{and} \tag{6.1}$$

$$W_2 = W_L \sin \varsigma + W_R \cos \varsigma \ . \tag{6.2}$$

Thus data can be parametrized in terms of the mixing angle ς and the mass ratio squared α , defined by $\alpha = M^2(W_L)/M^2(W_R)$. Note that the α parameter is identical to the parameter η that is conventionally used in discussing the double β decay experiments.

We have already discussed the double β decay experiments and the relevance that they have on this question of R-L symmetry. One might only add here the caveat that all the conclusions drawn from these data rest on the assumption that we are dealing with a Majorana neutrino.

The first experiment that we shall discuss is the study of the endpoint of the electron energy spectrum from a muon decay in a direction opposite to the muon spin.[77] The results of that experiment are illustrated in Fig. 47. When the spin is precessed, the experiment effectively integrates over all the directions with respect to the spin and we are merely measuring the Michel ρ parameter (or alternatively detection efficiency, resolution, etc). This is illustrated in curve (A). When the spin is held, we see the rapid drop-off to the zero yield at the endpoint, as is predicted by the V-A theory. Quantitatively, the result can be expressed as a lower limit on the product of μ decay parameters and muon polarization and is $\xi P_\mu \delta/\rho > 0.9959$(90% C.L.). This value should be unity for pure V-A interaction.

The authors summarize[77] the results of their experiment as well as those of other low energy experiments that have a bearing on the question of right-handed currents. They are displayed as allowed contours in the $\varsigma - \alpha$ plane in Fig. 48. It should be emphasized that all of these results, with the exception of

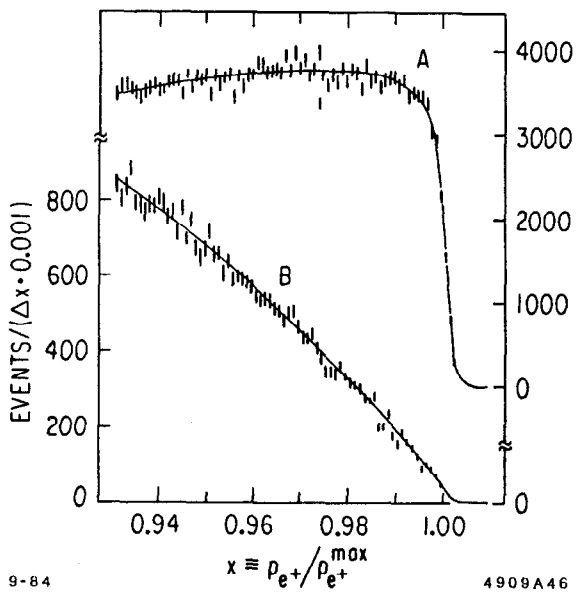

Figure 47 Distribution of the reduced positron momentum in the direction 180° away from the initial μ spin. Curve A is for the data taken with μ processing; curve B for μ spin held along the initial polarization direction.

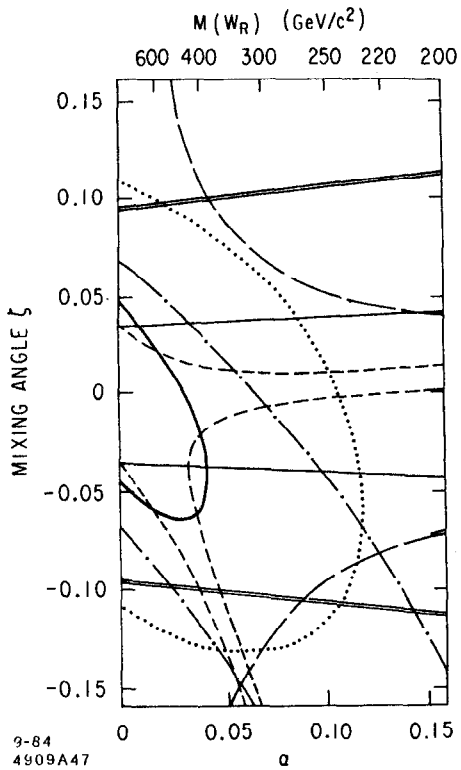

Figure 48 Experimental 90% -confidence limits on the W_L/W_R mass-squared ratio α and mixing angle ζ describing possible right-handed charged currents. The allowed regions are those which include $\alpha = \zeta = 0$. Muon-decay contours are derived from decay-rate measurements at the spectrum endpoint (bold curve), the polarization parameter ξP_μ (dotted curve) and the Michel parameter ρ (solid curve). Nuclear β-decay contours are obtained from the Gamow-Teller β polarization (dot-dashed curves); the comparison of Gamow-Teller and Fermi β polarizations (long-dashed curves); and the ^{19}Ne asymmetry A(0) and ft ratio, with the assumption of conserved vector current (short-dashed curves). Limits from the y distributions in νN and $\bar{\nu}$N scattering are shown as double lines.

the ν experiment to be discussed later, assume in their derivation of limits that $m_{\nu_R} \approx 0$.

A recent experiment at KEK[114] searched for the presence of right-handed currents in the decay $K^+ \rightarrow \mu^+\nu$. In principle, the expectation for this process could be independent of the μ decay experiment if the quark mixing angles are different in the right- and left-handed sectors. The specific experimental measurement is the polarization of the muon, predicted to be -1 in the V-A theory. The experimental value, $P_\mu = -0.970 \pm 0.047$ is fully compatible with that hypothesis.

The cross section for the reaction

$$\nu_\mu + e^- \rightarrow \mu^- + \nu_e$$

is sensitive to the handedness of the neutrinos and the nature of the charged leptonic current.[115] The experimental results are in perfect agreement[116] with the left-handed neutrinos and a V-A nature of the current.

The CDHS collaboration has searched[117] for possible admixtures of right-handed currents in the ν interactions. Experimentally these would show up as a deviation in the y distribution that one expects in a standard V-A picture. Thus, in the V-A picture the expected distribution for the ν scattering is

$$\frac{d^2\sigma^\nu}{dxdy} \;\alpha\; q(x) + (1-y)^2\bar{q}(x) \; .$$

If the Lagrangian has a right-handed contribution such as

$$L = \frac{G}{\sqrt{2}}\{\bar{\mu}\gamma_\mu(1+\gamma_5)\nu \times \bar{u}\gamma_\mu[C_L(1+\gamma_5) + C_R(1-\gamma_5)]d\}$$

then the differential distribution will be modified to

$$\frac{d^2\sigma^\nu}{dxdy} \;\alpha\; q(x) + \rho^2\bar{q}(x) + (1-y)^2[\bar{q}(x) + \rho^2 q(x)] \equiv q_L(x) + (1-y)^2 q_R(x)$$

where we have defined

$$\rho \equiv |C_R/C_L| \; .$$

For $\bar{\nu}$'s, we interchange the $q(x)$ and $\bar{q}(x)$ contributions (and $q_L(x)$ and $q_R(x)$).

Quantitatively, one compares the ratio of $\bar{\nu}$ to ν cross sections as a function of y and x (Fig. 49). Since this ratio vanishes at high x as $y \rightarrow 1$, we must have $q_R(x) << q_L(x)$. An upper limit on ρ^2 can be obtained by assuming that $\bar{q}(x) = 0$ in that limit, yielding a value of $|\rho^2| < 0.009$ with a 90 % confidence limit.

To relate this limit to our two standard parameters, we present in Fig. 50 the contribution of the right-handed currents to the neutrino quark scattering process. We assume that we have a pure beam of left-handed neutrinos and thus right-handed interaction occurs at the lower vertex by virtue of the mixing of W_L, or W_R, expressed previously in Eq. 6.1. Thus we have

$$C_R = \sin\,\varsigma\,\cos\,\varsigma\left(\frac{1}{M_{W_R}{}^2} - \frac{1}{M_{W_L}{}^2}\right) .$$

The left-handed interaction contribution has similar diagrams in this picture except that the coupling at the 2 vertices is either $\cos\,\varsigma$ or $\sin\,\varsigma$ depending on whether M_1 or M_2 is exchanged. We thus have

$$C_L = \frac{\cos^2\varsigma}{M_{W_L}{}^2} + \frac{\sin^2\varsigma}{M_{W_R}{}^2} \; .$$

For small values of the mixing angle we obtain

$$\varsigma \approx \rho/(1 - M_{W_L}{}^2/M_{W_R}{}^2) = \rho/(1-\alpha^2) \; .$$

Thus the experiment is mainly sensitive to the mixing angle; this fact is apparent from Fig. 48.

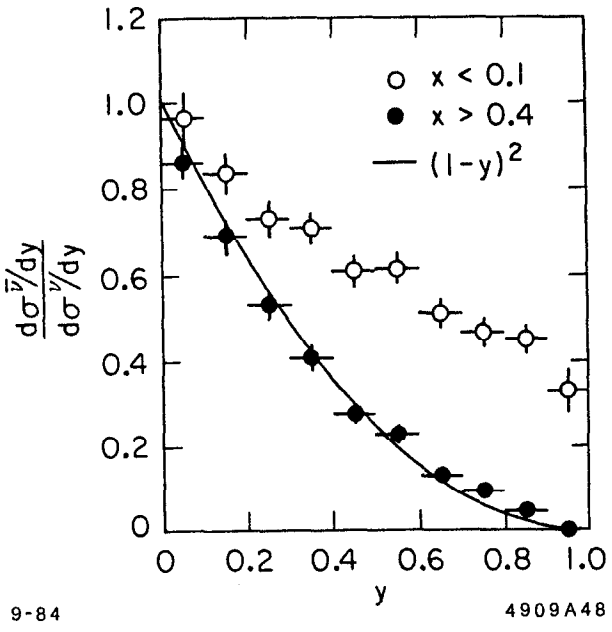

Figure 49 The ratio of antineutrino to neutrino cross sections as a function of y in two different regions of x.

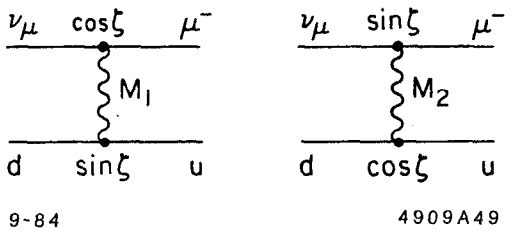

Figure 50 The 2 diagrams contributing to the right-handed interaction at the quark vertex if a left-handed neutrino initiates the reaction.

The CDHS Collaboration has also been able to explore[19] any possible contribution of the right-handed currents to interactions involving charm quarks, by studying the $\mu^+\mu^-$ channel that has been discussed previously in Chapter 2. Since that reaction has to proceed entirely off the quarks for incident neutrinos (and off the anti-quarks for incident $\bar{\nu}$'s), the right-handed currents are the sole possible contributor to the $(1-y)^2$ component for ν interactions (and to the isotropic component for $\bar{\nu}$'s). One can thus compare the Monte Carlo predictions for both the V-A and V+A predictions. Comparisons at 2 different energies are illustrated in Fig. 51. Clearly the data do not demand any V+A contribution and a quantitative analysis yields a 95% confidence limit on ρ^2 of $\rho^2 < 0.07$.

Finally, we might end this chapter by illustrating the sensitivity of a potential new high energy e^-p collider to right-handed currents. The cross sections[118] for the process $e^-p \to \nu_R + X$ are illustrated in Fig. 52. The projected rate of 1000 events/year assumes 10^7 secs of good running time. Thus even with these high energies the increase in M_{W_R} sensitivity is rather negligible over the lower energy experiments. It is important, however, to emphasize that these investigations would be independent of the mass of ν_R , provided only that $M_{\nu_R} << E_{cm}$.

Acknowledgements. I would like to thank L. Littenberg, M. Shaevitz, and B. Winstein for sending me copies of recent preprints and conference presentations that facilitated the preparation of these lectures.

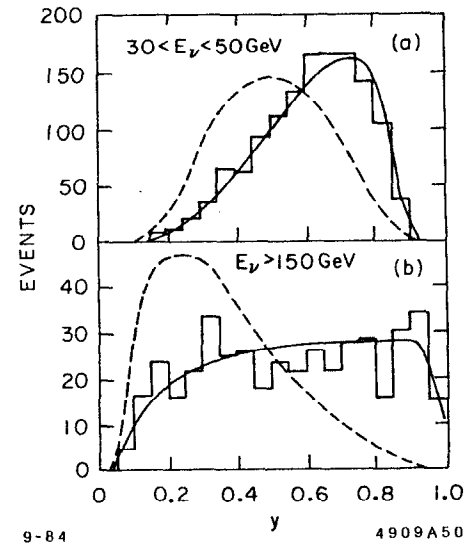

Figure 51 The y distribution of the observed $\mu^+\mu^-$ neutrino induced events for 2 different ranges of E_ν. The solid and dashed curves represent the V-A and V+A current predictions, respectively.

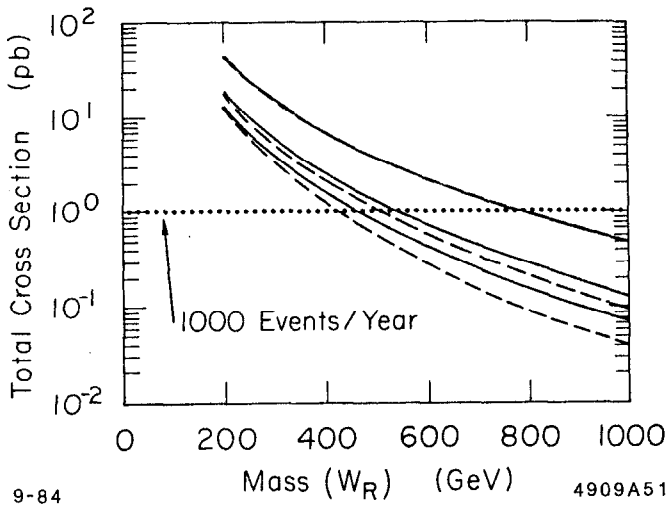

Figure 52 Cross section for the process $e^- p \to \nu_R + X$ computed in the limit $m_{\nu_R}, m_Q << E_{cms}$. (Q is the quark that emits or absorbs W_R.) The three sets of curves refer to electrons of energy 15 GeV, 30 GeV, and 200 GeV colliding with 20 TeV protons. The solid and dashed curves include angle cuts $\theta > 2°$ and $\theta > 10°$, respectively, on the produced fermions.

REFERENCES

1. It would be impossible for me to give appropriate credit to all the important experimental and theoretical work that contributed to the development of the subject under discussion. Accordingly I choose to avoid giving any references in this introductory chapter.
2. M. Kobayashi and K. Maskawa, Progr. Theor. Phys. 49, 652 (1973).
3. L. Maiani, **Proceedings of the 8th International Symposium on Lepton and Photon Interactions at High Energies**, Hamburg (1977), p. 867.
4. L. Wolfenstein, Phys. Rev. Lett. 51, 1945 (1983).
5. C. Rubbia, Recent Results from UA1 Experiment at CERN $\bar{p}p$ Collider, talk given at the Topical Conference at this Institute.
6. G. Kane and M. Peskin, Nucl. Phys. B195, 29 (1982).
7. S. Weinberg, Phys. Rev. Lett. 19 (1967) 1364; A. Salam, **Proc. 8th Nobel Symp.** (Almquist and Wiksells, Stockholm, 1968); S. Glashow, Nucl. Phys. 22, 579 (1961).
8. S. L. Glashow and S. Weinberg, Phys. Rev. D15 (1977) 1958.
9. CLEO Collaboration, paper C271 submitted to the 1983 International Symposium on Lepton and Photon Interactions at High Energies at Cornell; quoted by S. Stone, p. 217 of those Proceedings.
10. There have been several recent discussions of this question in the literature. The latest published work is probably by K. Kleinknecht and B. Renk, Phys. Lett. 130B (1983) 459.
11. E. A. Paschos and U. Turke, Phys. Lett. 116B 360 (1982).
12. R. E. Shrock and L. L. Wang, Phys. Rev. Lett. 41, 1962 (1978).
13. I. S. Towner and S. C. Hardy, Phys. Lett. 73B, 20 (1978); D. H. Wilkinson, Phys. Lett. 67B, 13 (1977).

14. M. Ademollo and R. Gatto, Phys. Rev. Lett. 13, 264 (1964).

15. M. Bourquin et al., Z. Phys. C21, (1983) 27.

16. Precision Measurement of the Decay $\Sigma^- \to ne^-\nu$, Fermilab Proposal No. 715, P. S. Cooper (Yale), spokesman.

17. R. H. Schindler et al., Phys. Rev. D24, 78 (1981).

18. D. Hitlin, Current Status of D Decays, talk given at the Topical Conference part of this Institute.

19. H. Abramowicz et al., Z. Phys. C15 (1982) 19.

20. Quoted by T. Nash in the **Proceedings of the 1983 International Symposium on Lepton and Photon Interactions at High Energies**, at Cornell, p. 359.

21. Heavy Hadron Decays, rapporteur talk by K. Schubert at the ν84 Conference in Dortmund.

22. S. Ahlen et al., Phys. Rev. Lett. 51, 1147 (1983).

23. W. Bacino et al., Phys. Rev. Lett. 43, 1073 (1979).

24. S. Pakvasa, S. F. Tuan, J. J. Sakurai, Phys. Rev. D23, 2799 (1981).

25. J. G. H. De Groot et al., Z. Phys. C1 (1979) 143.

26. K. Kleinknecht and B. Renk, Z. Phys. C16 (1982) 7.

27. C. Klopfenstein et al., Phys. Lett. 130B, 444 (1983).

28. A. Chen et al., Phys. Rev. Lett. 52, 1084 (1984).

29. M. K. Gaillard and L. Maiani, **Proc. Summ. Inst. on Quarks and Leptons, Cargese 1979** (Plenum, New York, 1980), p. 433.

30. E. Fernandez et al., Phys. Rev. Lett. 51, 1022 (1983); N. S. Lockyer et al., Phys. Rev. Lett. 51, 1316 (1983).

31. J. Jaros, Measurements of Heavy Quark and Lepton Lifetime at PEP, talk presented at the Topical Conference of this Institute.

32. D. E. Klem et al., submitted to Phys. Rev. Lett., SLAC-PUB-3379.

33. M. Davier, Recent Results from PETRA, talk presented at the Topical Conference at this Institute.

34. For a review of possible toponium decay modes, see J. D. Jackson, S. Olsen and S.-H. Tye, **Proceedings of the 1982 DPF Summer Study at Snowmass**, Colo., June 28 - July 16, 1982, p. 175.

35. L.-L. Chau and W.-Y. Keung, Phys. Rev. D29, 592 (1984).

36. L. Wolfenstein, Nucl. Phys. B160, 501 (1979).

37. J. Ellis, M. K. Gaillard, and D. V. Nanopoulos, Nucl. Phys. B109, 213 (1976).

38. P. H. Ginsparg, S. L. Glashow, and M. B. Wise, Phys. Rev. Lett. 50, 1415 (1983).

39. R. E. Shrock and S. B. Treiman, Phys. Rev. D19, 2148 (1979).

40. M. K. Gaillard and B. W. Lee, Phys. Rev. D10, 897 (1974).

41. J. F. Donoghue et al., Phys. Lett. 119B, 412 (1982).

42. See for example A. Buras, Phys. Rev. Lett. 46, 1354 (1980).

43. J. H. Christenson et al., Phys. Rev. Lett. 13, 138, (1964).

44. For a recent comprehensive review, see K. K. Kleinknecht, Ann. Rev. Nucl. Science 26, 1 (1976).

45. F. J. Gilman and M. Wise, Phys. Rev. D20, 2392 (1979); B. Guberina and R. D. Peccei, Nucl. Phys. B163, 289 (1980).

46. L. Wolfenstein, Phys. Rev. Lett. 13, 562 (1964).

47. F. J. Gilman and J. S. Hagelin, Phys. Lett. 133B, 443 (1983) and Phys. Lett. 126B, 111 (1983). See also Ref. 45.

48. B. Winstein, review talk given at the XIth International Conference on Neutrino Physics and Astrophysics at Dortmund, June 11-16, 1984.

49. J. Cronin, CP Violation in K Decays, talk given at the Topical Conference part of this Institute.

50. W. M. Morse, Measurement of ϵ' at the AGS, talk given at the 1984 Conference in Erice, Sicily, Italy.

51. A measurement of the magnitude of ϵ'/ϵ in the neutral Kaon system to a precision of 0.001, Fermilab Proposal E-731, Chicago, Fermilab, Saclay collaboration; B. Winstein, Chicago, spokesman.

52. Measurement of $|\eta_{oo}|^2/|\eta_{+-}|^2$, CERN/SPSC/81-110 , December 22, 1981; proposal to CERN SPS; H. Wahl, CERN, spokesman.

53. M. K. Campbell et al., Phys. Rev. Lett. 47, 1032 (1981).

54. W. M. Morse et al., Phys. Rev. D21, 1750 (1980).

55. Letter of intent by Backenstoss et al., CERN/PSCC/83-28; PSCC/I 65, June 9, 1983.

56. Fermilab proposal # 621; Wisconsin, Rutgers, Michigan, Minnesota collaboration; G. Thomson, U. of Wisconsin, spokesman.

57. Study of very rare K_L° decays, AGS proposal # 791 by UCLA-Los Alamos, Pennsylvania, Princeton, Stanford, Temple, William and Mary collaboration; S. Wojcicki, Stanford, spokesman.

58. F. J. Gilman and M. B. Wise, Phys. Rev. D21, 21 (1980).

59. P. Herczeg, Phys. Rev. D27, 1512 (1983).

60. L.-L. Chau, W.-Y. Keung, M. D. Tran, Phys. Rev. D27, 2145 (1983).

61. W. B. Dress et al., Phys. Rev. D15, 9 (1979).

62. D. V. Nanopoulos, A. Yildiz, and P. H. Cox, Phys. Lett. B87, 53 (1979); B. F. Morel, Nucl. Phys. B157, 23 (1979).

63. I. I. Bigi and A. I. Sanda, Nucl. Phys. B193, 85 (1981).

64. A. Bodek et al., Phys. Lett. 113B, 82 (1982).

65. I. I. Bigi and A. I. Sanda, Phys. Rev. D29, 1393 (1984).

66. J. S. Hagelin, Nucl. Phys. B193, 123 (1981).

67. R. N. Cahn and H. Harari, Nucl. Phys. B176, 135 (1980).

68. J. Ellis and J. S. Hagelin, Nucl. Phys. B217, 189 (1983).

69. F. Wilczek, Phys. Rev. Lett. 49, 1549 (1982).

70. A Study of the Decay $K^+ \to \pi^+\nu\bar{\nu}$, AGS Experiment # 787, BNL, Carnegie Mellon, Columbia, Princeton, TRIUMF Collaboration.

71. Y. Asano et al., Phys. Lett. 107B, 159 (1981).

72. A Search for the Rare Decay $K^+ \to \pi^+\mu^+e^-$, AGS experiment # 777, a Brookhaven, Washington, Yale collaboration; M. Zeller, Yale, spokesman.

73. A. M. Diamant-Berger et al., Phys. Lett. 62B, 485 (1976).

74. A Search for the Flavor Changing Neutral Currents $K_L^\circ \to \mu + e$ and $K_L^\circ \to e^+e^-$, AGS experiment # 780, BNL-Yale Collaboration, M. P. Schmidt (Yale) and W. M. Morse (BNL), spokesmen.

75. G. J. Feldman, in the **Proceedings of the 1981 DPF Annual Meeting**, Santa Cruz, Ca., C. A. Heusch and W. T. Kirk, ed; also K. G. Hayes et al., Phys. Rev. D25, 2869 (1982).

76. F. Scheck, Phys. Rep. C44, 187 (1978).

77. J. Carr et al., Phys. Rev. Lett. 51, 627 (1983).

78. W. Bacino et al., Phys. Rev. Lett. 42, 749 (1979).

79. J. A. Jaros et al., Phys. Rev. Lett. 51, 955 (1983).

80. For example see A. DeRujula et al., Nucl. Phys. B168, 54 (1980).

81. K. E. Berquist, Phys. Scripta 4, 23 (1971) and Nucl. Phys. B39, 317 (1972).

82. V. A. Lubimov et al., Phys. Lett. 94B, 266 (1980).

83. V. A. Lubimov, **Proceedings of the European Physical Society HEP 83**, Brighton, England; see also the review talk by M. Shaevitz, in the **Proceedings of the 1983 International Symposium on Lepton and Photon Interactions at High Energies**, Cornell, N.Y.

84. See the review paper by F. Boehm in the **Proceedings of the 4th Workshop on Grand Unification**, Birkhäuser Boston, p. 163, (1983).

85. A. DeRujula, Nucl. Phys. B188, 414 (1981).

86. J. U. Anderson et al., Phys. Lett. 113B, 72 (1982).

87. R. S. Raghaven, Phys. Rev. Lett. 51, 975 (1983).

88. R. Abela et al., Phys. Lett. 105B, 263 (1981).

89. C. Matteuzzi et al., Phys. Rev. Lett. 52, 1869 (1984).

90. R. Schrock, Phys. Lett. 96B, 159 (1980).

91. K. Winter, in **Proceedings of the 1983 International Symposium on Lepton and Photon Interactions at High Energies**, Cornell, N.Y., p. 177.

92. D. Silverman and A. Soni, **Proceedings of the Annual DPF Conference**, at Santa Cruz, 1981.

93. See for example J. N. Bahcall, R. Davis, Science 191, 264 (1976).

94. J. N. Bahcall et al., Rev. Mod. Phys. 54, 767 (1982).

95. R. Davis et al., **Proceedings of the International Neutrino Conference**, Purdue Ill., 1978, p. 53; W. Hampel, **Proceedings of the International Conference on Neutrino Physics and Astrophysics**, Erice, 1980, p. 61.

96. M. R. Krishnaswamy et al., **Proc. Roy. Soc. London A323**, 489 (1971); M. F. Crouch et al., Phys. Rev. D18, 2239 (1978).

97. M. M. Bolieu et al., **Proc. 1981 Intern. Conf. on Neutrino Phys. and Astroph.**, Maui, 1981, vol. I, p. 283; G. D. Davimus, ibid. p. 291.

98. R. M. Bionta et al., **Proceedings of the 4th Workshop on Grand Unification**, Birkhäuser: Boston, p. 46, 1983.

99. T. Gaisser, ibid., p. 87.

100. See for example I. E. Stockdale et al., Phys. Rev. Lett. 52, 1384 (1984); F. Bergsma, Phys. Lett. 142, 103 (1984); F. Dydak et al., Phys. Lett. 134B, 281 (1984).

101. F. Reines et al., Phys. Rev. Lett. 45, 1307 (1980); F. Boehm et al., Phys. Lett. 97B, 310 (1980). The Irvine experiment compared charged current and neutral current reactions, the latter being insensitive to any ν_e depletion due to oscillations.

102. H. Kwon et al., Phys. Rev. D24, 1097 (1981).

103. J. L. Vuillemier et al., Phys. Lett. 114B, 298 (1982).

104. J. L. Vuillemier, paper presented at the XIth International Conference on Neutrino Physics and Astrophysics at Dortmund, June 11-16, 1984.

105. D. Koang, paper presented at the XIth International Conference on Neutrino Physics and Astrophysics at Dortmund, June 11-16, 1984.

106. See for example W. C. Haxton, G. J. Stephenson, Jr., and D. Strottman, Phys. Rev. Lett. 47, 153 (1981).

107. B. Pontecorvo, Phys. Lett. 26B, 630 (1968).

108. E. Hennecke et al., Phys. Rev. C11, 1378 (1975).

109. T. Kirsten, H. Richter and E. Jessberger, Phys. Rev. Lett. 50, 474 (1983).

110. M. K. Moe and D. D. Lowenthal, Phys. Rev. C22, 2186 (1980).

111. B. Srinivasan et al., Econ. Geol. 68, 252 (1973).

112. F. T. Avignone, III et al., review talk given at the Fourth Workshop on Grand Unification, Philadelphia, Pa., April 21-23, Birkhaüser-Boston, publishers.

113. M. A. B. Bég et al., Phys. Rev. Lett. 38, 1252 (1977).

114. R. S. Hayano et al., Phys. Rev. Lett. 52, 329 (1984).

115. C. Jarlskog, Nuov. Cim. Lett. 4, 377 (1970).

116. N. Armenise et al., Phys. Lett. 84B, 137 (1979); M. Jonker et al., Phys. Lett. 93B, 203 (1980).

117. H. Abramowicz et al., Z. Phys. C12, 225 (1982).

118. C. Prescott, in the Summary Report of the PSSC Discussion Group Meetings, P. Hale and B. Winstein, editors.